Quality Assessment – Final Report for PMTACS-NY

(PM2.5 Technology Assessment and Characterization Study in New York)

April 1, 2001 – April 30, 2005

Kenneth L. Demerjian
Project Director for PMTACS-NY

Volker A. Mohnen
Quality Assurance Manager for PMTACS-NY

TABLE OF CONTENTS

FINAL QUALITY ASSESSMENT REPORT FOR PMTACS-NY

I. INTRODUCTION

A Quality Assurance Project Plan for the EPA Particulate Matter "Supersite": PM2.5 Technology Assessment and Characterization Study in New York was developed and adopted by EPA (QAPP Version 1.1, last revised July 15, 2002). It defined the Data Quality Objectives and audit responsibilities for the special intensive field studies that were carried out in the summer of 2001 and winter of 2004 . Accordingly, all measurements that are based on FRMs have been audited by:

New York State Department of Environmental Conservation
Division of Air Resources, Bureau of Technical Support
Quality Assurance Section

Measurements that are based on RPs have been quality assessed through specially designed quality assurance experiments based on three approaches:

(1) Filter Comparison- these start with evaluations of the filter methods

(2) Laboratory Evaluations and Comparisons- these require a substantial investment and effort to establish a benchmark facility.

(3) Instrument Inter-comparisons- these can establish "comparability and/or "agreement"; often requires substantial effort and/or equipment investment.

Methodology/instrument inter-comparisons were performed at the ASRC reference laboratory and/or during the field experiments. Purpose of these activities was to characterize instrument performance with regard to possible interferences, minimum detection level, precision (root mean square error) and accuracy (trueness). For all instruments (FRM and RM) a Standard Operating Procedure (SOP) was developed, approved by the QA-Manager and posted on the PMTACS-NY web site prior to their deployment in the field.

It must be recognized that no standard reference/calibration material or FRM procedure is currently available from EPA for suspended, atmospheric PM (specifically chemical composition, size distribution, number concentration etc).

This final Quality Assurance Report summarizes the results obtained to date with special focus on the summer 2001and the winter 2004 intensive field campaigns. All instruments operating under a RM protocol were located at the Queens College site.

II.SUMMARY OF RESULTS

II.1 Federal Research Method (FRM)

Staff from NYSDEC assumed principle responsibility for auditing all instruments operating under a FRM protocol deployed at Queens College II (7096-15) during the summer 2001 and winter 2004 intensives.

Summer 2001:

On July 26, 2001, QA staff from DEC conducted an annual performance audit at the Queens College II (7096-15) continuous air monitoring site. This site has continuous analyzers for ozone, SO_2, CO and NO-NO_2-NO_x and a TEOM and FRM PM2.5 particulate monitor. The results are summarized in Table II.1a.

Table II.1a

Compound	Average % Deviation	DQO Status
CO (TECO 48)	-0.6	Ok
O_3 (TECO 49C)	-2.8	Ok
SO_2 (TECO 43C)	-1.8	Ok
NO (TECO 42)	+0.7	Ok
NO_2 (TECO 42)	+2.8	Ok
NO_x (TECO 42)	+2.4	Ok
CH_4 (Horiba APHA 360)	4.3	Ok
NMHC (Horiba APHA 360)	0.2	Ok
THC (Horiba APHA 360)	1.3	Ok
NY PM2.5 (R&P 2025)	--	Passed
TEOM PM-10 (R&P)	--	Passed
*PM2.5 speciation (R&P 2300)	--	Passed

*The filters were sent to RTI for chemical analysis. An external system- and performance audit of this laboratory was performed by US EPA-QAQPS and National Air and Radiation Environmental Laboratory (see Appendix B). All relevant DQOs have been met. The QA results from DEC are detailed in Appendix A.

Winter 2004:

On October 28 and November 4, 2003, QA staff conducted annual performance audits at the Queen's College (7096-15) continuous air monitoring site. The results are summarized in Table II.1 b

The extraction efficiencies for Nylon filters are further discussed and quantified in:
http://www.epa.gov/ttnamti1/files/ambient/pm25/spec/nylstud.pdf
http://www.epa.gov/ttnamti1/files/ambient/pm25/spec/nylstu2.pdf
for both participating monitoring sites, IS 52 and Queens College

Table II.1b :PMTACS-NY Queens College Winter 2004 Field Intensive (DEC)			
Instrument	**Parameter**	**QA Status**	**Comments/Requirements**
TECO NO_s	NO_x	Passed Jan 18th (-1.8%) Jan 30th (-2.8%)	
TECO CO	CO	Passed Jan Audit (2.9%)	
TECO Pulsed Fluoresc.	SO_2	Passed Jan Audit (-.5%) Feb Audit (1.6%)	
TECO O_3	O_3	Passed Jan Audit (0.5%) Feb Audit (-4.7%)	Re-Calibrated 2/13 Audit (.2%)
Horiba THC	THC/NMHC/CH_4	Passed Methane Audit (-5.5%) Total HC Audit (0.0%)	November 2003
PE Auto GC	C2-C12 hydrocarbons	Passed EPA Std Cylinder	Limited Period of Data See Memo in Appendix:
TEOM FDMS	PM2.5 mass	Passed March Audit (-0.07%)	
TEOM Accu Samp. 50 C	PM2.5 metals & $SO_4^=$	Passed March Audit (-1.8%)	
Partisol 2300	PM2.5 Composition	Passed Jan Audit (.8%)	.8% = Average % Diff. (for all six channels)
PM2.5 FRM	PM2.5 mass	Passed Jan Audit (-3.25%) Feb Audit (0.36%)	
R&P 5400	PM2.5 carbon	Passed Span Ratio 0.76-0.79	Heating Bulb Failed 1/16 – 2/23/04
Toxic/PAMS Canister	Toxics/C2-C12 NMHC	Passed	Canister Volume and Lab Standard
Nano SMPS; 3025A, 3080	PM size distribution	No FRM audit method	See Table 1 c
Electr. Aerosol Det. 3070 & 3010	PM size distribution	No FRM audit method	See Table 1 c
TSI 3007 portable	Total CNC number	No FRM audit method	See Table 1 c
Nanomet PAS 2000	PM bound PAH	No FRM audit method	See Table 1 c

II.2 Particle Sizing and Counting Instrumentation Operated by NYDEC– PMTACS-NY Winter 2004, Data and QA Summary

These instruments were operated under a Research Method protocol by the NYSDEC Particle Research Group.

- Particle Sizing Instrumentation included
    - Scanning Mobility Particle Sizer with Nano Differential Mobility Analyzer and CPC 3025 (TSI Model 3936, NanoSMPS).
    - Electrical Aerosol Detector (EAD, TSI Model 3070A)
    - Portable Condensation Particle Counter (TSI Model 3007)
    - NanoMet; comprised of Photoelectric Aerosol Sensor (Matter Engineering, Model PAS2000) and Diffusion Charger (Matter Engineering, Model LQ1-DC), from Matter Engineering
- Instrument deployment period: 01/09/04-02/05/04

1. In-field QA procedures and checks included daily checks of operation parameters, necessary adjustments; weekly (or more often if needed) flow audits, dynamic filter blanks, replacement of Drierite in bypass flows of the SMPSs, inlet impactor orifice cleaning, and recharging of the CPC3007 wick (see below). All flow calibrations were performed right after setting instruments up in the field.

- Cycle length, scanned diameter, sample and sheath flows of each instrument are listed in Table II.1c.
- Bias and MDL are not applicable to these instruments. Accuracy values are given in Table II.1c.
- Percent of data capture is the ratio of valid data "samples" to maximum possible data "samples" can be also found in Table II.1c.
- The NanoSMPS measured size distribution over a specified diameter range (see Table II.1c). The instrument setup and inlet sampling parameters were identical to those implemented by ASRC at the Queens College site. Particle mean, median and mode diameters as well as total concentration are calculated. NanoSMPS data from the NYSDEC-operated instrument were compared to the ASRC-operated instrument (see section III.15 and Chapter V)
- The Electrical Aerosol detector (EAD) measures the parameter of "total aerosol length" of particles in a sample as mm/cc. Sampled particles are charged, and then the total charge for a sample is read by an electrometer after excess charges have been removed.
- The portable Condensation Particle Counter (CPC3007) is similar in operation to other CPCs, but employs isopropanol in an internal wick rather than butanol in an external reservoir. Over long sampling periods (the instrument is designed for portable, short-term use) the wick was found to dry out and had to be periodically swapped out with a fully charged wick ca. every 6 hours.

Table II.1.c. Operational parameters and data completeness

	NanoSMPS	EAD	CPC3007	NanoMet
Parameter	Size distribution	Total aerosol length (mm/cc)	Total particle concentration (#/cc)	Total PM-bound PAHs (ng/m3) & particle surface area (um2/cc)
Cycle Length	5 min	1 sec	1 sec	1 sec
Inlet Flow, l/min	0.6	1	1	1.5
Sheath Flow, l/min	6	N/A	N/A	N/A
Diameter Range, nm	4.6–163 nm*	10-1000 **	10-1000 **	0-1000 ng/m3 ** 0-2000 um2/cc **
Concentration Accuracy***	±10% up to 9.99 × 10^4/cm^3	±10% **	±20% of reading plus variation from counting statistics. **	Sensitivity limits: 10 ng/m3 ** 1 um2/cc **
% of data capture	90	90	75 ****	90

* - electrical mobility diameter, corresponds to physical diameter for spherical shape particles;
** - information is taken from corresponding manuals
*** - occasional unusually high values (800, 000 particles/cm^3 or higher) had been recorded by the NanoSMPS. These concentration "spikes" are random, not correlated either with the second NanoSMPS, or with the CPC 3022 measurements, and were considered artifacts. Corresponding samples were removed from the NanoSMPS data set.
**** - lower % of data capture is due to drying out of internal isopropanol wick.

III. SUMMARY OF RESULTS – Research Protocols (RP)

For assessing the data quality of instruments/methods operated under "Research Protocols" (RPs) and of new measurement technologies, quality assurance experiments and instrument/methods intercomparisons have been executed both in the ASRC Reference laboratory and in the field. Standard Operating Procedures were developed for all RP-instruments prior to their deployment in the field campaign. These are posted on the PMTAC-NY web site.

III.1 ASRC Reference Laboratory

The ASRC has established a special aerosol facility (Fig. III.1) where particle related QA experiments have been conducted for the purpose of characterizing aerosol instrument response and addressing other quality assurance issues in aerosol physics and the chemistry of aerosols. The purpose of the aerosol facility was to:

- Develop techniques for the generation of primary and secondary aerosol calibration standards
- Apply generated aerosol standards (i.e. aerosols of known size and composition within well-characterized ambient environments) to
  - Evaluate and characterize the performance of aerosol instrumentation (research and commercial)
  - Calibrate and quality assure aerosol size, mass and chemical speciation instrumentation

- Perform research associated with the formation and evolution atmospheric aerosols. Besides instrumentation for the generation and characterization of aerosols, the facility includes a large aerosol chamber along with support to provide controlled aerosol dilution and humidification. This facility has been designed to provide a capability that is as broad as possible to encompass a wide range of aerosol assessments in support of quality assurance. Aerosol generation includes spray atomization of solutions that are used for the generation of polydisperse aerosols in the 0.02 micrometer to 1 micrometer size range. Monodisperse aerosols over this size range can be produced by mobility classification. Production of larger monodisperse aerosols (0.5 micrometer to 20 micrometer) is accomplished through the use of a Vibrating Orifice Aerosol Generator (TSI Model 3450). Both inorganic and organic compounds have been used to generate test aerosols.

Aqueous solutions of the following chemical compounds were used to generate polydisperse test aerosol:

Inorganic - NaCl, $NaNO_3$, KNO_3, NH_4NO_3, $(NH_4)_2SO_4$, NH_4HSO_4, etc.
Organic - DOP, Acids, Nitrates, etc.
Mixed - Organic/Inorganic

The aerosol generation system is shown in Fig. III.2.

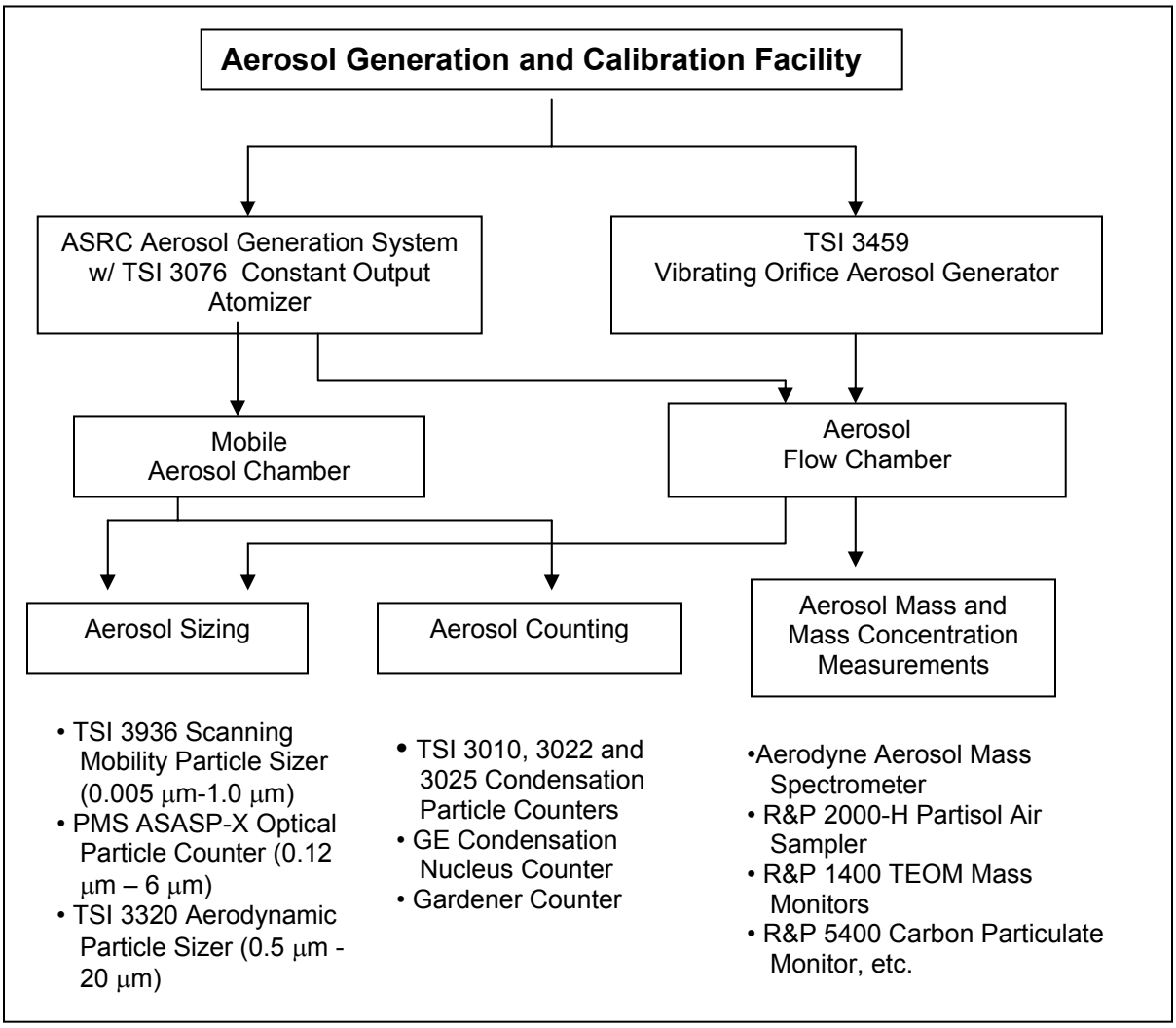

Figure III.1 Aerosol Generation and Calibration Facility

Test aerosols were generated using a Constant Output Atomizer, operating in a recirculation mode. When generating small size sulfate aerosol, a flat-plate impactor was installed at the generator outlet (to remove droplets larger than 3 μm)). The aerosol, after pre-dilution with dry particle-free air and passing through an Aerosol Neutralizer, was directed into a dilution tube, where it underwent main dilution with particle-free air with controlled relative humidity, and then was introduced into the slow flow 480 L chamber (Fig. III.3). The airflow rate used for main dilution varied from 20 to 55 l/min. Size of aerosol particles sampled from the middle of the chamber was less than 1 μm. Typical mass concentrations for the experiments ranged from 1 to ~ 60 $\mu g/m^3$. The tests were conducted with the flow chamber RH below 5%, with the exception of ammonium nitrate experiments, for most of which RH was maintained around 50-60%.

Physical characterization of small test aerosols includes concentration measurement using several condensation nucleus counters as well as size distribution measurements with a mobility

spectrometer (TSI Model 3080L). Concentrations and sizes of larger aerosols are obtained using an optical scattering instruments (PMS ASASP-X) as well as an aerodynamic particle sizer (TSI Model 3220). The combination of these instruments, deployed in PMTACS-NY, allows a detailed size and concentration characterization over the size range 20 nanometers to greater than 1 micrometer. The characteristics of test aerosols generated in the aerosol facility to challenge this instrumentation are summarized in Table III.1. Quality assurance experiments using the aerosol facility included the evaluation of TEOM mass monitors (Rupprecht & Patashnick Model 1400, R&P 5400 for carbon particulate monitoring, R&P 8400 for nitrate particulate monitoring and newly developed R&P instruments for monitoring sulfate aerosol.

Table III.1. Physical Characteristics of Generated Aerosol

Aerosol	Size	Mass Concentration	Relative Humidity	Generation Instrument
Polydisperse	0.01-0.5 µm	5-200 µg m^{-3}	10%-90%	Constant Output Atomizer
Monodisperse Small	0.01-0.5 µm	5-50 µg m^{-3}	10%-90%	Constant Output Atomizer + Electrostatic Classifier
Monodisperse Large	0.5-20 µm	5-100 µg m^{-3}	< 50%	Vibrating Orifice Aerosol Generator

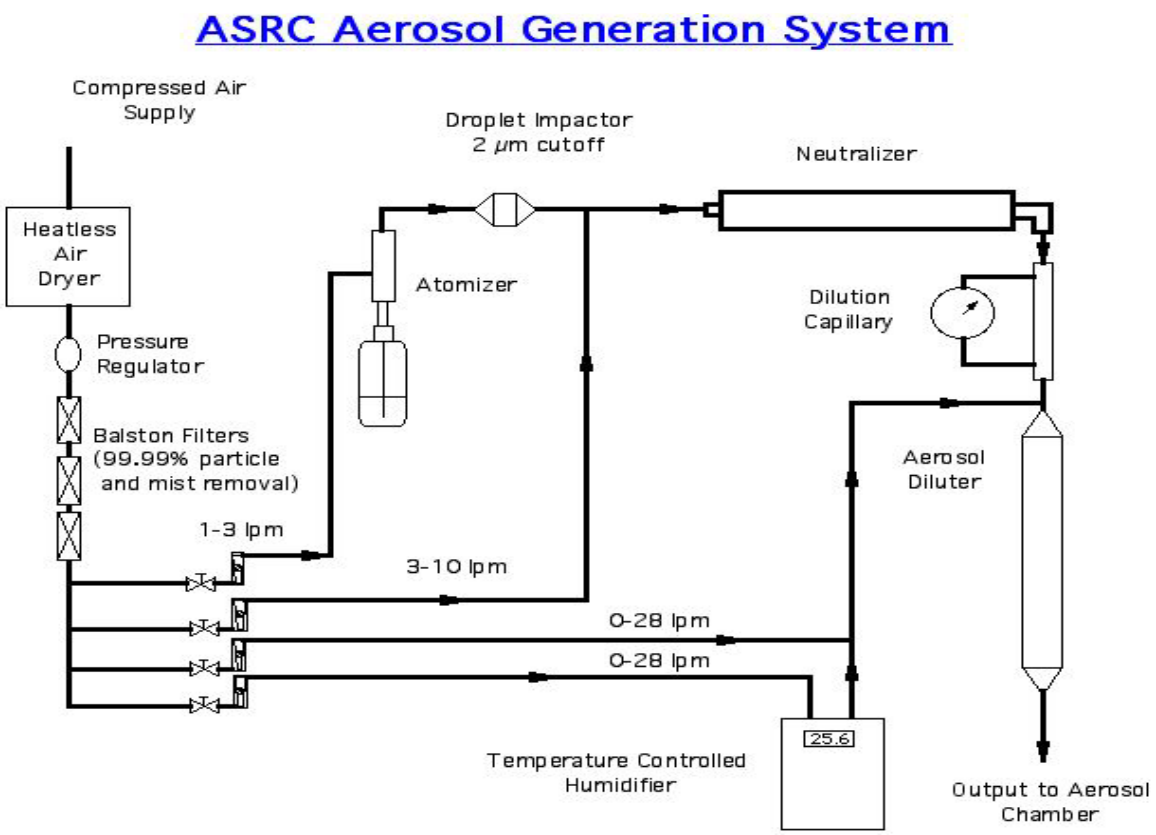

Figure III.2 Aerosol Generation System

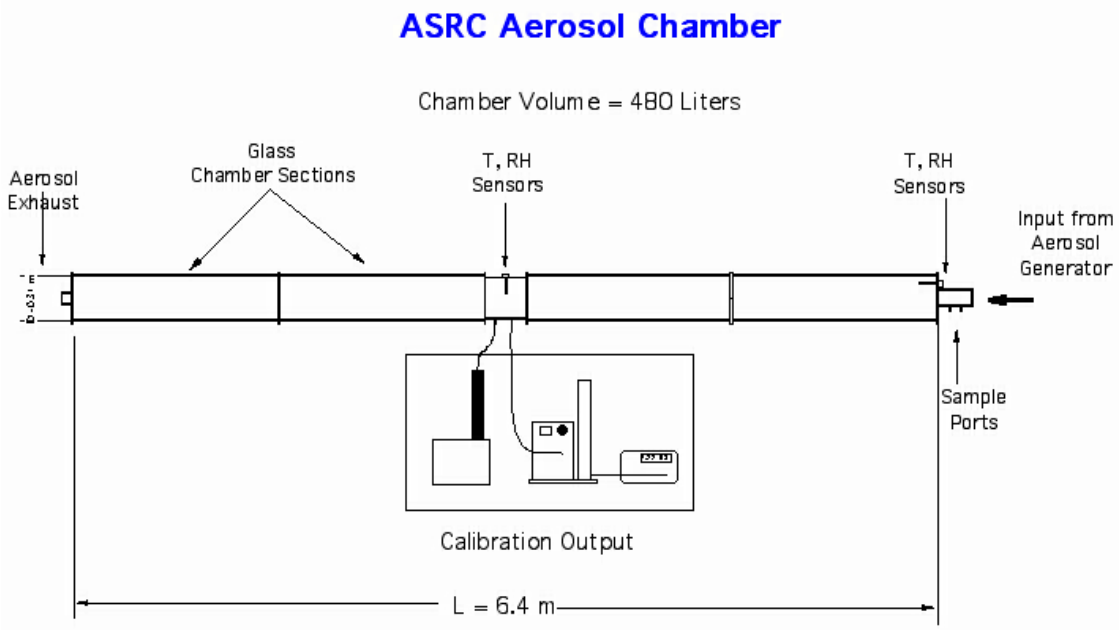

Figure III.3 Aerosol Chamber

During several tests, the size distribution of aerosol particles in the flow chamber was measured using a Scanning Mobility Particle Sizer (SMPS). The SMPS consisted of an Electrostatic Classifier, a Long Differential Mobility Analyzer and a Condensation Particle Counter. The SMPS measurements can serve as an additional reference measurement for nonvolatile test aerosols.

Examples of the aerosol facility applications are shown for:

- Size distribution of polydisperse ammonium sulfate aerosol generated by the constant output atomizer (Fig. III.4)
- Special aerosol distributions produced by the electrostatic classifier (Figures III.5-7).

III.2 R&P TEOM – SES

A continuous mass monitor based on the tapered element oscillating has been modified to operate at 30^{o}C and sample a de-humidified ambient air stream passed through a Nafion dryer.

III.2.1 Ammonium sulfate generation experiments

After testing the generation and measurement systems with NaCl aerosol, we turned to $(NH_4)_2SO_4$ for a set of experiments. Ammonium sulfate is non-volatile, very soluble, and easy to handle like NaCl, but it is of greater interest to atmospheric scientists because it is often a major component of the atmospheric aerosol, especially in the Eastern U.S., and other places downwind of transportation and industrial activity (Finlayson-Pitts and Pitts, 1986). $(NH_4)_2SO_4$ aerosol was generated with the atomizer, and measured with the TEOM monitors and the DMA/SMPS/CPC instrumentation. Table III.2 lists some parameters characterizing the aerosol produced. Mass concentrations measured with the TEOM monitors typically agreed to within

20% to the mass concentrations determined by the SMPS system. The estimates of mass concentration for the SPMS system were obtained by multiplying the cumulative volume determined by the TSI software by the density of ammonium sulfate.

The data indicated that a significant amount of particle bound water remained with the generated particles from the atomizer. In an experiment with NaCl, aerosol was generated for about 5 hours with a mean mass concentration near 500 µg/m^3. At a sample flow rate of 1 LPM, this resulted in a total deposition of 112.11 µg on the 50°C TEOM filter. Overnight the filter lost mass and stabilized at 88.70 µg. The measured mass loss was 23.41 µg. If all the lost mass is attributed to water vapor, then the original aerosol was at least 20.9% water.

Table III.2.

Chemical Composition	Solution Concentration	Mass Concentration	Median Diameter of Mass Distribution	Cumulative Number Concentration
Ammonium Sulfate	.01-2.0 g/liter	4-1000 ug/m^3	35-70 nm	1.3E(9) to 8E(10) cm^{-3}
Ammonium Nitrate	0.2-1.2 g/liter			

Figure III.4

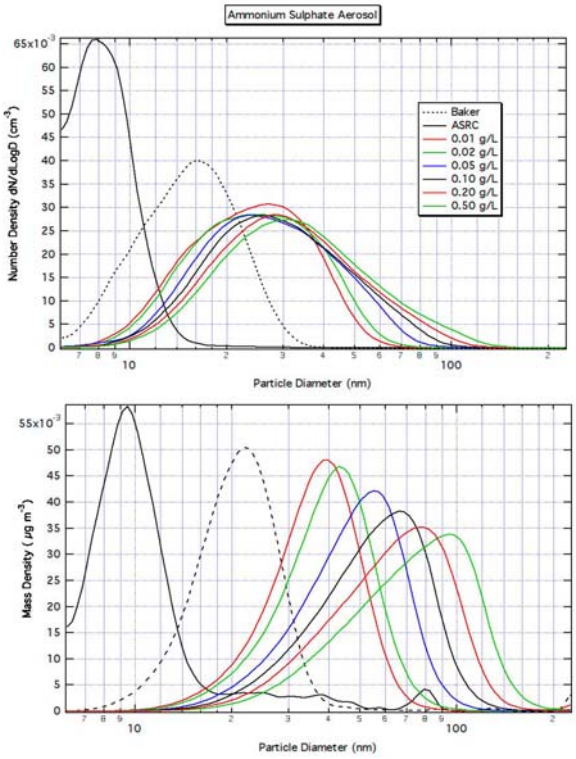

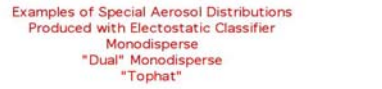

Figure III.5

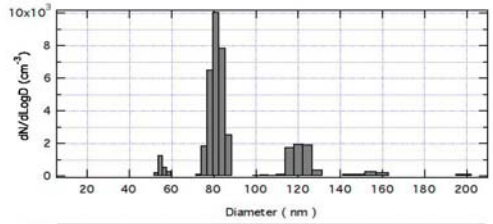

Figure III.6

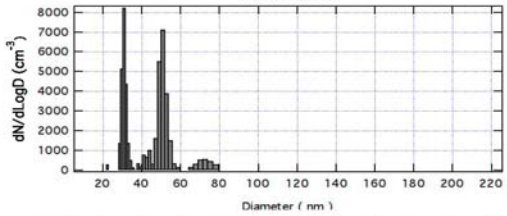

FigureIII.7

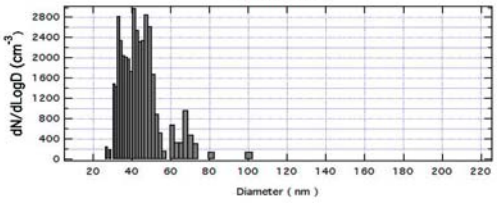

III.2.2 Ammonium nitrate generation experiments

Generation and measurement of ammonium nitrate presents a variety of challenges compared to sodium chloride and ammonium sulfate. Particle concentrations and size distributions continued to change for the whole 10 to 30 minutes they were in the aerosol chamber. The 50°C TEOM typically collected no ammonium nitrate – only at the highest mass concentration was any appreciable mass gain on the filter observed. Mass collected on the 30°C SES TEOM evaporated away with a half-life of 13 hours (1/e time constant of 16.5 hours). The constant evaporation of ammonium nitrate from the TEOM filter means that, even at 30°C, only some of the aerosol is collected, and that eventually, it all evaporates away. Collection and evaporation of ammonium nitrate is described by Furuchi et al. (paper by Fissan's group in POWDER TECHNOLOGY, Japan).

Collection of ammonium nitrate using the FRM Partisol sampler was also performed. The Partisol collects sample at ambient temperature in the laboratory, which varies between 21 and 26°C. The first comparison experiments used very high concentrations of aerosol, and are summarized in Table III.3. The very warm laboratory temperature during the first Partisol sample collection may explain the observation that apparently a greater mass concentration was measured by the 30°C TEOM. Later experiments presented below, used lower aerosol concentrations. For low aerosol concentrations (below 50 $\mu g/m^3$ in this case), the 30°C SES TEOM does a poor job of accurately collecting and measuring ammonium nitrate. The experiments in Table III.3 are presented mainly to show that, at very high mass loadings, one can collect an appreciable fraction of the generated ammonium nitrate on a TEOM filter at 30°C. In contrast to ammonium nitrate deposited on the TEOM filter, ammonium nitrate collected on a

PTFE filter and stored in a weighing chamber held between 20 and 23°C, and between 30 and 40% RH remains stable. Specifically, over the course of four days, the filter exposed on 9/5/00 was weighed four times, with each weighing within 2 μg of the mean. To further test the stability of ammonium nitrate on the filter during sampling, we then ventilated this filter with particle-free air for 5 hours at a flow rate of 16.7 LPM. The average filter temperature during this ventilation period was 20.7°C. There was measurable mass loss during ventilation, 45 μg of the 1550 μg initially deposited was lost. This amounts to 2.9% of the deposited aerosol. These experiments demonstrate that one can collect and measure 95% or more of the ammonium nitrate aerosol using filter collection and gravimetric analysis, as long as collection and weighing temperatures are below 25°C.

Table III.3

Date	Collection Time	Partisol - Mass Collected	Partisol-Total Volume	Partisol-Mass Conc.	Average Temp. for Partisol Sample Collection	TEOM – Mass Collected	TEOM-Total Volume	TEOM-Mass Conc.	% Diff. Ref. To Partisol
9/5/00	300 min	1550 μg	5.0 m^3	310 $\mu g/m^3$	26.4° C	306.42 μg	0.9 m^3	340.5 $\mu g/m^3$	+9.8%
9/11/00	300 min	1113 μg	3.0 m^3	371 $\mu g/m^3$	21.4° C	311.97 μg	0.9 m^3	346.6 $\mu g/m^3$	-6.6%

III.2.3 Effects of humidity on TEOM sensors – Evaluation of the SES TEOM system

A number of types of experiments were performed to test and quantify the behavior of the TEOM sensor to changes in relative humidity. We tested the bare TEOM sensor (without a filter), new (unloaded) and heavily loaded filters, the effectiveness of the Nafion dryer at reducing sensitivity to humidity changes, and response of the sensor to changes in humidity while measuring generated aerosol. Initially, tests were performed without any conditioning of the sample flow by the Nafion dryer. These measurements provided the baseline for comparison with later tests.

A typical ramped humidity test occurred as follows: 1) initially relative humidity in the aerosol chamber was very close to zero, and total flow was about 20-30 LPM; 2) three step changes in relative humidity (usually to 30-40%, 65-70%, and 90-95%) were introduced by decreasing dry particle free air flow, and increasing saturated or humid air flow into the chamber; 3) after a period of time at the highest humidity, the procedure was reversed to ramp the humidity back to near zero. Each change in humidity (relative dry and humid flow) was maintained for 60-120 minutes.

III.2.4 Summary of humidity tests with particle free air

Figure III.8a-d illustrates the findings described above for humidity tests with particle free air. Figures III.8a and III.8b show the total mass gained by the TEOM as the humidity in the chamber is increased. These figures correspond to the increasing side of the total mass plots shown in Figures III.9 and III.10. The conclusions from these plots are that more water condenses on the cooler 30°C sensor than on the 50°C sensor, that the presence of the filter

(whether loaded or unloaded) accounts for most of the mass gain, and use of the Nafion dryer to condition the air reduces the apparent mass gain to that shown by the bare sensor. Figures III.8c and III.8d show that this effect is a transient response, and that water vapor which condenses on the filter will evaporate and reach a new equilibrium once the humidity is lowered.

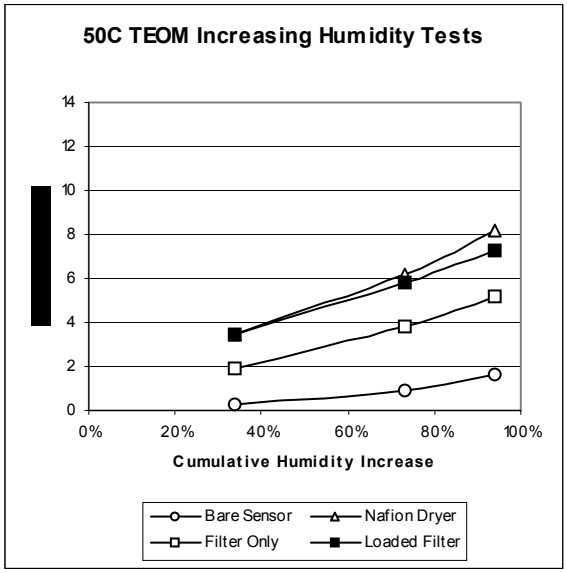

Figure III.8a

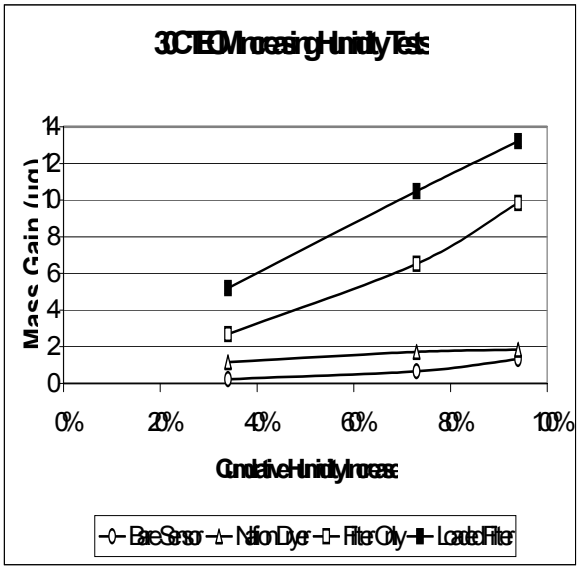

Figure III.8b

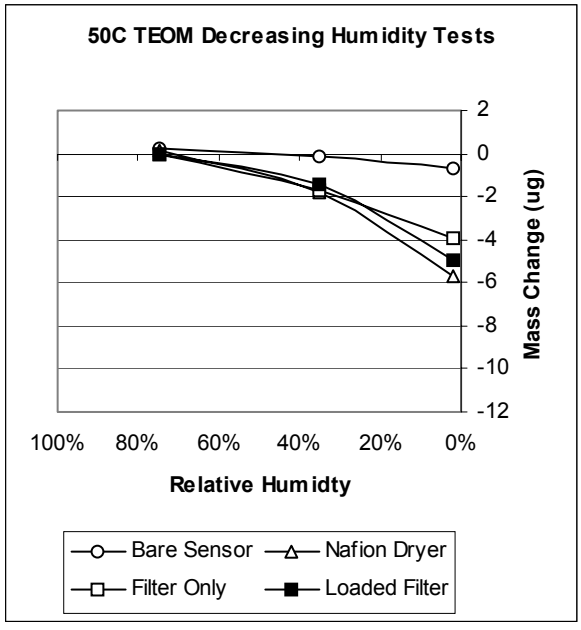

Figure III.8c

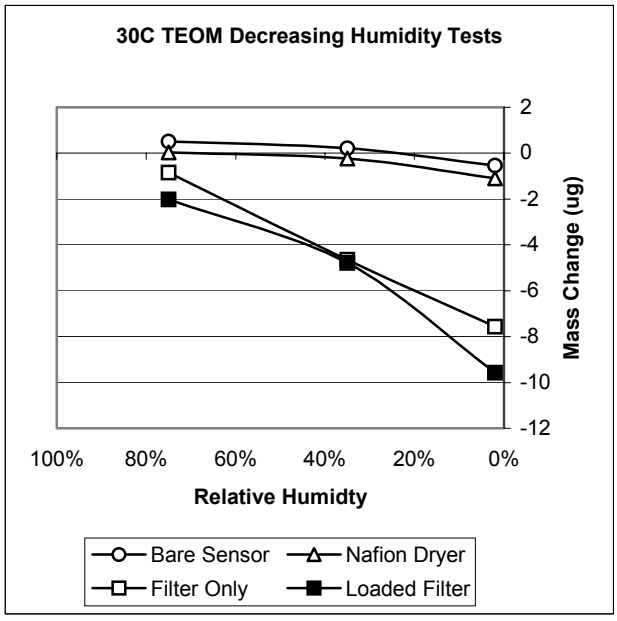

Figure III.8d

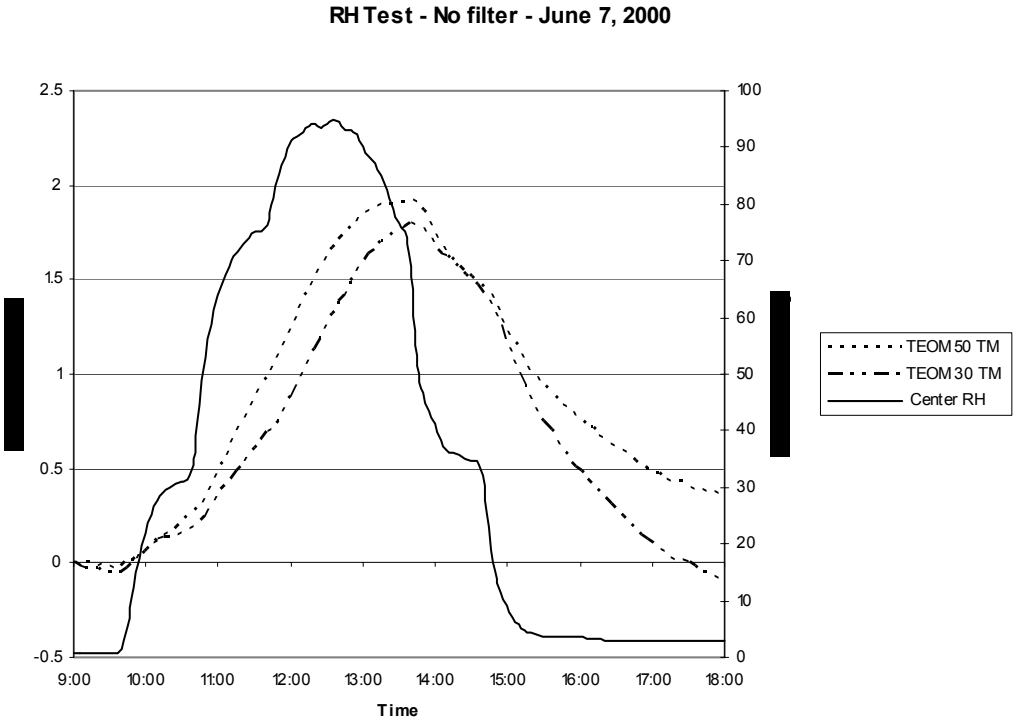

Figure III-9

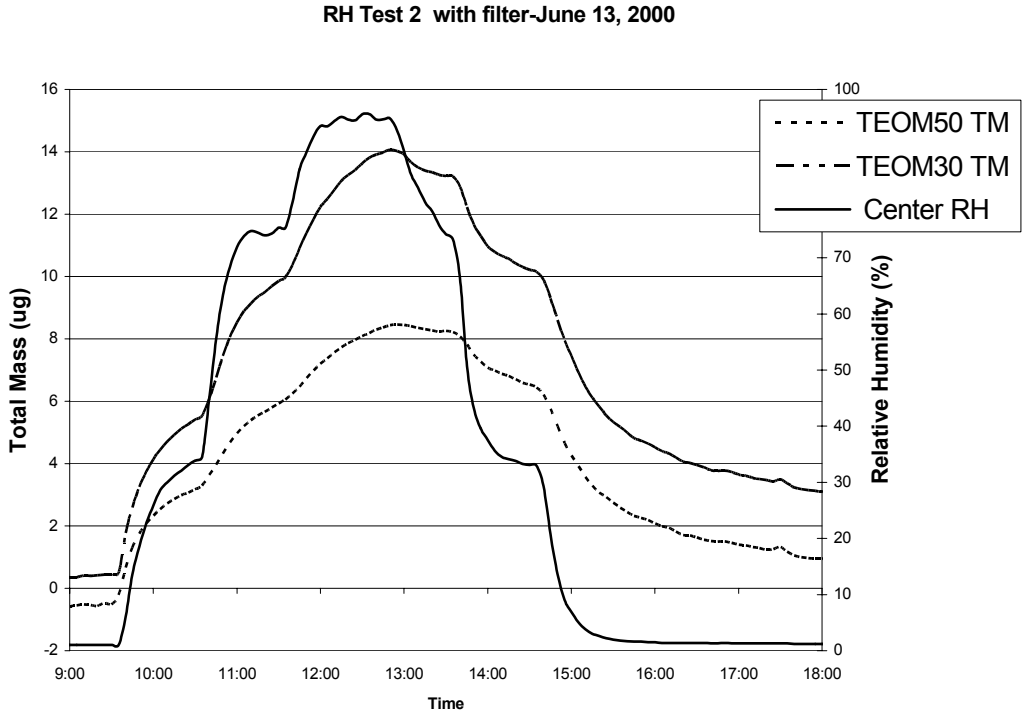

Figure III.10

III.2.5 Ramped humidity during stable particle generation

For measurement of aerosol mass concentration in ambient air, the sensitivity of the TEOM sensor to changes in humidity while measuring aerosol is the critical consideration. We tested this sensitivity with three different synthetic aerosols ($(NH_4)_2SO_4$, $CuSO_4$, and KNO_3) and at two different sample flow rates (1 LPM and 3 LPM). Figures III.11a-c show the response of the mass concentrations reported by the 30°C SES TEOM with the Nafion dryer and the 50°C TEOM without and sample conditioning. There are very large swings in apparent mass concentration by the 50°C TEOM when step changes in humidity occur. These swings are greatly damped and

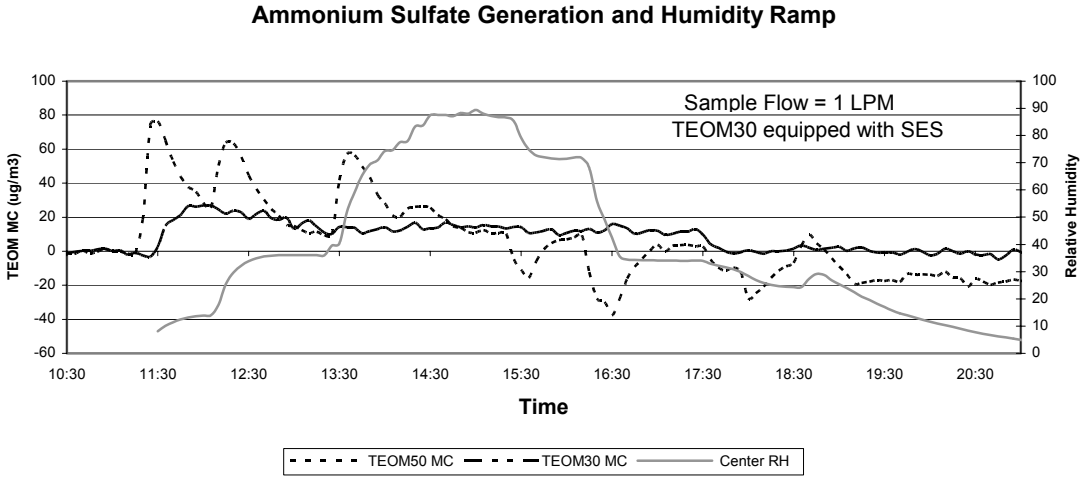

eliminated on occasion by conditioning the sample air with the Nafion dryer. The sensitivity of the 30°C SES TEOM to changes in humidity is lower at a sample flow of 1 LPM than at the usual sample flow rate of 3 LPM.

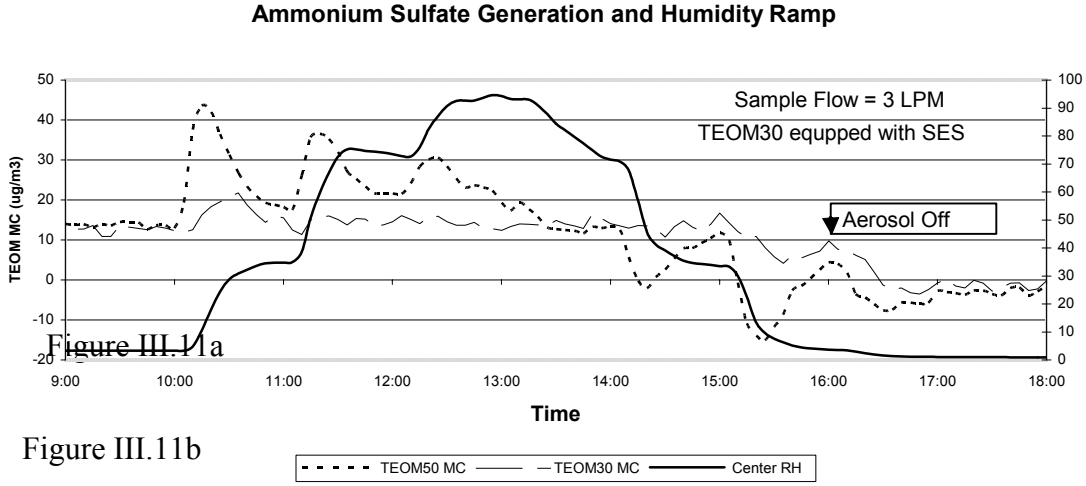

Figure III.11a

Figure III.11b

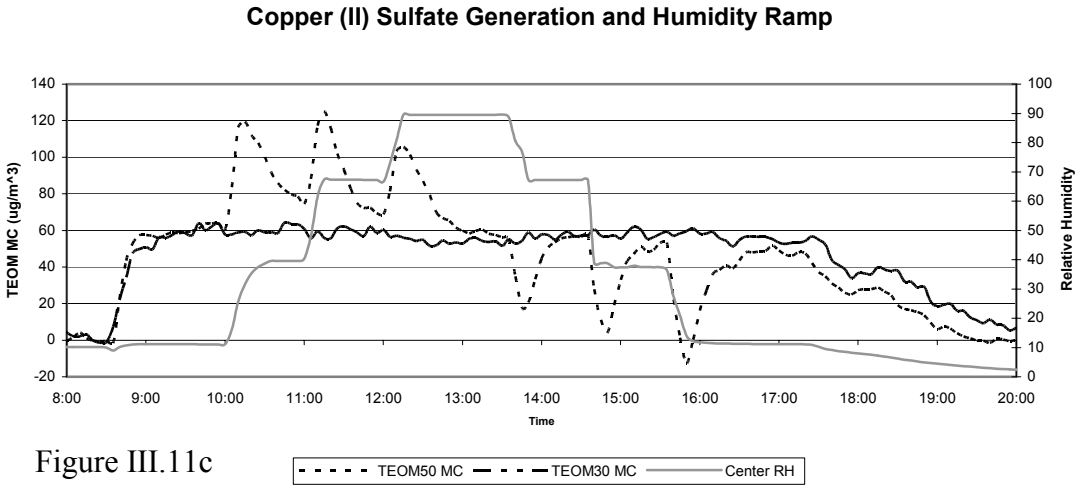

Figure III.11c

This is as expected, since the dryer should more effectively remove the water vapor from the sample stream at the lower flow rate.

III.3 R&P Differential Self Correcting Differential TEOM-ESP

The instrument is based on the direct mass reading and real-time capability of the TEOM system. Downstream from a common size selective inlet and ahead of the TEOM sensor is an electrostatic precipitator (ESP). The ESP is alternately switched on and off. The ESP is on or off for a time period, Δt. Frequency data is collected for the TEOM sensors on a continuous basis. The effective mass is the mass that is calculated from the frequency of the TEOM sensor including all sources that affect the frequency during the given time period. The difference between the effective masses during ESP on and off periods provides a direct measure of the non-volatile and volatile component of particle mass collected during the time interval.

III.3.1 Self-correcting ESP TEOM – Measurement of nonvolatile aerosol

Initial experiments with the ESP TEOM system focused on the intercomparison of aerosol mass concentrations measured by the ESP and SES TEOMS. Nonvolatile aerosols used for these tests were NaCl, $(NH_4)_2SO_4$, and $NaNO_3$. The ESP TEOM used in these tests operated by switching the ESP high voltage on and off every five minutes. Measurements of the sensor oscillation frequency recorded every five seconds were used to calculate the mass of the filter plus aerosol, and the mass concentrations of sampled aerosol. Figure III.12 shows the results for NaCl. The difference in the running average of the TEOM mass concentrations measured with the ESP "off" and "on" is used to calculate the true mass concentration. For a nonvolatile aerosol in conditioned and filtered laboratory air, TEOM mass measurements with ESP "on" should average to zero and the mass measurements from the SES TEOM and ESP TEOM systems to give comparable results. Figure III.12 shows results from such a comparison with good agreement between the systems, with a ratio of reported mass concentrations from the SES TEOM and the ESP TEOM very close to unity.

III.3.2 Self-correcting ESP TEOM – Measurement of a volatile aerosol – NH_4NO_3

As indicated above, ammonium nitrate evaporates from the TEOM filter at a steady rate at 30°C. The evaporation is slow enough that a very large mass concentrations (over 300 μg/m^3 in Table III.4), there is significant buildup of ammonium nitrate solid on the TEOM filter. Since ambient atmospheric mass concentration levels of ammonium nitrate range from near zero to somewhere around 50 μg/m^3, one would like to evaluate the ESP TEOM in this range. However, as one attempts to decrease the concentration of ammonium nitrate to concentration levels below 50 μg/m^3, evaporation from the TEOM filter is significant enough that the SES TEOM does not reliably measure aerosol mass. Figure III.13 shows quite clearly the competing effects of particle deposition and evaporation, and the ability of the ESP TEOM to separate these effects. During the ESP off periods, there is mass deposition on the filter, and evaporation of particles causing simultaneous mass loss. During the ESP on periods, the only significant change of mass on the filter is due to the evaporation of ammonium nitrate, and negative mass concentrations are reported for those periods. During ESP on periods, the ESP and SES TEOMs report similar mass concentrations, but the truest measure of aerosol mass is the ESP calculated mass, which subtracts the ESP on readings from the ESP off readings.

Further confirmation of the ability of the ESP TEOM to accurately measure ammonium nitrate came by comparing the ESP TEOM mass concentration measurements with those measured using the Partisol filter sampler, since our earlier experiments indicated that 95% or more of the ammonium nitrate is captured and retained on the FRM filter, as long as the sampling and storage temperature is kept to 25°C or lower. Two tests were run, with chamber humidities of roughly 5% and 40%. Samples were collected on Partisol filters for four hours, and conditions are summarized in Table III.4. It is quite reasonable that the Partisol mass concentration is lower than the ESP TEOM mass concentration when the average filter temperature for Partisol sample collection is 27.3°C. The apparent 10% under collection by the ESP TEOM for the second run is harder to explain, but is firmly within the uncertainty limits of the combined instruments. For comparison, the mass concentrations calculated from the SES TEOM using the same method as in Table III.3 yield results 25% and 17% lower than the Partisol respectively. The ESP clearly does a better job measuring the volatile ammonium nitrate.

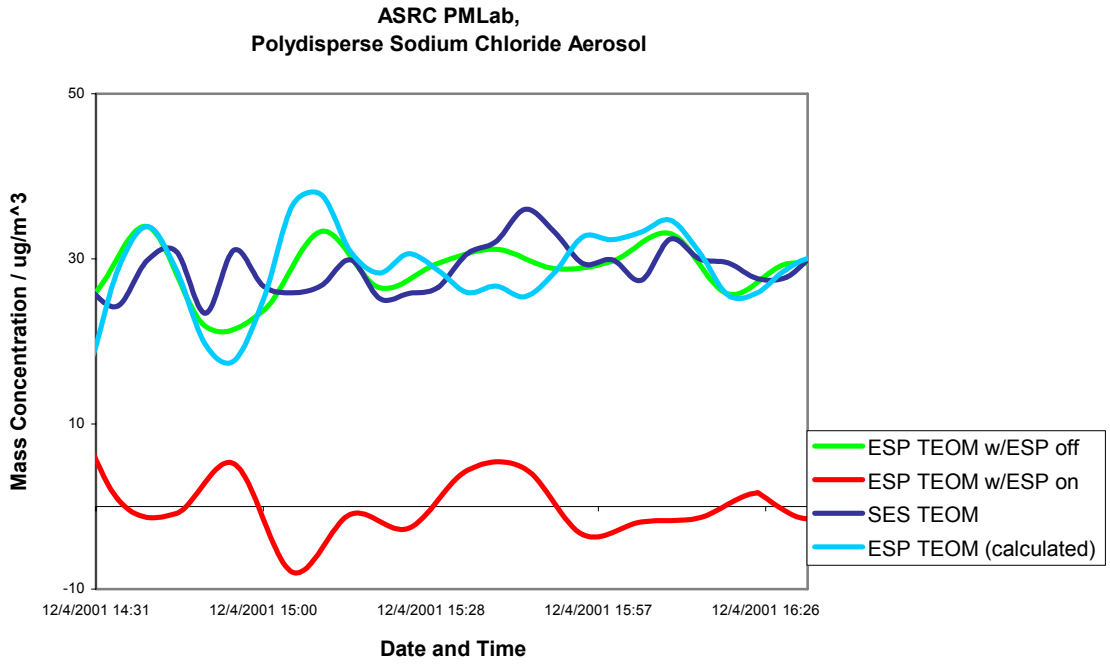

Figure III.12

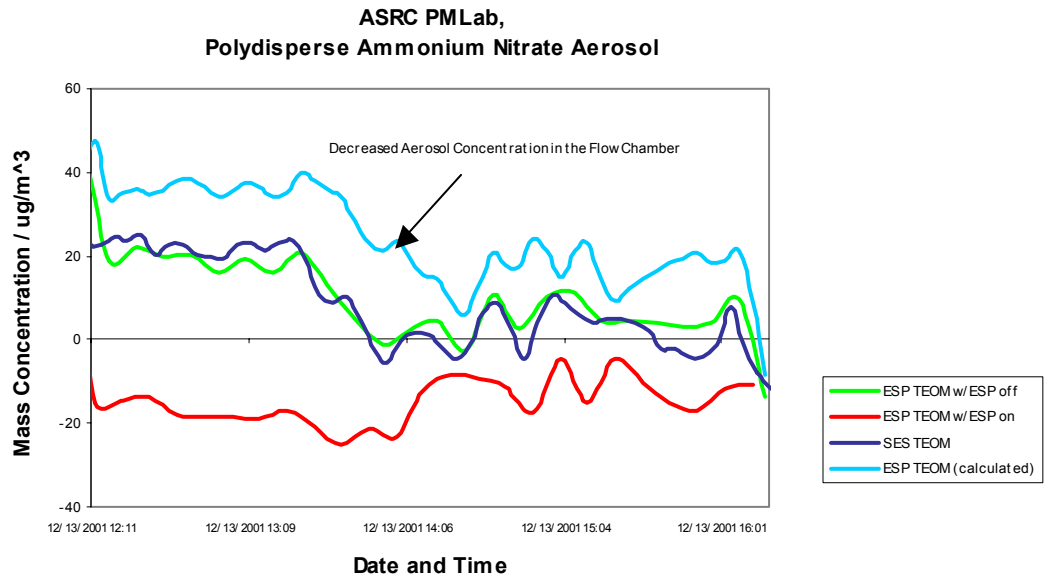

Figure III.13

Table III.4

Date	Collection Time	Partisol - Mass Collected	Partisol-Total Volume	Partisol-Mass Conc.	Average Temp. for Partisol Sample Collection	ESP TEOM-Mass Conc.	RH during collection	% Diff. Ref. To Partisol
1/4/02	240 min	462 µg	4.0 m3	115.5 µg/m^3	27.3° C	122.2 µg/m^3	40 %	+5.8%
1/8/02	240 min	960 µg	4.0 m3	240 µg/m^3	25.0° C	216.4 µg/m^3	5%	-9.8%

III.3.3 Self-correcting ESP TEOM – Measurement of a volatile/nonvolatile mixture

Further tests of the ESP TEOM used a mixed aerosol consisting of a nonvolatile sulfate salt and a volatile dicarboxylic acid. Results for ammonium sulfate (2 g/l) and oxalic acid (6 g/l) are shown in Figure III.14. It appears that re-adsorption of oxalic acid vapor is dominating the ESP on data, so that even with the ESP on, a positive mass concentration is reported. Nearly all of the measured aerosol is ammonium sulfate, even though the mass ratio in the solution used to generate aerosol is 3:1 oxalic acid to ammonium sulfate. This means that there has been a large amount of evaporation of oxalic acid from the mixed particles, so there is a large amount of oxalic acid vapor available to condense on the TEOM filter in this case. Like ammonium sulfate, any oxalic acid that deposits on the TEOM filter evaporates away continuously, so by shutting off aerosol generation and observing the total mass on the TEOM filter, one can observe this phenomenon, and then determine the amount of ammonium sulfate and oxalic acid deposited during aerosol generation.

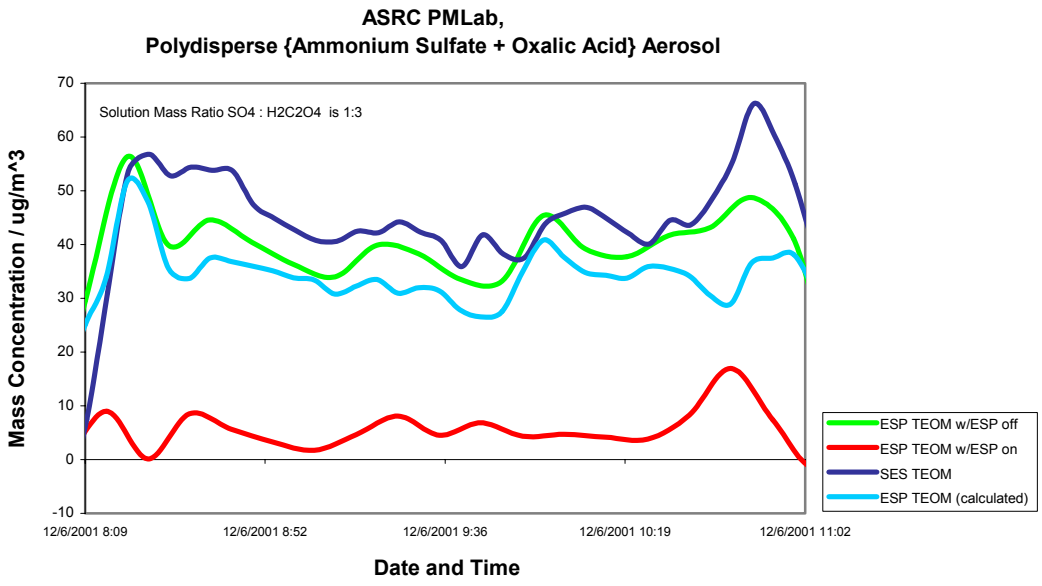

Figure III.14 Mixed Polydisperse Generated Aerosol Mass Concentrations

III.3.4 Efficiency of the ESP at removal of aerosol particles

As a check of the efficiency of the ESP at the removal of generated aerosol particles, an Ultrafine Condensation Particle Counter (TSI Model 3025) was connected at a Tee fitting downstream of the ESP outlet (but before the TEOM sensor). Size distributions of the particles were measured using the Scanning Mobility Particle Sizer (SMPS; TSI Model 3936), which consisted of an Electrostatic Classifier (TSI Model 3080) and a long Differential Mobility Analyzer tube (TSI Model 3081). Total particle counts, and particle size distributions were measured during ESP off and ESP on periods. Removal efficiency tests were done with pure ammonium sulfate and ammonium nitrate aerosols, and with mixtures of ammonium nitrate with oxalic and glutaric acids.

For all test aerosols, particles were observed during ESP on periods. Particle number concentrations with the ESP on ranged from about 6000-20,000 cm^{-3}. These compare with number concentrations of 50,000-400,000 cm^{-3} with the ESP off. This corresponds to particle removal efficiencies of 88-95%. Figure III.15 shows results from tests using a mixed aerosol of ammonium sulfate and oxalic acid with a mass concentration of around 50 $\mu g/m^3$. Comparing the particle number distributions during ESP on and ESP off periods shows that essentially all of the particles not collected by the ESP during its on period are small, less than 100 nm aerodynamic diameter. The median number diameter in the ESP on case is around 25-30 nm, a size range where it is difficult to get very high charging efficiency. These particles contribute less than 2% to the aerosol mass for the aerosol distributions used in these experiments. Since ambient aerosol distributions nearly always have median diameters much larger than the 60-80 nm measured in these tests (Seinfeld and Pandis, 1998), one expects the ESP to remove an even greater fraction of the mass under ambient conditions.
Once again, ammonium nitrate experiments were more challenging than those using ammonium sulfate. Even with aerosol mass concentrations equal to or greater than those used for ammonium sulfate (i.e., around 60 $\mu g/m^3$ as measured by the ESP TEOM), the particle concentrations measured by the CPC and SMPS/CPC combined system are as much as a factor of ten lower for ammonium nitrate compared to ammonium sulfate. It appears that ammonium nitrate suffers much greater inlet and/or evaporation losses in the CPC and SMPS/CPC instruments than ammonium nitrate. Ammonium nitrate exhibits similar behavior to ammonium sulfate and ammonium sulfate/organic acid mixtures based on the relative measurement of number concentration and size distribution with the ESP on and off. That is, not all small particles are removed by the ESP, but the contribution of these "unremoved" particles to the aerosol mass is very low, and in most cases insignificant.

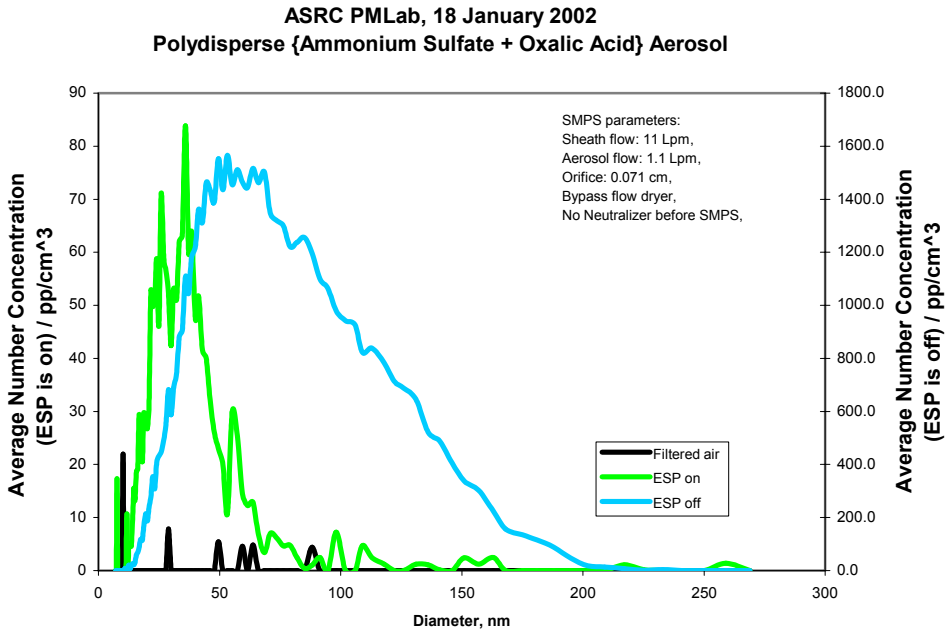

Figure III.15 Mixed Polydisperse Generated Aerosol Number Concentration vs. Diameter

III.3.5 Effects on the ESP TEOM of exposure to NO_2 and SO_2 gases

A final set of tests of the ESP TEOM involved checking for potential interferences caused by gas-to-particle conversions in the ESP. For these tests levels of the precursor pollutant gases NO_2 and SO_2 were introduced into the aerosol chamber along with ammonium sulfate or ammonium nitrate aerosol. SO_2 and NO_2 levels were set to around 50 or 100 ppbv, to simulate typical ambient urban pollution levels. These gas loadings correspond to between 90 and 250 $\mu g/m^3$ of mass, which could deposit on the TEOM filter if converted into particle form by the ESP. Changes in mass concentration as measured by the TEOM were not observed for either test aerosol due to addition of SO_2 or NO_2 . There were some indications of changes (on the order of 10 or 20%) in particle number downstream of the ESP during ESP on periods. As before, the particles measured downstream of the ESP had small diameters, with number median diameters less than 50 nm. In the case of ammonium sulfate aerosol with added NO_2 at 100 ppbv, total number concentration measured by the CPC during ESP on periods dropped slightly from 18,000 to 15,000 cm^{-3}. The opposite effect was observed with the addition of NO_2 during ammonium nitrate generation. In this case, particle number concentration increased from 5500 to 6800 cm^{-3} with the addition of 50 or 100 ppbv of NO_2. The increase in number of particles in this second case is likely due to the shift of the gas/particle equilibrium towards particles caused by the high concentration of gaseous NO_2. There was no evidence in these tests that the presence of the NO_2 or SO_2 gas affected the ESP performance.

III.4 R&P 8400N & S (PM2.5 Nitrate & Sulfate Analyzer)

This automated monitor for semi-continuous measurement of nitrate and sulfate is based on the method of Stolzenburg and Hering (2000). Particles are collected by a humidified impaction process and analyzed in place by flash vaporization. The approach is based on the manual method that has been used for over twenty years to measure the size distribution of sulfate aerosols (Hering and Friedlander, 1982). In the new instrument design, particle collection and analysis have been combined into a single, integrated collection and vaporization cell, allowing the system to be automated. Particles are humidified prior to impaction to eliminate the rebound of particles from the collection surface without the use of grease (Winkler, 1974; Stein et al 1994). Interference from vapors such as nitric acid is minimized by use of a denuder upstream of the humidifier. The flow system is configured such that there are no valves on the aerosol sampling line. Analysis is done by flash-vaporization with quantitative detection of the evolved gases. For sulfate the evolved gases are analyzed for SO_2 and for nitrate the evolved vapors are analyzed for nitrogen oxides.

III.4.1 Status of data processing

- Raw nitrate and sulfate mass concentration data were processed and flagged. 10-min and hourly averages are currently available.
- Inercomparisons between four semi-continuous sulfate instruments and three semi-continuous nitrate instruments were performed.
- 8400S sulfate mass concentrations were compared with those measured by the Aerosol Mass Spectrometer (AMS), Particle into Liquid Sampler with IC (PILS) and a continuous sulfate monitor developed by George Allen at Harvard School of Public Health (HSPH). The intercomparisons yield correlations with slopes ranging from 0.90 to 0.96 and intercepts ranging from 0.06 to 0.50. Correlation coefficient R^2 ranged from 0.88 to 0.93.
- 8400N nitrate mass concentrations were compared with those measured by AMS and PILS, resulting in coefficients close to 0.9, but with quite different slopes indicating that PILS measures higher nitrate concentrations than 8400N monitor, while AMS measures lower concentrations. These differences could be related to PILS denuder issues, AMS collection efficiency, and/or 8400N strip issues.
- Average diurnal patterns for sulfate and nitrate were calculated, using hourly data. Nitrate concentration exhibits a diurnal pattern with a maximum around 8 am. Sulfate concentration does not exhibit a diurnal pattern.
- Frequency distributions of sulfate and nitrate mass concentrations were also calculated.

III.4.2 Data processing (reduction)

If operation parameters were not within an acceptable range, cycle data were removed. Acceptable ranges for various operation parameters are listed in corresponding SOPs. For the data set discussed here, parameters, which sometimes fell outside the acceptable range, were the cell pressure (above half-atmospheric) and the flash time of the collection strips. The flash time were considered acceptable if they were 50-100 msec (8400N) and 10-15 msec (8400S). However, in some cases, even when flash time was outside the acceptable range, but flash time

did change abruptly, and no unusual changes were observed in the measured data, the data were not removed, but were flagged by a V6 flag (see below).

Summer 2001:

Data were adjusted to account for the following:
1) Aqueous standard calibrations (typical calibration charts are shown in Fig. III.16-17),
2) Variations in analyzer audit span, and 3) Blanks

8400S

Date and Time	Filter Blank, µg/m^3
7/12/2001 9:56	0.40
7/12/2001 10:06	0.36
7/27/2001 14:20	0.38
7/27/2001 14:30	0.17
8/3/2001 10:30	0.34
8/3/2001 10:40	0.47
	MDL = 3 * St. Dev = 0.36

8400N

Date and Time	Filter Blank, $\mu g/m^3$	Comments
7/12/2001 12:51	0.08	
7/12/2001 13:01	0.10	
7/27/2001 12:10	0.39 [a]	
7/27/2001 12:20	0.31 [a]	
7/27/2001 15:00	0.43 [a]	
7/27/2001 15:10	0.37 [a]	
7/27/2001 15:24	0.16	Carbon denuder was replaced
7/27/2001 15:34	0.14	
8/3/2001 11:00	0.17	
8/3/2001 11:10	0.22	
	MDL = 3 * St. Dev = 0.15	

[a] – these blanks were not used to calculate the MDL.

For both data sets, blanks used to calculate the MDL were obtained during "blank tests", when filter was inserted in a sampling line. During one of the 8400N blank tests it was discovered that a carbon denuder (which removes gaseous interferences) is either saturated or very close to being saturated. Denuder was replaced as soon as the problem was discovered. Although, high filter blanks measured on 07/27/01 indicate that during some part of the period of 07/12/01-07/27/01 denuders may not have removed all the gaseous interferences with 100% efficiency, it does not warrant making all the data obtained during this period, invalid.

Winter 2004:

The Instrument deployment period covered the time period 01/08/04-02/06/04

In-field QA procedures and checks included daily checks of operation parameters, necessary adjustments; bi-daily gas analyzer audits, weekly (sometimes more often) flow audits, aqueous standards calibrations, dynamic filter blanks; periodic leak tests, cyclone cleaning, inlet orifice cleaning, flow filters replacement; 8400N molybdenum converter efficiency test performed shortly before the campaign.

Raw nitrate and sulfate mass concentration data were processed and submitted to the data bank. Ten-minute and hourly averages are currently available. If operation parameters were not within an acceptable range, cycle data were removed. Acceptable ranges for various operation parameters are listed in the corresponding SOPs.

Data were adjusted to account for the following:

1. Aqueous standard calibrations
2. Variations in analyzer audit span
3. Blanks: for 8400S dynamic blank is 1.04 $\mu g/m^3$, for 8400N dynamic blank is 1.52 $\mu g/m^3$ (before 1/20/04 19:00, when the analyzer cell was cleaned and rebuilt) and 0.90 $\mu g/m^3$.

LODs (calculated as 3*dynamic blank) is 1.41$\mu g/m^3$ for 8400S, 2.49 $\mu g/m^3$ for 8400N before 1/20/04 19:00 and 1.79 $\mu g/m^3$ for 8400N after 1/20/04 19:00.

Data were flagged (next section will describe this process in more details)
In this final report, data summary and statistics were obtained using the following data: 10 min cycles, sampling period: 06/30/01 – 08/03/01 for the summer 2001 and 01/08/04-02/06/04 for the Winter 2004 field campaign respectively:

III.4.3 Data flagging

1. For flagging of the 8400N and 8400S data, the following flags from the NARSTO Data Qualification Flag set were used

V0	Valid Value	All valid 10-min data, that are not qualified in any way
V1	Valid Value, but wholly or partially below detection limit [a]	For all valid 10-min data, where the mass concentration during this cycle is below the detection limit
V6	Valid value, but qualified due to non-standard sampling conditions	For data collected under conditions outside the range specified in SOP or an instrument operating manual, e.g. cell pressure is slightly above half-atmospheric values, strip flash time is different than specified in SOP, but the difference is "acceptable"
M1	Missing Value, because no value available	Value missing. Reasons: 1) the instrument memory failure, 2)the instrument was not sampling, either because calibrations or maintenance procedures were performed, or due to a NiCr strip failure of the 8400N and strip-failure-related procedures
M2	Missing Value, because invalidated by Originator	Value invalidated, because operating parameters were outside "the acceptable range"

[a] - The detection limit was calculated as MDL = 3 * standard deviation of the average blank mass concentration. All data values below the detection limit were left as they were and flagged with V1 (data were not set to value of MDL). If data qualified to be flagged with both the V6 and V1 flags, V6 was considered to be more important, and V1 was not used.

2. Data Flags Statistics

Summer 2001:

Flag	**8400S**	**8400N**
V0	4486 (89.0%)	3298 (65.6%)
V1	274 (5.4%)	1151 (22.9%)
V6	10 (0.2%)	83 (1.6%)
M1	171 (3.4%)	479 (9.5%)
M2	99 (2.0%)	17 (0.3%)
Maximum possible data points	5040 (100%)	5028[a] (100%)

[a] – at the beginning of the campaign, cycle time 8400N monitor was accidentally set to 10 min 08 sec, instead of 10 min. The cycle time was reset to 10 min on 07/07/01.

Winter 2004:

III.4.4 Data summary

Summer 2001:

Data Summary (10 min data). All mass concentrations in μg/m^3

	8400S	**8400N**
Minimum	-0.41	-0.10
25%	1.12	0.14
Median	2.70	0.32
Mean	3.82	0.53
75%	5.64	0.68
Maximum	20.91	5.87

Winter 2004:

Data Summary (10-min data). All mass concentrations in μg/m^3

	8400S	**8400N**
Minimum	-0.96	-1.03
25%	1.32	0.14
Median	2.39	0.87
Mean	2.68	1.5
75%	3.71	2.23
Maximum	11.80	9.32

III.4.5 Data completeness

Summer 2001:

	8400S	**8400N**
Maximum possible cycles	5040	5028[a]
Completed cycles	4770 (94.6%)	4532 (90.0%)
Missed/rejected cycles	270 (5.4%)	496 (10%)
Cycles missed due to • Routine maintenance • Instrument failures • Other	 124 32 114	 97 378[b] + 12[c] 12

[a] – at the beginning of the campaign, cycle time 8400N monitor was accidentally set to 10 min 08 sec, instead of 10 min. The cycle time was reset to 10 min on 07/07/01
[b] – cycles were missed or rejected due to NiCr strip failures
[c] – cycles were missed due to data loss from the instrument memory

Winter 2004:

Data completeness (ratio of valid data "samples" to maximum possible data "samples") was calculated using hourly averages. For the 8400N instrument, the completeness is 86%, and for the 8400S instrument, completeness is 83%. Scheduled maintenance, calibrations, audits, dynamic blanks and emergency repairs account for all "missing" data.

III.4.6 QA and QC experiments

- In-field daily checks of operation parameters, necessary adjustments;
- In-field bi-weekly and monthly maintenance procedures and checks;
- In-field comparisons of raw data (8400 monitors, AMS, PILS);
- Data adjustment to in-field aqueous standards calibrations, gas analyzer audits, blanks;
- Comparison of processed data (8400 monitors, AMS, PILS, Continuous Sulfate Monitor);
- ASRC PMLab tests and intercomparisons. For more details on aerosol generation, equilibration and reference measurements, refer to Appendix A.

1. Nitrate and sulfate aerosols were generated in the ASRC PMLab. The aerosols were than introduced in a slow flow chamber. Residence time of aerosol in a flow chamber was about 5-15 min (depending on a flow rate).
2. Chemical compounds used to generate aerosol, included ammonium nitrate, sodium nitrate, ammonium sulfate, ammonium hydrogen sulfate, and sodium sulfate. Generated sulfate aerosol contained organic acids (oxalic or glutaric). Presence of organic acids is a necessary condition for efficient operation of the 8400S monitor.
3. The aerosol mass concentrations were simultaneously measured using 8400N or 8400S monitor and SES TEOM. For some experiments another 8400N monitor, the ESP TEOM, SMPS, PILS and AMS instruments were operated to provide additional mass concentration measurements. 8400 monitors performance is described in terms of 8400/TEOM mass concentration ratio: the higher the ratio, the better the 8400 performance.

4. The mass concentration measurements were conducted using various
   - chamber relative humidities,
   - aerosol concentrations,
   - mass fractions of organic component in aerosol-generating solution (for sulfate aerosols)
5. 8400N tests (see Fig. III.18-20):
   - an agreement between the 8400N, the TEOM and the SMPS measurements improves when test aerosol has the mass median aerodynamic diameter 250 nm or higher (Fig. III.18, 19).
   - the best agreement between the 8400N and the reference instruments was obtained with sodium nitrate (nonvolatile salt) aerosol when the flash strip of the 8400N monitor was pre-exposed to the ambient aerosol (Fig. III-19, 20).
   - relative humidity did not seem to significantly affect the performance of the 8400N
   - an increase of aerosol concentration in the chamber did not affect the 8400N performance as long as the mass concentration stays within the instrument calibration range (12-15 $\mu g/m^3$ for a 10-min sampling cycle). For higher mass concentrations, the 8400N/TEOM mass ratio decreases.
6. 8400S tests (see Fig. III.21-23)
   - 8400S tests were conducted with test aerosol with the mass median aerodynamic diameter below 200 nm, which may have affected an agreement between the 8400S and the reference instruments. Experiments with larger size aerosol are currently underway in the ASRC PMLab.
   - using results of the previous tests: increase of relative humidity in the chamber did not affect the 8400S performance with NH_4HSO_4, but in $(NH_4)_2SO_4$ experiments lead to an apparent decrease in 8400S/SES TEOM mass concentration ratio (see Fig.III.21). An increase in the aerosol mass concentration in the chamber lead to a worse agreement between the 8400S and a TEOM (Fig.III.22), effect of an organic fraction in an aerosol-generating solution is shown in Fig.III.23.
7. The 8400N monitor (which was deployed in Queens) was operated side by side with another 8400N monitor, sampling ambient aerosol. A comparison plot is shown in Fig. III.24.
8. The same experiment was conducted with two 8400S monitors (see Fig. III.25).

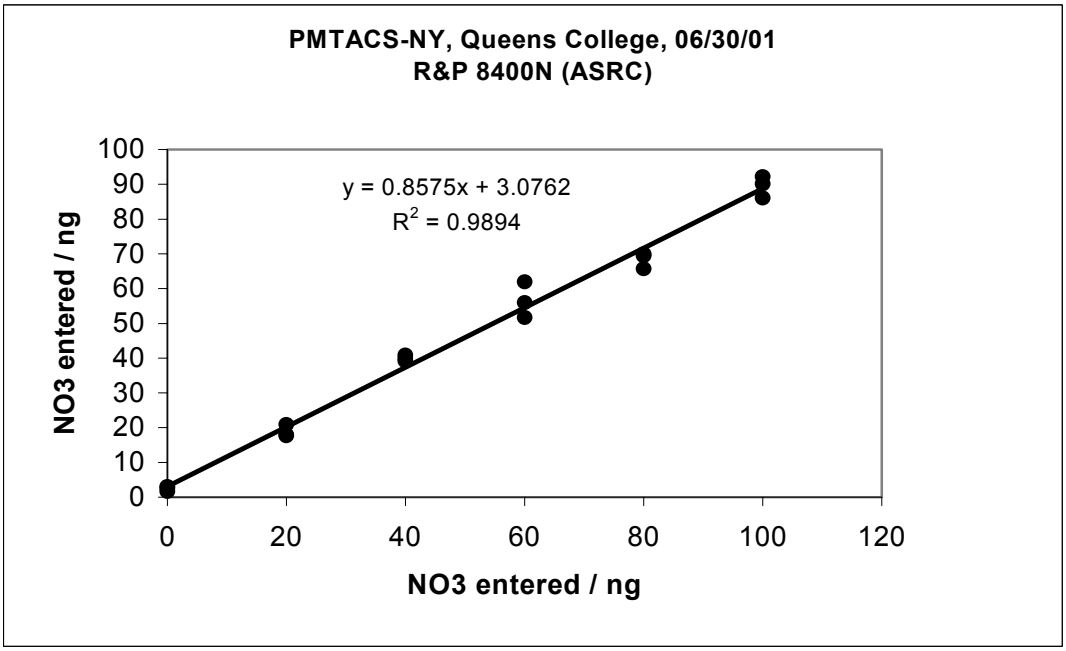

Figure III.16. Aqueous standards calibration chart for the R&P 8400N monitor.

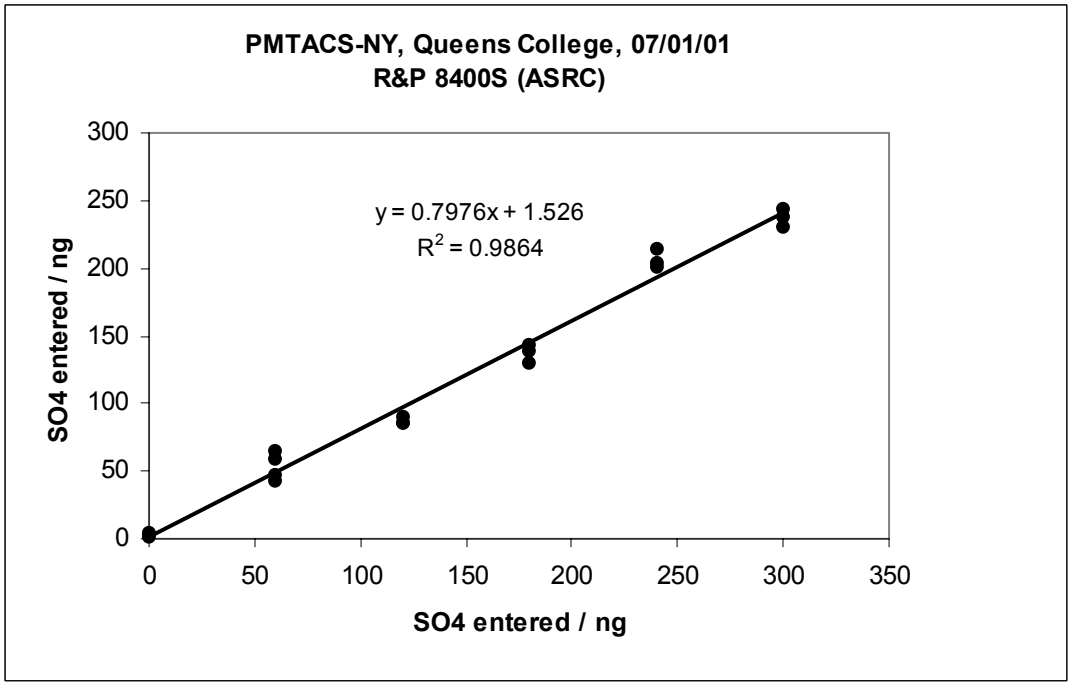

Figure III.17. Aqueous standards calibration chart for the R&P 8400S monitor.

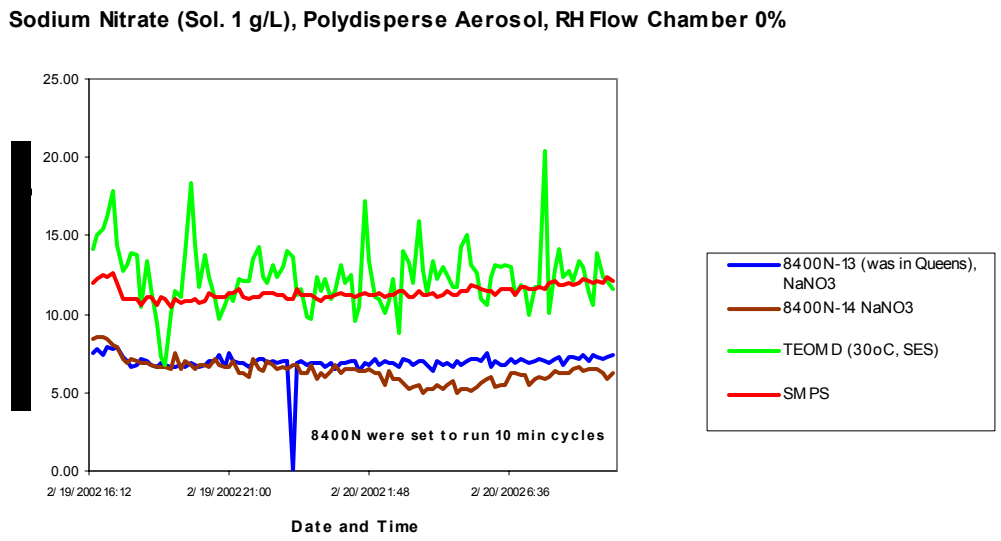

Figure III.18. PMLab measurements of $NaNO_3$ aerosol with the average mass median aerodynamic diameter 114 nm. 8400N strips were pre-exposed to ambient aerosol.

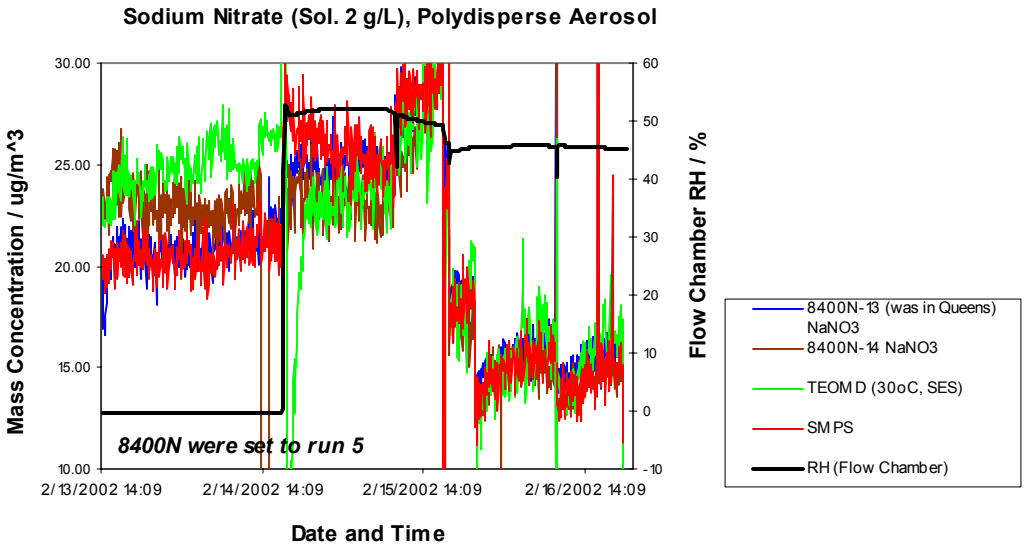

Figure III.19.PMLab measurements of $NaNO_3$ aerosol with the mass median aerodynamic diameter 240-280 nm. 8400N strips were pre-exposed to ambient aerosol.

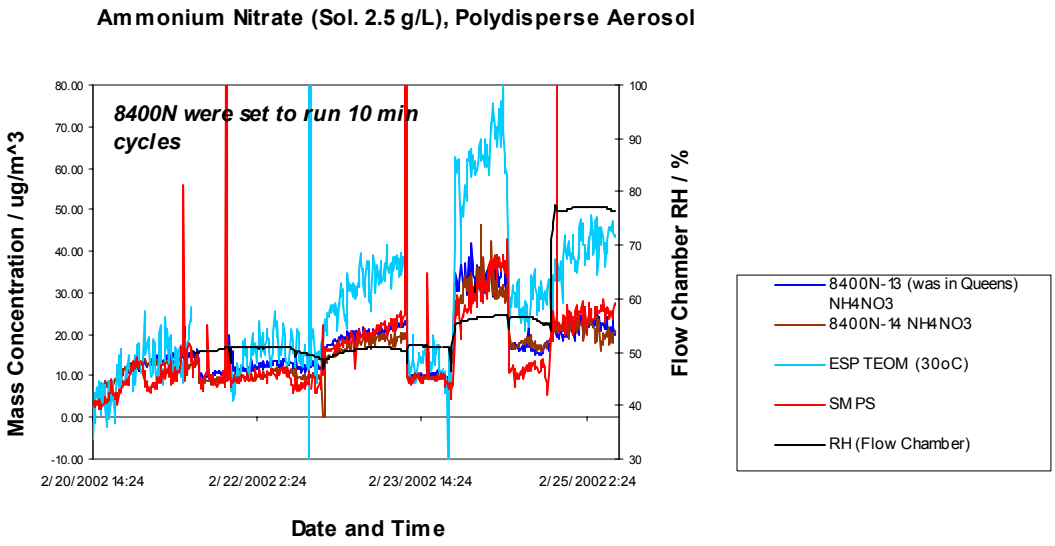

Figure III.20. PMLab measurements of NH_4NO_3 aerosol with the mass median aerodynamic diameter 290-310 nm. 8400N strips were pre-exposed to ambient aerosol.

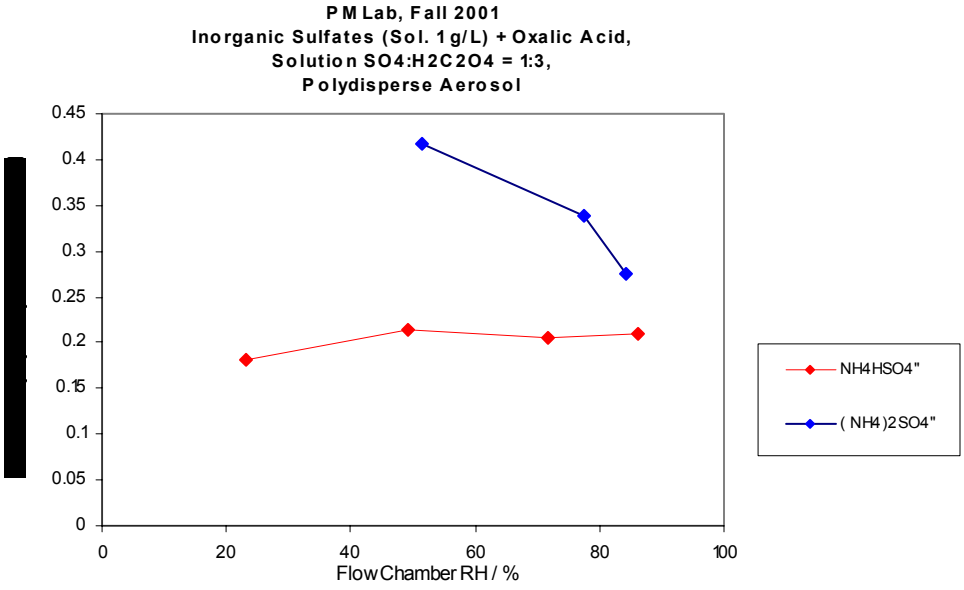

Figure III.21. Summary of 8400S humidity tests.

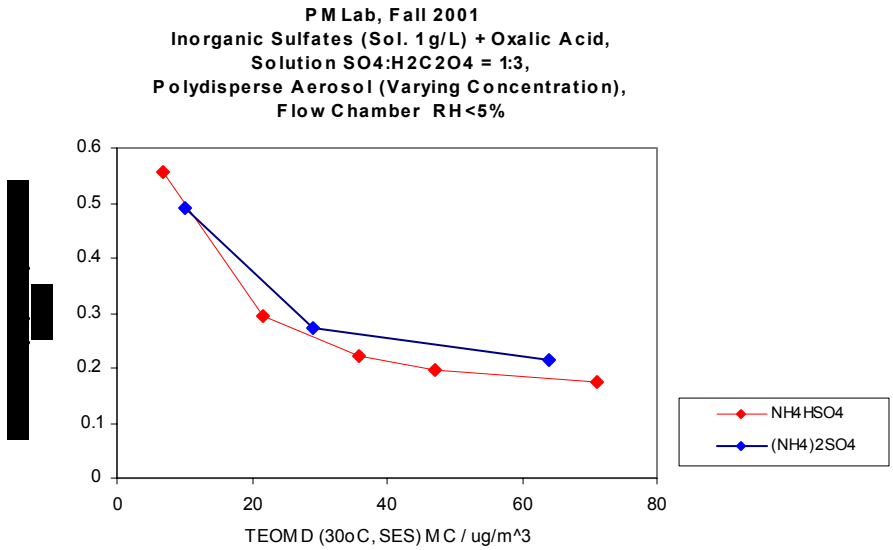

Figure III.22. Summary of 8400S "changing aerosol mass concentration" tests.

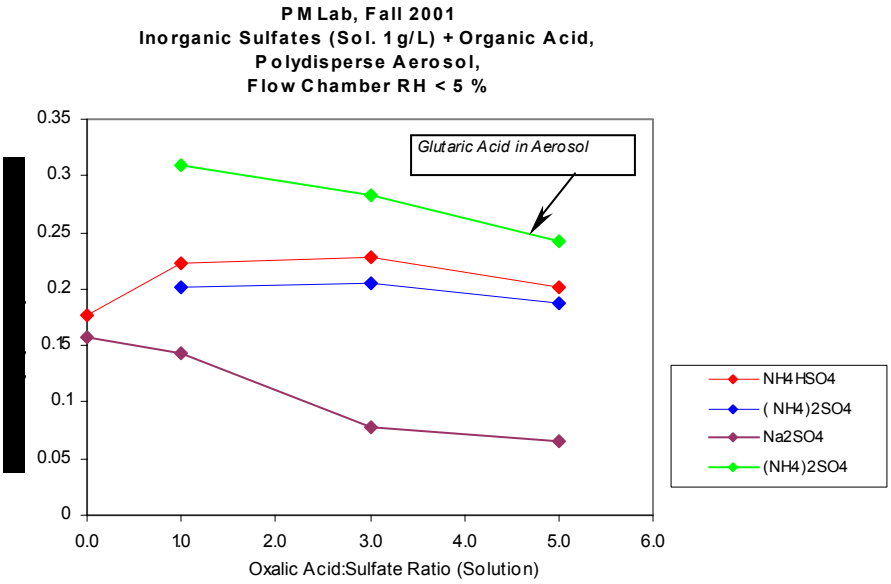

Figure III.23. Summary of 8400S "organic fraction" tests.

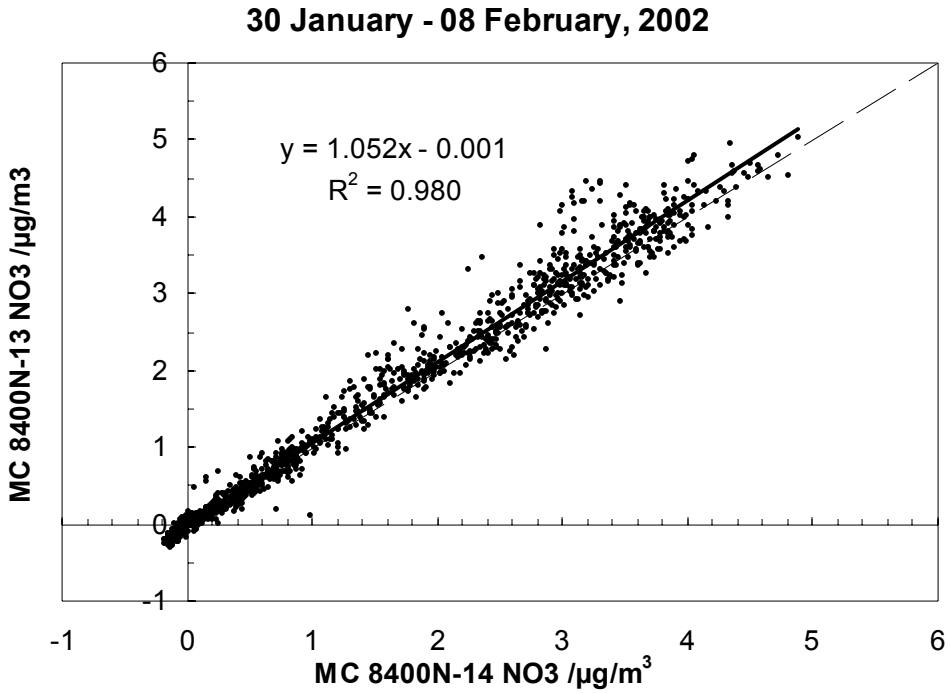

Figure III.24. Comparison of two 8400N monitors sampling ambient aerosol (8400N-13 was used in Queens).

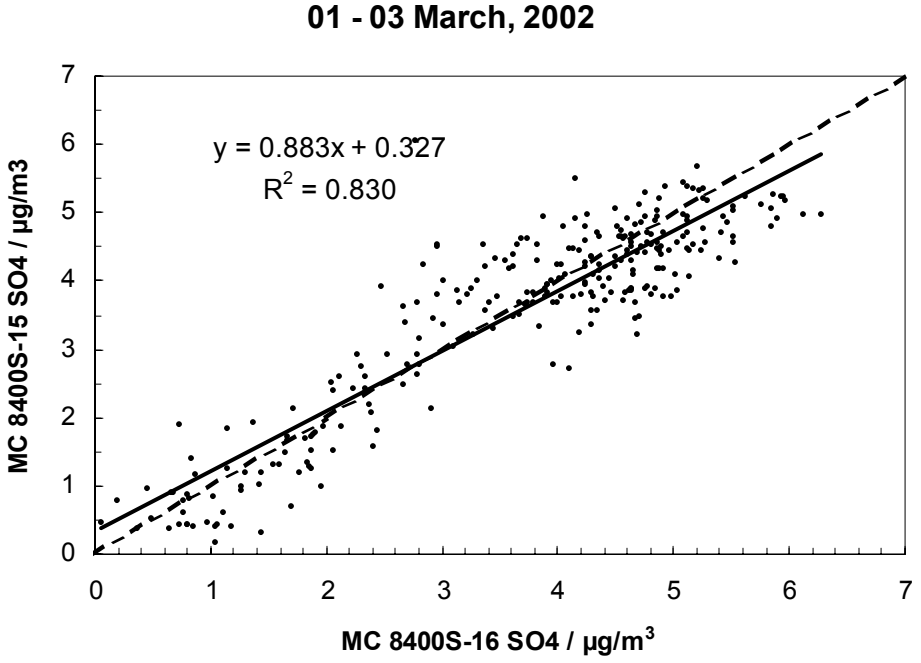

Figure III.25. Comparison of two 8400S monitors sampling ambient aerosol (8400S-15 was used in Queens).

III.4.7 Major problems with 8400 monitors field operation

- 8400N – short lifetime of a NiChrome collection strip. This issue is currently solved: R&P now uses a new strip designs. Experiments, conducted in the ASRC PMLab showed that those strips last much longer.

- 8400S monitor had no major operational problems during Summer 2001 field campaign.

III.5 Aerosol Mass Spectrometer (Aerodyne Research, Inc. (AMS))

Ambient aerosol particles in the size range 0.05 up to 1 micrometers are focused into a high vacuum system. Particle velocity measurements determine particle aerodynamic diameter. Volatile and semi-volatile chemical components are thermally vaporized and detected via electron impact ionization quadrupole mass spectrometry. Detection sensitivity for the base system corresponds to aerosol loading of 0.1 to 1 microgram/m^3, depending on the molecular mass interferences and background levels.

III.5.1 Status of AMS data processing

<u>Summer 2001</u>:

- Mass Spectrum Mode raw data are processed, leading to 10-min averages of sulfate, nitrate, ammonium, chloride and total organics aerosol mass concentration. 1-hour, 6-hour and daily averages are also available.
- Minimum Detection Limits for all five species groups have been determined for every 10-min interval. Data have been flagged.
- Comparison of AMS data with TEOM total mass data: On average 67% of the total mass (TEOM) was identified with AMS. 11% of total mass was assigned to particle water. Particle water was calculated from AMS total ion current signal, corrected for water vapor using local relative humidity and air temperature data. The correlation of the AMS total mass signal (including particle water) with the TEOM signal is pretty good (MC_{AMS}= 0.69 * MC_{TEOM} – 0.24 μg/m^3, R=0.95) and much better than the correlation of the uncorrected AMS signal with TEOM.
- Intercomparison of 4 semi-continuous sulfate instruments yield to very good correlations between these instruments with slopes close to 1, intercepts close to 0 and correlation coefficients of 0.96 and above.
- Intercomparison of 3 semi-continuous nitrate instruments show larger differences between these instruments. It is not yet resolved, which of these instruments (if any) gives the right concentrations. PILS had some denuder issues, R&P 8400N shows strange behavior in the laboratory.
- Comparison of AMS (and other semi-continuous sulfate instruments) with 6-hour and 24-hour filter data show pretty good correlations, but the AMS only ‘sees’ about 80% of the filter sulfate. Most likely explanation for the difference is sulfate accumulation on the filters by gas-to-particle conversion during sampling.

- Average diurnal patterns of sulfate, nitrate, ammonium, chloride, total organics and total non refractory mass concentrations have been calculated: Only nitrate shows a clear diurnal pattern with a maximum during early morning hours.
- AMS size distribution data have been averaged for 2-hour intervals for sulfate, nitrate, total organics and their fragments (mass 30, 46 amu (nitrate); 48, 64, 80 amu (sulfate); 55, 57, 69, 71 amu (organics)). More detailed investigation of events like particle production events or 'large particle events' are in process. Investigation of information derived from the fraction ratios is in progress as well.
- Average diurnal patterns of AMS size distribution data have been calculated and investigated for sulfate, nitrate and total organics (and their fractions).

Winter 2004:

- Minimum Detection Limits for all five species groups have been determined for every 10-min interval. Data have been flagged. Detection Limits for organics and chloride are quite high compared to the detection limits for sulfate, ammonium and nitrate. This is due to the contribution of noise from a large number of low signal-to-noise mass lines that all contribute to the total signal of the respective species.
- Beam Width Probe (BWP) data was evaluated. Leading to the result that particles were not lost by beam broadening.
- To determine collection efficiency (CE) for AMS data, AMS sulfate mass concentrations were compared to the Particle-into-liquid sampler with IC (PILS-IC) sulfate mass concentration for the period January 23rd until January 31st 2004. From this comparison a CE of 0.42 was determined. This factor was applied to all other species.
- Intercomparison of 2 semi-continuous sulfate instruments yield to very good correlations between these instruments with slopes close to 1, and correlation coefficient of 0.8.
- Intercomparisons of 2 semi-continuous nitrate instruments show larger differences between these instruments. It seems that for some periods a collection efficiency of 0.42 for nitrate is too low. Collection efficiency varies for example with the shape and size of the particles and the compound. Further research is necessary.
- Average diurnal patterns of sulfate, nitrate, ammonium, chloride and organics mass concentrations have been calculated: All species show a clear diurnal pattern.

III.5.2 Data summary

Summer 2001:

Statistical Summary for the whole campaign (all data in µg/m^3):

Species	Sulfate	Nitrate	Ammonium	Organics
Minimum	0.049	-0.040	-0.739	0.456
25 % Percentile	1.221	0.084	0.334	1.805
Median	2.563	0.177	0.850	2.718
75 % Percentile	5.478	0.390	1.770	3.996
Maximum	53.165 (23.077)*	4.511	7.193	28.653
Mean	3.695	0.346	1.174	3.071

* 53.165 µg/m^3: Maximum value during huge sulfate event on first day of AMS deployment. At this time only R&P 8400S was operating and measured much lower sulfate concentrations. 23.077 µg/m^3: Maximum sulfate concentration without this event on the first day (6/30).

Winter 2004:

Statistical Summary for the whole campaign (all data in µg/m^3):

Species	Sulfate	Nitrate	Ammonium	Organics
Minimum	0.34	0.06	- 0.08	- 0.55
Median	1.99	1.54	1.16	5.20
Maximum	9.74	19.61	9.11	64.95
Mean	2.41	2.58	1.70	5.98

III.5.3 Data completeness

Summer 2001:

Deployment of AMS: June 30, 15:00 - August 05, 18:00

10 min averaging intervals → during deployment 5202 possible intervals

Number of complete cycles:	4758	91.46 %
Number of incomplete cycles:	153	2.94 %
Incomplete, > 75 %:	99	1.90 %
Incomplete, < 75 %:	54	1.04 %
Number of missing cycles:	291	5.59 %
Number of useable cycles:	**4857**	**93.37 %**

Number of lost cycles:	**345**	**6.63 %**
Reasons:		
Calibration:	76	22.03 %
Computer Crash:	257	74.49 %
Maintenance:	6	1.74 %
Others:	6	1.74 %

Winter 2004:

Deployment of AMS: January 9, 09:00 - February 06, 09:00

10 min averaging intervals → during deployment 4032 possible intervals

Number of measured cycles:	**3920**	**97 %**
Number of lost cycles:	**112**	**3 %**
Reasons:		
Calibration:	73	65 %
Computer Crash:	13	12 %
Maintenance:	19	17 %
Others:	7	6 %

III.5.4 Data flagging

For flagging of the AMS MS data parts of the NARSTO Data Qualification Flag set was used. The following flags have been used in the PMTACS-NY 2001 dataset:

V0	Valid Value	All valid 10-min data, that are not qualified in any way
V1	Valid Value, but wholly or partially below detection limit	For all valid 10-min data, where the average during this interval is below the detection limit, determined for this interval
V2	Valid estimated Value	All valid 10-min data, where the actual sampling and averaging time is below 7.5 min but not below 5 min
V6	Valid value, but qualified due to non-standard sampling conditions	Used for one data point, where the heater was off during part of the 10-min interval
M1	Missing Value, because no value available	Value missing, because instrument was not sampling – either due to a computer crash or because calibration or maintenance was performed
M2	Missing Value, because invalidated by Originator	Value invalidated, because instrument was sampling less than 5 min during 10 min interval

Detection Limit (V1): The detection limit was determined for every 10 min interval for which data are available (not M1). The detection limit was calculated as DL = 3 * standard deviation of the blank (background, measured at the masses of the fractions of the actual species), calculated for the 12 background measurements (2-hour interval) closest to the actual interval. All data

values below the corresponding detection limits were left as they are and flagged with V1 (data were not set to value of MDL).

Incomplete Sampling Periods (V2, M2): Data were saved every 10 min as 10 min averages. If maintenance or calibration procedures were performed during part of a 10 min interval or if the instrument was started after a computer crash during a 10 min interval, the data saved at the end of this interval were collected over an interval of less than 10 min. If collection time was more than 75 % (7.5 min) the data were flagged as 'V0'. For collection times from 5 to 7.5 min they were flagged as 'V2'. Data with collection times below 50 % (5 min) were invalidated (-9999.99) and flagged with 'M2'.

Non-standard sampling conditions (V6): One 10-min interval was flagged with 'V6', because the heater (that evaporates the particles) was turned off during parts of this interval. This happened when Children from a nearby High School were visiting the trailers.

Missing Data (M1): Data were missing when the instrument was not sampling and measuring. This was mostly due to computer crash or during maintenance or calibration times.

Flagging summary for all species:

Summer 2001:

Fla	Sulfate	Nitrate	Ammonium	Chloride	Organics
V0	4853 (93.3%)	4678 (89.9%)	3952 (76.0%)	2344 (45.1%)	4711 (90.6%)
V1	3 (0.06 %)	178 (3.42%)	906 (17.4%)	2522 (48.5%)	145 (2.79%)
V2	35 (0.67%)	35 (0.67%)	35 (0.67%)	35 (0.67%)	35 (0.67%)
V6	1 (0.02%)	1 (0.02%)	1 (0.02%)	1 (0.02%)	1 (0.02%)
M1	291 (5.59%)	292 (5.61%)	291 (5.59%)	291 (5.59%)	291 (5.59%)
M2	19 (0.37%)	19 (0.37%)	19 (0.37%)	19 (0.37%)	19 (0.37%)
Data Points	5202 (100%)	5202 (100%)	5202 (100%)	5202 (100%)	5202 (100%)

Winter 2004:

Flag	Sulfate	Nitrate	Ammonium	Chloride	Organics
V0	3800 (97.0%)	3800 (97.0%)	3181 (81.2%)	150 (3.8%)	2156 (55.0%)
V1	0 (0%)	0 (0%)	619 (15.8%)	3650 (93.2%)	1644 (42.0%)
M1	117 (3.0%)	117 (3.0%)	117 (3.0%)	117 (3.0%)	117 (3.0%)
Data Points	3917 (100%)	3917 (100%)	3917 (100%)	3917 (100%)	3917 (100%)

III.5.5 Quality assurance experiments

Summer 2001:

- Frequent calibration of the multiplier and the ionization and transmission efficiency with single ions and laboratory particles during the field campaign
- Continuous Monitoring of inlet flow and multiplier performance for correction of data
- In-field comparison of raw data of AMS with R&P 8400N, R&P 8400S and PILS
- Comparison of processed data of AMS with R&P 8400N, R&P8400S, PILS, HSPH continuous sulfate monitor, TEOM and filter data

Winter 2004:

- Frequent calibration of the multiplier and the ionization and transmission efficiency with single ions and laboratory particles during the field campaign
- Continuous Monitoring of inlet flow and multiplier performance for correction of data
- In-field comparison of raw data of AMS with PILS-IC
- Comparison of processed data of AMS with R&P 8400N, R&P 8400S, PILS-IC, TEOM and OC Sunset Laboratory data

III.5.6 Major problems in AMS field operation:

Summer 2001:

- Frequent and randomly occurring Computer Crashes of the Data Acquisition Computer caused loss of 75% of the loosed data and made frequent reboots of the computer necessary
- During the first two weeks the ionization and transmission efficiency calibration was done with 200 nm particles due to limitations of the equipment. Therefore these calibrations have higher uncertainties than the later ones with 350 nm particles. No trend was found for the IE value measured before the campaign and during the campaign in the last 4 weeks, therefore the average IE value was used for the whole campaign.
- For a period of 48 hours the inlet flow was lower by 5% due to a misaligned pinhole. The mass concentrations were corrected for this lower flow, but the size distribution data could be affected as well, they are not corrected for the low flow.

Winter 2004:

- The beam width probe data yielded that the aerosol beam was not focused well. This issue is being corrected by applying the CE factor.
- One pump failed during the campaign.
- The beam width probe failed on February 2nd because the motor of the wire stopped working. This had no effect on the data.

III.5.7 Other data issues

Summer 2001:

- Due to incomplete sampling of sulfate particles on the heater and/or less efficient evaporation and ionization of the vapor, the sulfate mass concentrations have to be corrected. This correction was done by a single factor of 2.9 for the whole campaign. The correction factor was determined by comparison of AMS and PILS.
- Due to interferences with water and oxygen at masses 16 – 18 amu, the ammonium signal was calculated from mass 15 amu signal, multiplied by a factor of 10 to account for the omitted fragments.
- According to lab experiments, the organics have to be scaled by a factor of 0.7 to account for lower ionization efficiency. This was done for the 'total organics' signal.
- The transmission for the aerodynamic lens inlet of the AMS is well below 100 % for particles smaller than 40 nm and larger than ca. 1000 nm. There is no correction for the lost small and large particle mass.
- The size distribution data produce useless results for time periods with low mass concentrations for the measured species. The sizes are always aerodynamic.

III.6 PILS/IC Analyzer: Particle into Liquid Sampler

III.6.1 Ion chromatograph (IC) operational description

The liquid sample from the Particle Into Liquid Sampler (PILS) is injected into an IC column where the individual ionic species elude off separately. A conductivity detector measured the concentrations of each species. The conductivity response/concentration relationship is produced from injecting a range of known concentrations and producing a calibration curve.

III.6.2 Uncertainty

The ion liquid concentrations reported by IC software are converted into corresponding atmospheric concentrations. This conversion is dependent on the airflow rate, the liquid flow rate, and the liquid concentrations.

The airflow rate was measured daily with a Bios DryCal, which has a reported accuracy uncertainty of 1%. The precision of the DryCal is calculated from the thirty daily airflow measurements. the standard deviation is 0.15 LPM, or about 1% of the total 10.6 LPM flow rate. During the winter 2004 intensive, the flow rate was increased to 16.5 LPM to accommodate a redesigned PILS impactor which complies with a standard sampling rate of 1 cubic meter per hour.

The liquid flow rate pumped by the 8-channel IsmaTech peristaltic pump is dependent upon the condition of the flexible tubing used with the pump. The flow rate was measured with an Acculab portable scale with a stopwatch. The density of 1 g/ml was assumed for all liquids. The accuracy uncertainty of this measurement was 2%. We report a liquid flow rate accuracy precision of 5% to account for the additional uncertainty related to the variability of the

peristaltic pump flexible tubing. The peristaltic pump flow rate precision is not reported by the manufacturer. However, daily checks showed variation of less than 1% provided that the peristaltic pump tubing was in acceptable condition.

The dilution factor is the concentration of the lithium (Li) transport flow with steam divided by the concentration of the Li transport flow without the steam. The uncertainty of the dilution factor is 5%. The precision of the dilution factor measurements is 6%.

The Metrohm-IC calibration curves and the uncertainty associated with the conductivity detector result in a cumulative 3% accuracy uncertainty in the liquid concentrations. The precision of the Metrohm-IC was calculated as 1% from several measurements of the same standard solution.

Using the sum of the squares equation with these variables, the collective accuracy uncertainty of the PILS-IC measurements is 8%.

III.6.3 PILS Limits of Detection (LOD)

The LODs for each reported species from the PILS-IC system are based on the signal to noise ratio from chromatographs produced by the Metrohm-Peak IC data acquisition hardware. Figure III.26 shows a chromatograph baseline with an insert illustrating the noise. Figure III.27 shows a chromatograph from the PMTACS-NY PILS-IC data. Each integrated peak area represents the integrated conductivity response from the baseline for each corresponding ion. The LOD is determined to be the concentration where the signal is three times the standard deviation of the noise.

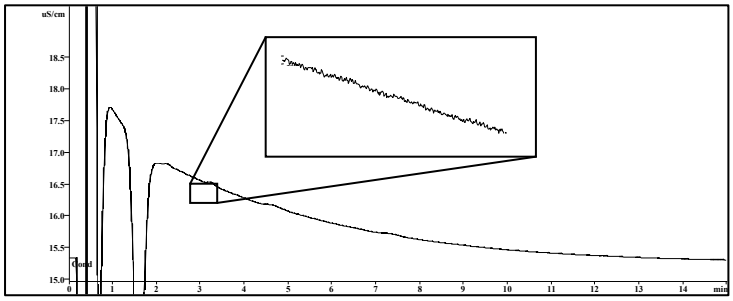

Figure III.26. Chromatogram baseline with insert illustrating baseline noise found with Metrohm-Peak IC software.

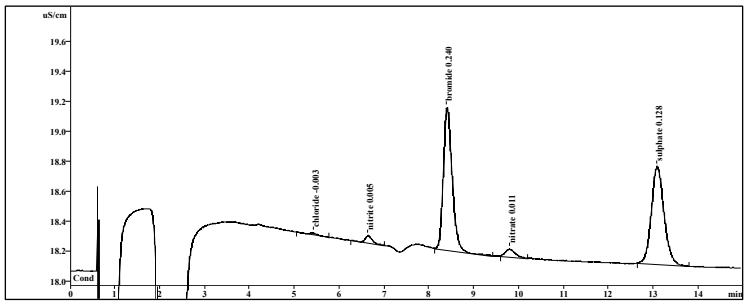

Figure III.27. Typical anion chromatogram taken from the PMTACS-NY PILS-IC data from Summer 2001. Numbers indicate the concentration in mg/L before conversion to $\mu g/m^3$.

The following table reports the LOD's for the reported PILS-IC species:

Anions	LOD ($\mu g/m^3$)
chloride	0.05
nitrite	0.05
nitrate	0.05
sulfate	0.05
Cations	LOD ($\mu g/m^3$)
sodium	0.10
ammonium	0.60
potassium	0.10
calcium	0.10
magnesium	0.10

The cation LODs are larger than the anion LODs due to the greater noise amplitude of the cation chromatograph baseline. The anion IC includes a suppressor to decrease background noise due to interfering ions, such as carbonate. Other than ammonium, these LODs are identical to those reported for the PILS-IC setup for the Texas Supersite in Texas, and the Atlanta Supersite in Georgia. The ammonium LOD is explained in the next section. Examining several chromatograms throughout the summer and winter dataset revealed a relatively constant level of noise found in flat sections of the baselines. Therefore, the LODs are held constant for the entire dataset.

Ammonium

Ammonium is the primary aerosol base for the PILS-IC data set, comprising 91% of all recorded cations by mass during the summer 2001 intensive. The charge balance for the PMTACS-NY PILS-IC summer 2001 data appears to have an apparent offset from neutrality, suggesting a possible systematic error or correction factor. This feature is also found in data sets from other recent PILS-IC field studies where the PILS was operated in a similar manner.

Linear regression of the recorded versus calculated NH_4, as shown in Figure III.28, produces a y-intercept of 0.0313 µmol/m^3 (0.56 µg/m^3), suggesting that adding 0.0313 µmol/m^3 to the recorded ammonium would make the apparent isolated neutral data set neutral.

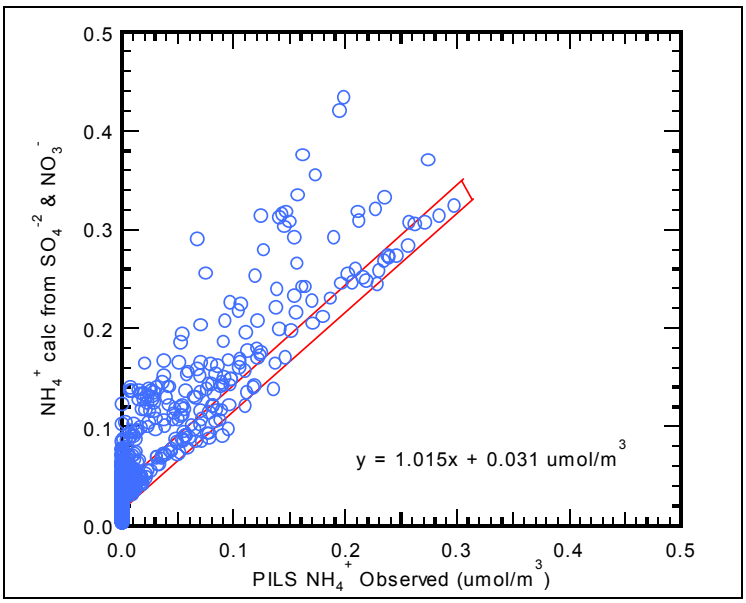

Figure III.28. Observed versus calculated NH_4.

Extrapolating this correction to the entire ammonium data set creates a corrected ammonium trace. Figure III.29 shows the inorganic charge balance with the recorded ammonium in red (top trace), and the corrected ammonium in blue (bottom trace). The corrected charge balance still produces acidic events correlating to sulfate and PM events, but periods of neutrality now exist. With all of this in mind, the consensus for the LOD for ammonium is 0.60 µg/m^3.

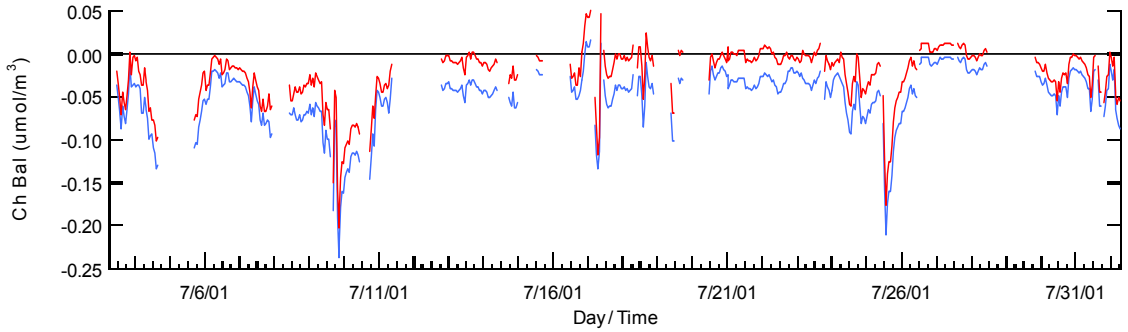

Figure III.29. Charge balance with correction.

This theoretical correction is reclassified as an experimental error or sample loss due to supporting tubing experiments. Research conducted after the PMTACS-NY field intensive relates ammonium loss from the liquid sample to the tubing material used. Figure III.30 illustrates several different solutions of ammonium run through the ICs with varying residence times to determine the effect. The solutions are denoted in the legend. With increased residence time, the measured ammonium decreased with the Teflon tubing. This did not occur with the polyetheretherketone (PEEK) tubing. The entire sample flow path in the PILS system was replaced with PEEK tubing prior to the winter 2004 intensive.

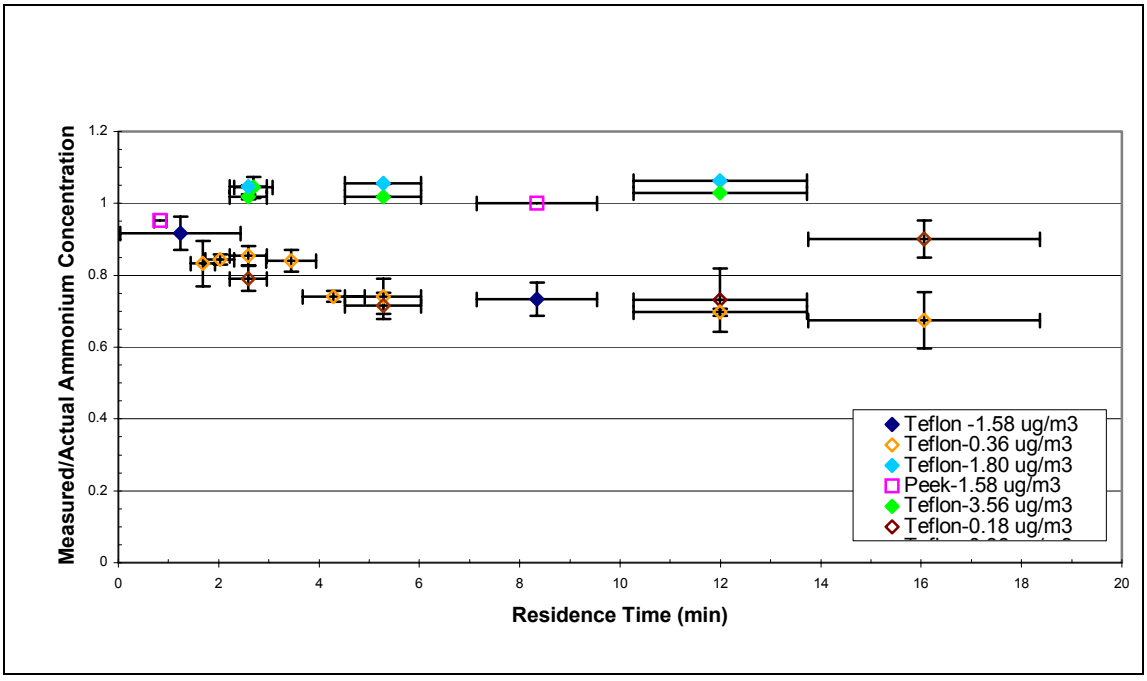

Figure III.30. Residence time experiments run with Teflon and PEEK tubing. The legend indicates the concentrations of the ammonium solution injected into the ICs.

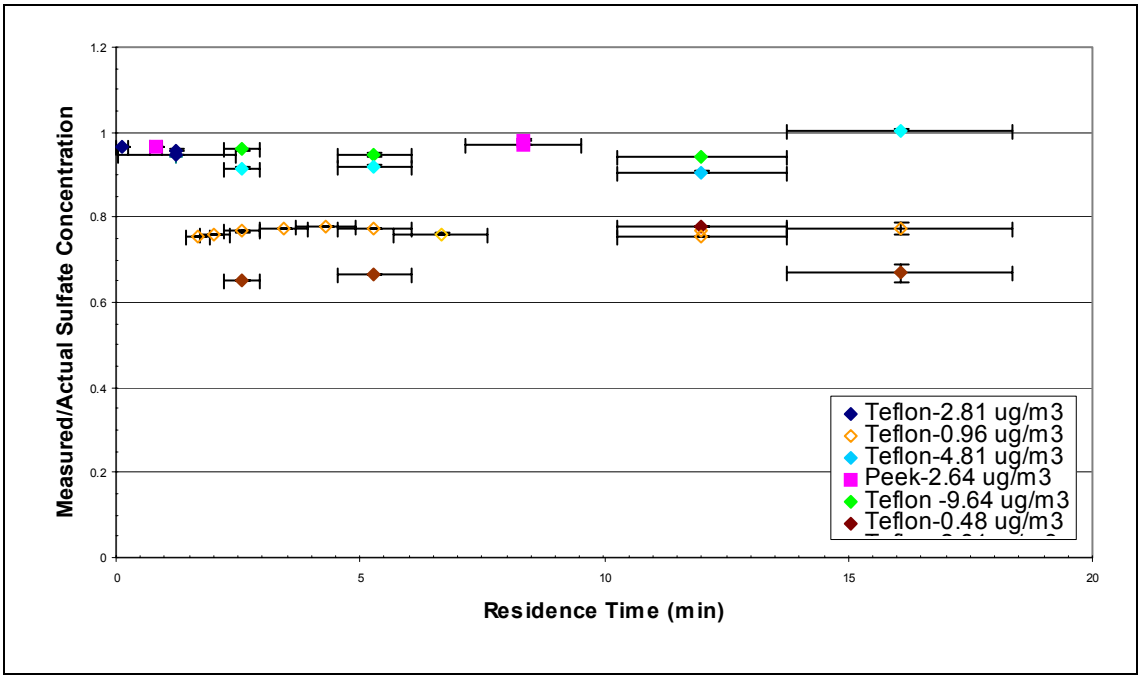

Figure III.31. Residence time experiments run with Teflon and PEEK tubing. The legend indicates the concentrations of the sulfate solution injected into the ICs.

Figure III.31 shows that this decrease in concentration with longer residence times did not occur for sulfate, except at very low concentrations.

The research concluded that the Teflon tubing carrying the liquid sample from the PILS to the IC effectively stripped away a fraction of the ammonium. The loss rate is a function of the liquid sample residence time in the tubing. As the liquid flow rate is increased, the tubing has less of an effect. Conversely, the alternative PEEK tubing showed no significant ammonium loss. The tubing experiments produced a constant ammonium loss dependent on the sample residence time. This verifies the 0.60 $\mu g/m^3$ experimental error assigned to the ammonium values reported for the summer 2001 experiment.

III.6.4 Quality Assurance

The majority of the QA for the PMTACS-NY PILS-IC data was done in the field on the day after the data was recorded. All of the 15-minute chromatographs recorded were reviewed to confirm that the peaks were correctly identified with the corresponding species. The resulting time series from the entire study was reviewed further by checking any anomalous structure.

The IC calibration was checked three times during each of the 4-week studies by running four levels of standards. A 10 level calibration was performed immediately prior to the beginning of the data collection. A standard solution of known concentrations for all species was injected directly into the IC and compared against the NIST traceable reported values. The calibration checks were typically within 5% of the predicted values. Henceforth, the 10 level calibration was only performed in the field at the beginning of each study.

Throughout the summer 2001 campaign, particulate matter was simultaneously collected upon filters as part of the PILS unit. These filters were then added to a sample bottle filled with distilled deionized water and sonicated for a minimum of 24 hours. The solution from the sample bottle was then injected into the anion ion chromatograph. The sulfate concentration was compared to the average sulfate concentration measured online by the PILS-IC over the same sample period. Figure III.32 illustrates the compared sulfate values. It is important to note that the large differences between the filter and online measurements usually coincide with low concentrations of sulfate.

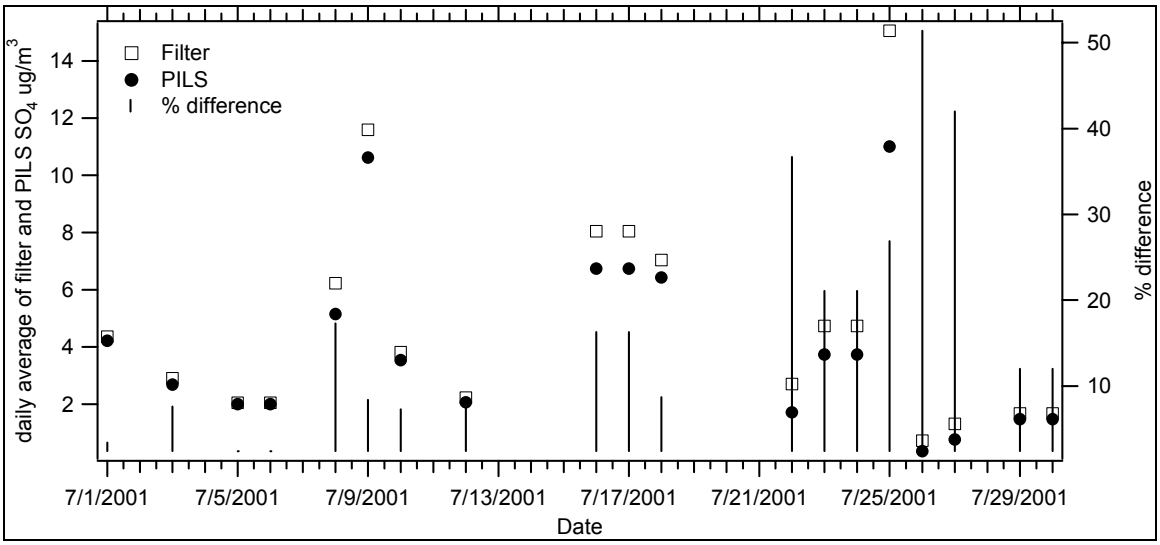

Figure III.32: Measured sulfate as reported by the internal filter check and the average of the online PILS-IC measurements over the same time period during the summer 2001 experiment.

III.6.5 Data completeness

The following tables summarizes the PMTACS-NY PILS-IC data completeness:

Summer 2001:

Data Period: 7/1/2001 0:00 - 8/4/2001 0:00
Total possible hours:
816

Ions	Hours recorded	Data completeness
Cation	551	68%
Anion	611	75%

Winter 2004:

Data Period: 1/9/2004 19:00 - 2/5/2004 0:00
Total possible hours:
630

Ions	Hours recorded	Data completeness
Cation	548	87%
Anion	523	83%

The next tables summarize the data loss causalities:

Summer 2001:

IC problems	45%
Operational errors	25%
PILS problems	20%
Daily operations	10%

Winter 2004:

IC problems	35%
Operational errors	25%
PILS problems	30%
Daily operations	10%

III.6.6 Flagging

All data has been flagged and turned into the NARSTO template for review. Unlike most instruments, the PILS-IC has irregularly spaced periods of downtime. The IC software does not activate upon specified timeslots, so sampling periods were not started or stopped at regular intervals. When an irregular period of down time occurred, this anomalous time period was marked as "*999*" in both the start and end points. Each corresponding ion data block was left blank and flagged with "M1." The utilized flags are as listed:

M1 Missing value because no value is available (PILS-IC was down)
M2 Missing value because invalidated by data originator
V0 Valid value
V1 Valid value but comprised wholly or partially of below detection limit data
V5 Valid value but qualified because of possible contamination (e.g., pollution source, laboratory contamination source)
V6 Valid value but qualified due to non-standard sampling conditions (e.g., instrument malfunction, sample handling) ammonium values.

III.7 HSPH/Allen Sulfate

This instrument measures sulfate aerosol mass by converting it in a stainless steel reduction over at 900°C to sulfur dioxide which is measured by a commercial low level pulse detector (TECO 43S). The SO_2 detector is calibrated with NIST traceable mixture of SO_2 in air.

Ambient air stream passes through 5 LPM sharp-cut cyclone, then sodium carbonate denuder, carbon monolith denuder, and Nafion dryer. About 0.5 LPM passes through an 8-10 foot long coil of 1/8" O.D. SS tubing heated to 900°C in a tube furnace, then a PTFE filter. The sulfate converted to SO_2 in the sample is detected in a low-level pulsed fluorescence SO_2 analyzer. Once each hour for 10 minutes, the ambient air stream is diverted through a capsule filter, then through the oven and into the analyzer. This provides a continuous measure of the zero response of the instrument. The SO_2 analyzer was operated on the 20 ppbv full scale range. If there is 100% conversion of SO_4 to SO_2, 20 ppbv SO_2 corresponds to nearly 80 $\mu g/m^3$ of SO_4 at 1 atmosphere and 25°C. Data is generated continuously by the TEI Model 43S SO_2 analyzer. The instrument time constant is set to 60 seconds, and the analog output terminals of the analyzer are connected to an ESC Model 8816 data logger. The data logger stores the data as minute and hour averaged values. A computer at the site running EDAS Ambient software downloads data from the data logger to the computer each hour.

III.7.1 Data reduction

- Minute data stored on the computer is "exported" to an ASCII file in one day increments. These ASCII files are imported into EXCEL for further manipulation. The EXCEL worksheet begins with columns for 1) time; and 2) minute averaged analyzer signal.
- Within EXCEL, the data from 4 to 10 minutes past each hour is used to calculate the zero response signals for that hour. Five three minute averages (4-6, 5-7, 6-8, 7-9, and 8-10) are computed, and the minimum from these three minute averages is taken as the zero. A new zero value is computed for each hour.
- The zero correction signal is subtracted from all of the minute averaged data points for each hour. This results in minute averaged difference signals.
- The minute averaged data is collected in ten minute periods and averaged to yield 10 minute averaged data. Each hour yields up to five 10 minute averaged data points, the first ten minute period having been used for the zero correction.
- The difference signals were multiplied by 3.93 to convert from ppbv SO_2 gas concentration to $\mu g/m^3$ SO_4 concentration.
- Based on a zero air gas replacement test on July 25, 2001 (described below), an additional zero offset of 1.03 $\mu g/m^3$ was measured. This zero offset was subtracted from the final data.

III.7.2 Period of operation and operations log

<u>Summer 2001</u>:

- Instrument began operation on July 21, 2001 at 16:00. The SO_2 analyzer had been calibrated earlier in the day. There was a large (off scale) signal as the SS coil was heated to 900°C for the first time.

- Initially the zero response was measured every 90 minutes.
- On July 23, 2001 the flow demand of the SO_2 analyzer was checked, and the PTFE filter was changed.
- On July 24, 2001 at 12:00 the zero checks were reprogrammed to occur every 60 minutes.
- July 25, 2001: The SO_2 analyzer was calibrated through the heated SS coil. Zero air was directed through the coil and into the analyzer for about 90 minutes. This provided the basis for the "additional zero offset" described above. Following the zero air, a flow containing 10 ppbv of SO_2 was introduced to the heated coil/analyzer system for two hours.
- July 27, 2001: Sodium carbonate denuder in the inlet sample train was changed. The bypass flow was checked and determined to be 4.6 LPM.
- August 5, 2001: Instrument was turn off (oven only initially).

The instrument was not deployed during the Winter 2004 field campaign

III.7.3 Data flagging

The following flags are used for the data generated by this instrument during this campaign:

V0 - Valid Value
V1 - Valid Value, but wholly or partially below the detection limit (se below)
M2 - Missing Value because invalidated by data originator (i.e., zero checks, calibrations, and instrument maintenance.)

The detection limit was determined to be 0.80 $\mu g/m^3$ SO_4, which was calculated as 3* standard deviation of the blank signal determined in the July 25 zero check period. (As noted above, the mean signal during this period was 0.26 ppbv SO_2, which corresponds to1.03 $\mu g/m^3$ SO_4. Thus the detection limit measures the ability to detect signals above the 1.03 $\mu g/m^3$ zero offset.)

III.7.4 Summary statistics

Summer 2001:

Data from the eight hour warm up period from 16:00 to 23:59 on July 21, 2001 is considered pre-deployment. Deployment period is from 00:00 on July 22, 2001 to 18:00 on August 5, 2001. This makes 2124 ten minute averaging periods, and 354 hour averaging periods. Completeness statistics will be calculated using these totals.

	10 minute averages	Hour averages
Number of unqualified valid values	1656 (78%)	336 (94.9%)
Number of MDL valid values	109 (5.1%)	14 (4.0%)
Total valid values	1765 (83.1%)	340 (98.9%)
Number of missing values	359 (16.9%)	4 (1.1%)

III.7.5 Data summary

Summer 2001:

Summary of SO_4 concentrations measured during period of operation (all data in $\mu g/m^3$):

	10 minute averaged data	Hour averaged data
Minimum	-.30	.25
25^{th} percentile	1.55	1.54
Median	3.10	3.18
75^{th} percentile	5.19	5.04
Maximum	19.98	18.93
Mean	3.88	3.89

III.7.6 Quality Assurance Experiments

- SO_2 analyzer was calibrated with a mixture of SO_2 in air 1)directly (through PTFE filter only); and 2)through the zero valve and heated SS coil. The SO_2 came from a NIST certified reference standard cylinder from Scott-Marrin. This was dynamically diluted with UHP zero air using an Environics S100 calibrator.
- Instrument flow and bypass flow were checked with a BIOS DryCal Lite to assure a total flow of 5 LPM for the cyclone.
- Processed data was compared with data from filters, R&P 8400S, PILS, and AMS (ongoing work).

III.7.7 Problems or issues with the instrument and/or data

- The zero check valve arrangement uses a solenoid pinch valve to cut off the flow of ambient air with particles, while at the same time opening a PFA solenoid valve downstream of a Balston capsule filter. This arrangement substitutes particle free ambient air to the oven and analyzer during the zero check. One possible problem with this set up is that a roughly four inch long piece of latex tubing was used in the pinch valve. It was necessary to use latex because the conductive rubber tubing was too stiff for the solenoid to effectively pinch it shut.
- The data from the instrument showed a characteristic "waveform" pattern that was quite clearly instrumental, and not environmental in nature. Namely, at the end of each "zero period" the analyzer signal would rebound to a higher level, and invariably decay as the hour progressed; until the next "zero period" began and the signal dropped sharply. No good explanation has been discovered for this behavior. It is recommended that the zero check valve arrangement be modified to see if it is responsible for the waveform pattern of the data.

III.8 ICP/MS – PM2.5 Sulfate and Metals

The sulfate analysis was assessed by means of method intercomparison, whereby split samples were analyzed with Standard Ion Chromatography that was calibrated with NIST traceable

chemicals. The following relationship was established: (ICP-MS) = 1.01 (IC) + 0.26 with a correlation coefficient of 0.99. It follows that the (ICP-MS) – sulfate analysis essentially measures the sulfate concentration with a precision of 1%, i.e. well within the stated DQO.

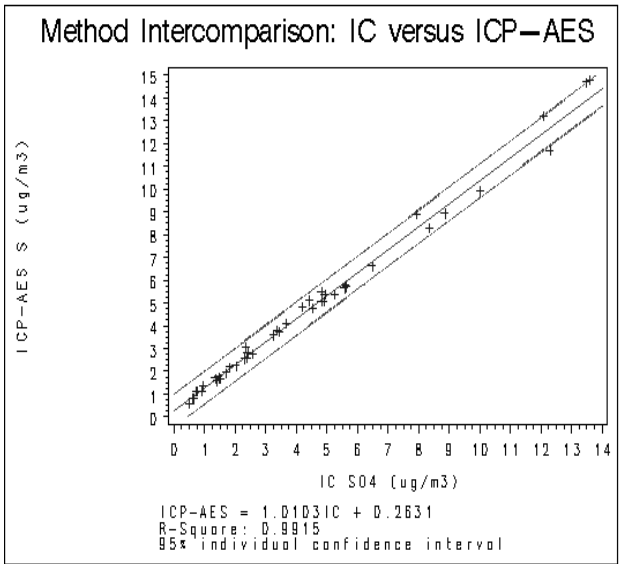

With regard to the ICP/MS analysis for metals (Mg, Al, K, Ca, V, Cr, Mn, Ni, Fe, Zn, As, Se, Cd, Sb, Hg and Pb), the DOH laboratory established through internal audits, that the ICP/MS meets or exceeds values reported in EPA Compendium Methods for Inorganic Air Pollutants (IO-3.3, -3.5, -3.7 and –4.0). EPA/625/R-96/010a, June 1999.

III.9 PM2.5 Carbon – R&P Model 5400C

III.9.1 Overview of instrument operation and data generation

Ambient air stream passes through a 16.7 LPM URG cyclone, then into the instrument where it is diverted to one of two identical collectors, Collector A or Collector B.

During collection cycle the 16.7 LPM (nominal) sample air flows though a specially designed stainless steel impaction type collector. The collector is toroidal, with a series of precision drilled holes acting as impactor jets, and a flat stainless steel plate acting as collector for particles. The manufacturer's design parameters specify a 50% collection efficiency for particles of size 140 nm or 0.14 μm (i.e., D_{50} = 0.14 μm).

Flow control is achieved by the pressure drop across the collector. This means there is no active flow control and no flow controller. Flow is measured by a mass flow meter and converted to volumetric flow using values for average seasonal temperature and pressure entered by the user. Pressure at the collection plates is about 22" Hg, or about 0.73 atm.

The collector temperature is held constant at 50°C.

After the collection period (one hour for this campaign), valves switch the sample flow and collection to the other collector, and the previously collected sample is analyzed. Thus, during normal operation, one collector is collecting sample, and the other is undergoing analysis.

During the analysis cycle the collector, afterburner, CO_2 sensor, and a circulating pump are isolated as a closed analysis loop.

The complete analysis phase consists of about 24 steps for this configuration of the instrument. It is beyond the scope of this report to detail all these steps, but instead a condensed description of the analysis sequence will be attempted.

After analysis begins, the loop is purged with filtered ambient air, the afterburner is heated to 750°C, and the loop is purged again.

The CO_2 sensor then measures the amount of CO_2 in the analysis loop before performing the stepwise oxidation of the material collected in the collector(M0).

The collector is heated to 275°C (340°C in winter 2004) and held for 8 minutes and the amount of CO_2 in the loop is measured (M3).

The collector is heated to 750°C and held for 4 minutes and the amount of CO_2 in the loop is measured (MF).

The collector and afterburner are cooled and purged. Filtered purge air is "collected " for 90 s to form the basis of the instrument's residual measurements and computations.

The afterburner is heated to 750°C and the loop is purged again.

The CO_2 sensor then measures the amount of CO_2 in the analysis loop before performing the stepwise oxidation to compute residuals ($M0_{res}$).

The collector is heated to 275°C (340°C in winter2004) and held for 8 minutes and the amount of CO_2 in the loop is measured($M3_{res}$).

The collector is heated to 750°C and held for 4 minutes and the amount of CO_2 in the loop is measured (MF_{res}).

The collector and afterburner are cooled and purged.

Data collection and computations are done by the instrument's electronics and computer. At the end of each analysis cycle about 40 parameters are stored in memory. This data can be displayed on the front panel, or downloaded to a computer. For this campaign the data was

downloaded to a computer using the RPCOMM software provided by the manufacturer. (The instrument can store approximately 45 days of hourly cycle data–or approximately 1000 cycles.)

III.9.2 Data Reduction

- Instrument data records include about 40 fields, as noted above. Key parameters include the instrument status codes and the computed carbon mass concentrations in micrograms per cubic meter for the intermediate (275°C in summer 2001, 340°C in winter 2004) and final (750°C) oxidation steps (referred to as "burns").
- Ambient background CO_2 concentrations, purge and residual concentrations are also included in the data record, but these parameters are not needed under normal circumstances.
- The recorded data is insufficient to rigorously check the instrument's computation of mass concentrations from the CO_2 sensor's measurements because the pressure in the sample loop during analysis varies, and this information is not stored. However, assuming the CO_2 amounts measured are correct, and using the collection volumes, one can check the calculation of mass concentrations.
- Based on instrument status codes and operator notes, the data records are assigned a flag. (NARSTO flags are used – see below.)
- A zero offset correction is subtracted from each MC3 and MCF value to obtain the final data with fields denoted as "275 Burn" in summer 2001 ("340 Burn" in winter 2004) and "TC".

III.9.3 Period of operation and operations log

Summer 2001:

- Instrument was set up and began running on June 28, 2001 in an outdoor enclosure.
- Reported data begins with cycle 9, beginning at 00:00 on June 29, 2001.
- July 7,2001 – audits and checks (see below).
- July 18, 2001 – filter blank test 15:00-17:59.
- July 20, 2001 – vacuum blank test 10:00-13:59.
- July 23, 2001 – afterburner on loop B fails at 4:00; not replaced until July 27 at 14:00. All 275 Burn data on loop B flagged for this period.
- July 31, 2001 – audits and checks (see below).
- August 6, 2001 – instrument off at 12:00. Last valid data point at 10:00.

Winter 2004:

- Instrument was running in an outdoor enclosure on January 1, 2004 at Queens College, PS219.
- Reported data begins with cycle 8734, beginning at 00:00 on January 6, 2004.
- January 2- February 7,2004 – zero and span audits and checks (see below).

- January 16, 2004 –afterburner lamp on loop B fails at 14:00; not replaced until January 23 at 14:00. Instrument shutdown. No data available during this period.
- Feb 26, 2004 – sample flow audit and leak checks.

III.9.4 Data flagging

The following flags are used for the data generated by this instrument during this campaign:

- V0 Valid Value
- M2 Missing Value because invalidated by data originator (i.e., zero checks, calibrations, malfunctions and instrument maintenance.)

III.9.5 Summary statistics

Summer 2001:

There were 923 hours starting at 00:00 on June 29 and ending at 11:00 on August 6. This is the total used for completeness statistics of the hourly data. Daily or 24 hour averages were considered valid if 75% of hours (18 or more) were valid values. Days from June 29 to August 5 are considered (37 days).

	Hour averages		24 hour averages	
	275 Burn	TC	275 Burn	TC
Number of valid values	835 (90.5%)	881 (95.4%)	32 (86.5%)	36 (97.3%)
Number of missing values	88 (9.5%)	42 (4.6%)	5 (13.5%)	1 (2.7%)

Winter 2004:

There were 768 hours starting at 00:00 on January 6 and ending at 24:00 on February 6, 2004. This is the total used for completeness statistics of the hourly data. Daily or 24 hour averages were considered valid if 75% of hours (18 or more) were valid values. Days from January 6 to February 6 are considered (32 days).

	Hour averages		24 hour averages	
	340 ^{o}C Burn	TC	340 ^{o}C Burn	TC
No.of valid values	497 (65%)	497 (65%)	24 (75%)	24 (97.3%)
No. of missing values	271 (35%)	271 (35%)	8 (25%)	8 (2.7%)

III.9.6 Data summary

Summary of concentrations measured during period of operation (all data in $\mu g/m^3$):

Summer 2001:

	Hour averaged data 275 Burn	Hour averaged data TC
Minimum	0.559	0.698
25th percentile	1.191	1.664
Median	1.516	2.357
75th percentile	1.889	3.242
Maximum	2.963	9.348
Mean	1.545	2.576

Winter 2004:

	Hour averaged data 340 Burn	Hour averaged data TC
Minimum	0.25	0.24
25th percentile	1.22	1.66
Median	1.78	2.35
75th percentile	2.36	2.89
Maximum	4.65	6.56
Mean	1.87	2.41

III.9.7 Quality assurance experiments

Summer 2001:

- On July 7, a number of checks and audits were performed. First a manual CO_2 audit was done. The expected values for the zero, low CO_2 , and high CO_2 were 0, 1501, and 3987, respectively; and the measured values were –25, 1405, and 4028. A calibration of the LICOR sensor was then done, followed by a leak check and flow audit. The instrument passed the leak check and flow audit (16.66 LPM indicated while the BIOS calibrator measured 16.89). Another manual audit was done, this time with measured values of 3, 1445, and 4064. The percent errors for the low CO_2 points were –6.8% before and –3.7% after. The percent errors for the high CO_2 points were +1.0% before and +1.9% after.
- A second and final set of audits and checks were done on July 31. Both A and B channels passed leak checks. Manual audits of the CO_2 sensor were done twice. As before, the expected values were 0, 1501, and 3987 for zero, low CO_2 , and high CO_2 . Measured values for the first audit were –21, 1398, and 3995; and those for the second audit were +41, 1408, and 4000. The percent errors for the low CO_2 points were –6.9% and –6.2%. The percent errors for the high CO_2 points were +0.0% and +0.0%.
- Blank tests were attempted on July 18 and July 20. On July 18, a Zeflour filter was placed in a metal housing and placed upstream of the 5400 inlet. Three 5400 cycles ran sampling filtered air and mass concentrations measured. The average reported value for MC3 was

about 2.6 μg/m^3 and for MCF was nearly 5 μg/m^3. These values are higher than most of the ambient data, and could not reasonably be "zero offsets". On July 20, a cap was placed on the inlet and "vacuum blanks" were attempted. In this case one cannot look at reported mass concentrations (because the sample volume is almost zero), but instead at the increase in carbon measured during the thermal oxidation cycles. Fro these vacuum blanks with sample volumes of 2 liters or less (compared with 940-1000 liters), the carbon difference signal was within 5% of those from the Zeflour filter blanks.

- Zero offset corrections were determined from comparisons with TEOM and speciation filter data since the attempts to generate "blanks" using filters or zero sample flow were unsuccessful. Estimates of the zero offset were obtained by considering very low PM periods as measured by the TEOM. Three periods were chosen: July 2, July 26-27, and July 29. Average TEOM MC's for these periods were between 1 and 2 μg/m^3. From speciation filter measurements, and from AMS measurements during the same periods, we expect total carbon to generally contribute at most 65% of the mass, and organic carbon to contribute at most 50% of the mass. If one uses these numbers, the estimated zero offset corrections used in this data set are 0.32 μg/m^3 for the 275 Burn, and 0.48 μg/m^3 for total carbon.

Winter 2004:

- A total of seven automatic three point LICOR sensor calibrations(Zero, low CO_2 and high CO_2 spans) were performed from January 2 to February 7 2004. The expected values were 0, 1503 and 3974. The measured values ranged from –202 to –173 for zero, 859 to 949 for the low CO_2 and 2802 to 2960 for the high CO_2. The average percentage deviation on the low CO_2 span was -40% and -27.9% for the high CO_2. Due to the very cold conditions, when ambient temperatures were below 0^{o}C, the LICOR sensor could not be calibrated. The carbon mass concentration data was corrected using the slopes from each of the three point calibrations which varied from 0.76 to 0.79. A series of leak checks were performed from January 2 to February 7 2004. The instrument passed the leak checks.
- A set of audits and checks were done on February 26, 2004 when the weather was warmer. The sample flow audit indicated 16.9 LPM compared to the FTS Flow audit device of 16.2 LPM. This is within the 10% recommended by the manufacturer. Both A and B channels passed leak checks.
- No Blank tests were performed during the period as this was found to be problematic during the Summer 2001 campaign. Blanks were therefore estimated by considering very low PM periods for example at 1:00 AM Jan 14 and 3:00 AM on Jan 16. The R&P 5400 average Total carbon for these two periods was 0.32 μg/m^3 and the 340C burn average was 0.29 μg/m^3. These values are similar to those obtained during Summer 2001 (0.32 and 0.48 μg/m^3 respectively).

III.9.8 Comparisons with filter data

Summer 2001:

- Comparison data is available from the EPA Speciation sampler (R&P 2300) at PS219. The sampler collected 24 hour samples every third day during the intensive. One of the filters collected (a quartz substrate) was analyzed for OC (organic carbon), EC (elemental carbon),

and TC (total carbon) using the thermal-optical transmittance (TOT) method specified in NIOSH 5040.

- Filter data is shown both with and without an average blank correction determined from approximately 60 filter blanks from the five New York sites using the R&P 2300.
- Figures III.34-39 show the comparisons of the 5400 data and the Speciation filter data for carbon. The 5400 measures much lower total carbon than the filters as seen in Figures III.34 and III.35. If the three very low (and potentially incorrect) filter measurements are rejected, the difference is about 70% (i.e., filters measure 70% more total carbon than the 5400). For the selected data, the correlation is high (.967), and the blank corrected data has an intercept (-0.173) that is fairly close to zero. [NOTE: The standard deviation on the blank correction for total carbon is 0.26 $\mu g/m^3$ – out of a total blank of 1.10 $\mu g/m^3$.]
- Agreement is even worse for organic and elemental fractions, as seen in Figures III.36-III.39. Part of this may be due to the different collection temperatures; and oxidation temperature profiles of the analysis methods.
- There are errors in the organic and elemental fractions, which partially compensate for each other, but as noted above, even the total carbon values do not agree between the methods.
- As currently operated, it appears that the methods are not comparable. There is good correlation in some cases, but quantitative results are so different that one or both of the methods is clearly in error.

Winter 2004:

- Comparison data is available from the EPA Speciation sampler (R&P 2300) at PS219. The sampler routinely collects 24 hour samples every third day which would result in 10 days of filter data. The sampler was operated for an additional 13 days during the intensive which provided a total of 23 days of filter data for comparison. One of the filters collected (a quartz substrate) was analyzed for OC (organic carbon), EC (elemental carbon), and TC (total carbon) using the thermal-optical transmittance (TOT) method specified in NIOSH 5040.
- Filter data is shown both with and without an average blank correction determined from approximately 78 filter blanks from the Queens PS219 site using the R&P 2300.
- Figures III.40-III.45 show the comparisons of the 5400 data and the Speciation filter data for carbon. The 5400 measures much lower total carbon than the filters as seen in Figures III.40 and III.41. If the two very low (and potentially incorrect) filter measurements are rejected, the difference varies from 20 to 50% and on average is about 30% (i.e., filters measure 20-50% more total carbon than the 5400). For the selected data, the correlation is high (.78), and the intercept (0.15 $\mu g/m^3$) is fairly close to zero. However the fit to the blank corrected data has a significant positive intercept, 0.77 $\mu g/m^3$. [NOTE: The standard deviation on the blank correction for total carbon is 0.53 $\mu g/m^3$ – out of a total average blank of 1.15 $\mu g/m^3$.]
- Agreement is not as good for organic and elemental carbon as shown in Figures III.43-III.45**.** However there are potentially two high concentration outliers for organic carbon which would significantly improve the fit. There were three outliers for the Elemental carbon plot and the fit is slightly better than for organic carbon (slope of 0.47 compared to 0.45). Part of this may be due to the different collection temperatures; and oxidation temperature profiles of the analysis methods. The R&P 5400 collector temperature is set at 50^{o}C which could be lead to significant evaporative losses of the semi-volatile components.

- There are errors in the organic and elemental fractions, which partially compensate for each other, but as noted above, even the total carbon values do not agree between the methods.
- As currently operated, it appears that the methods are not comparable. There is good correlation in some cases, but quantitative results are so different that one or both of the methods is clearly in error.
- Comparison of the R&P 5400 with the SUNSET OCEC Analyzer operated during the Winter 2004 intensive are shown in Figures III.46-III.48**.** These results also show similar trends as the filter comparisons i.e. the R&P 5400 measures less carbon than the SUNSET Analyzer.

More information regarding potential problems with the carbon analysis is summarized in the NAREL report under:

http://www.epa.gov/ttnamti1/files/ambient/pm25/spec/rtiaudit4.pdf

III.9.9 Problems or Issues with the Instrument and/or Data

- The lack of an experimental procedure to determine the zero offsets for the instrument is troubling – see discussion above.
- The poor comparison with filter data, even when the data is selected to remove data that seems to be outliers, is also troubling.
- It would be very useful for the manufacturer to provide to the user community a detailed description of the low level data collection, transfer, and computation routines for this instrument.

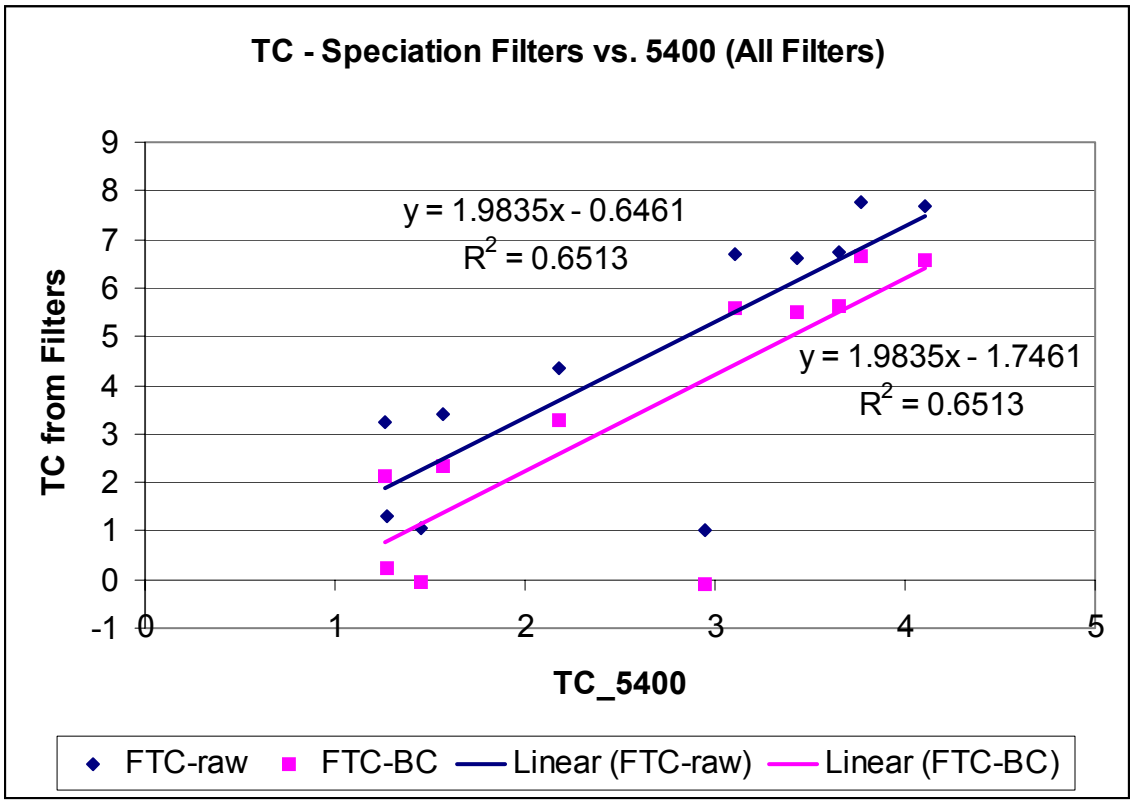

Figure III.34. Total Carbon scatter plot – all data.

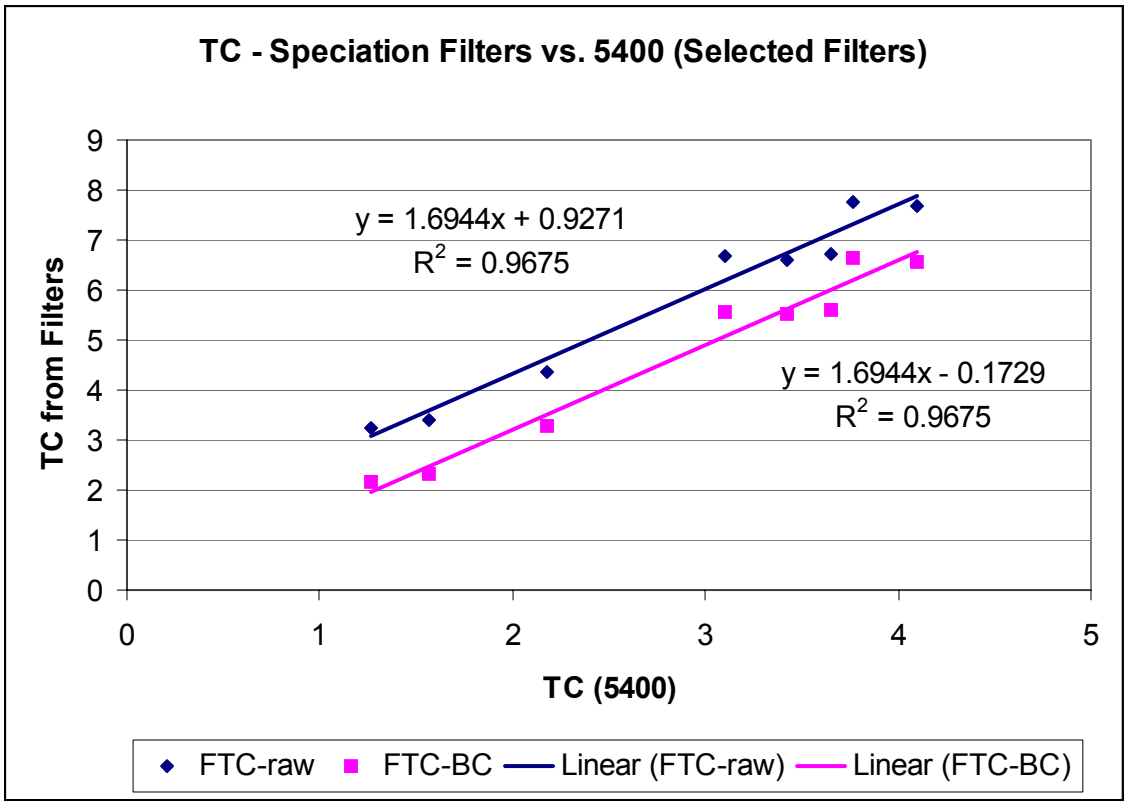

Figure III.35. Total Carbon scatter plot – selected filters only.

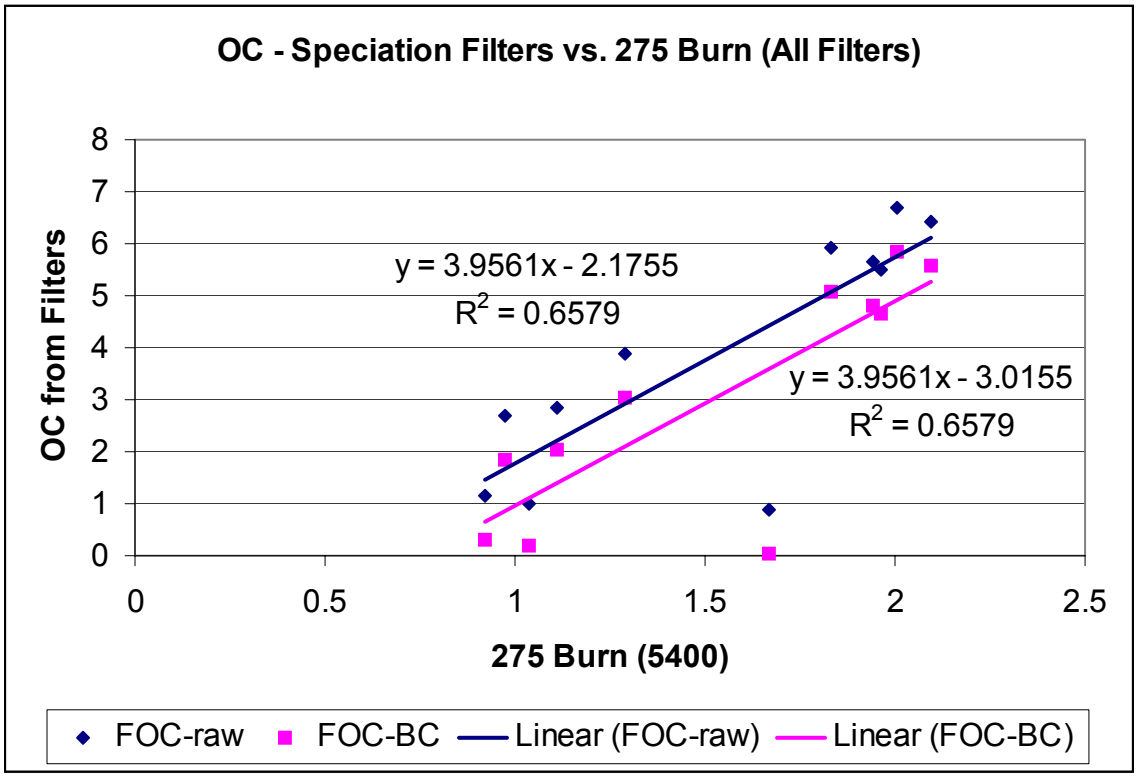

Figure III.36.

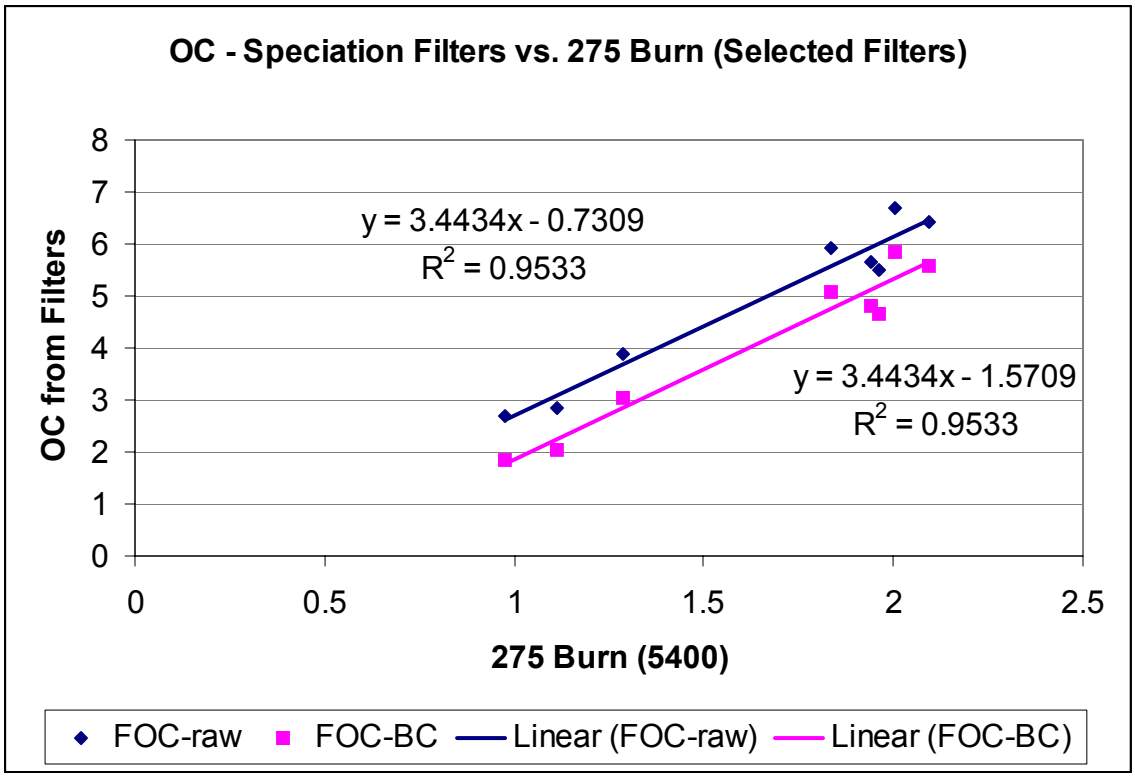

Figure III.37.

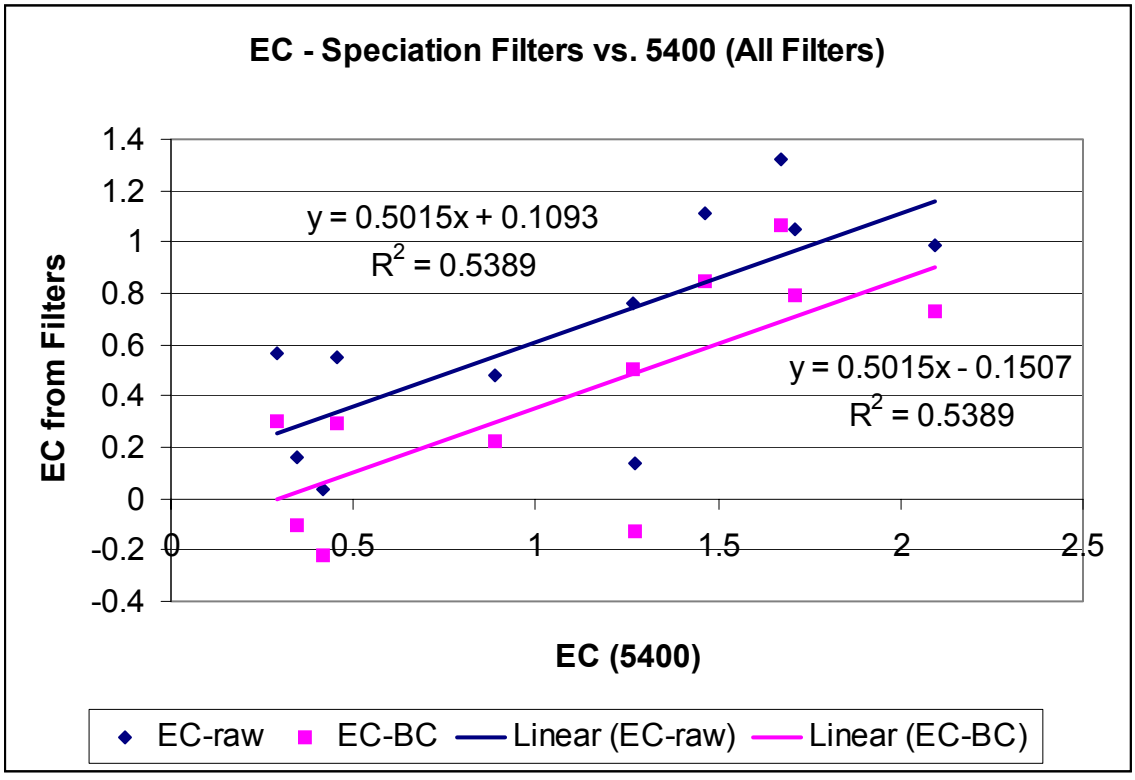

Figure III.38.

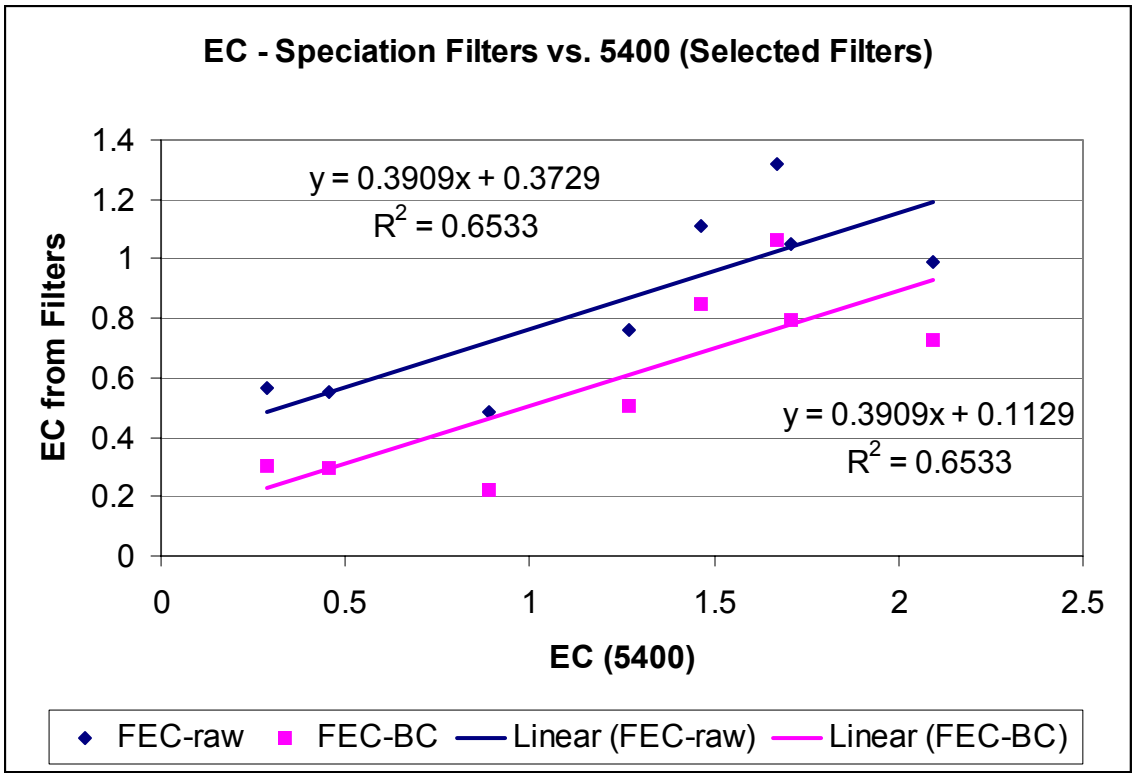

Figure III.39.

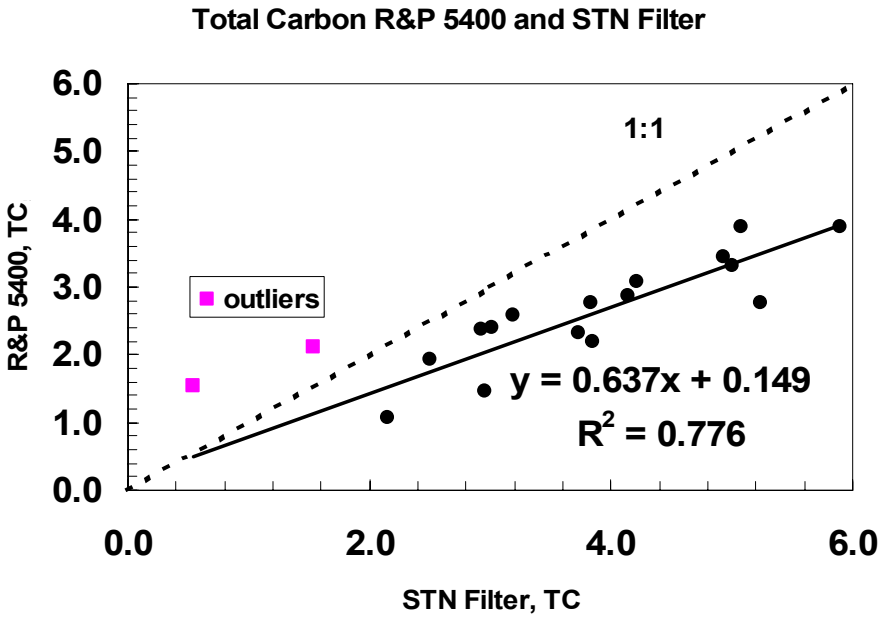

Figure III.40. Comparison of 24 hr average Total Carbon (μ/m^3) from R&P 5400 and EPA Speciation Filter Sampler. The solid line is the least squares fit to the data not including the outliers (solid squares). Data is not blank corrected.

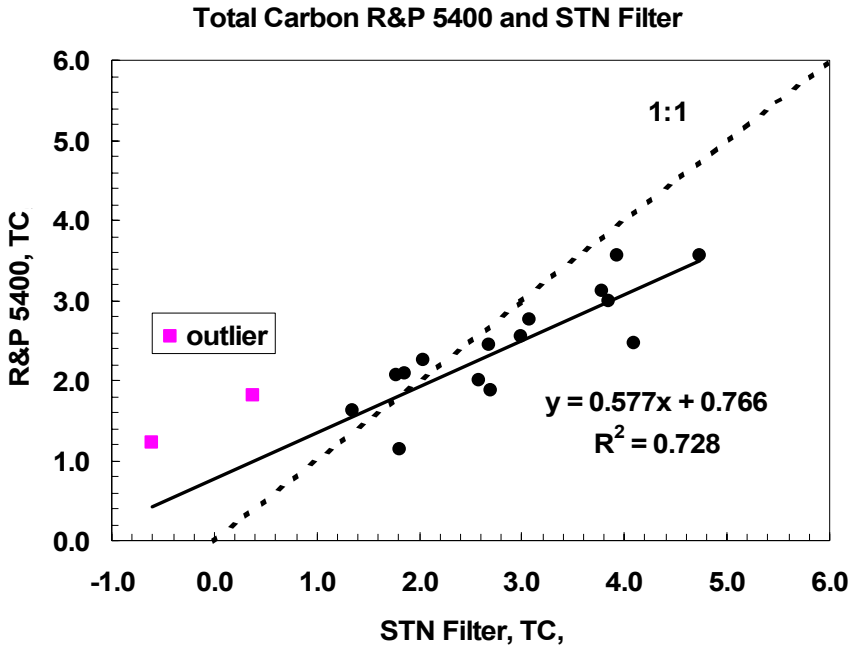

Figure III41. Comparison of blank corrected 24 hr average Total Carbon (μg/m^3) from the R&P 5400 and EPA Speciation Filter Sampler. The solid line is the least squares fit to the data not including the outliers (solid squares).

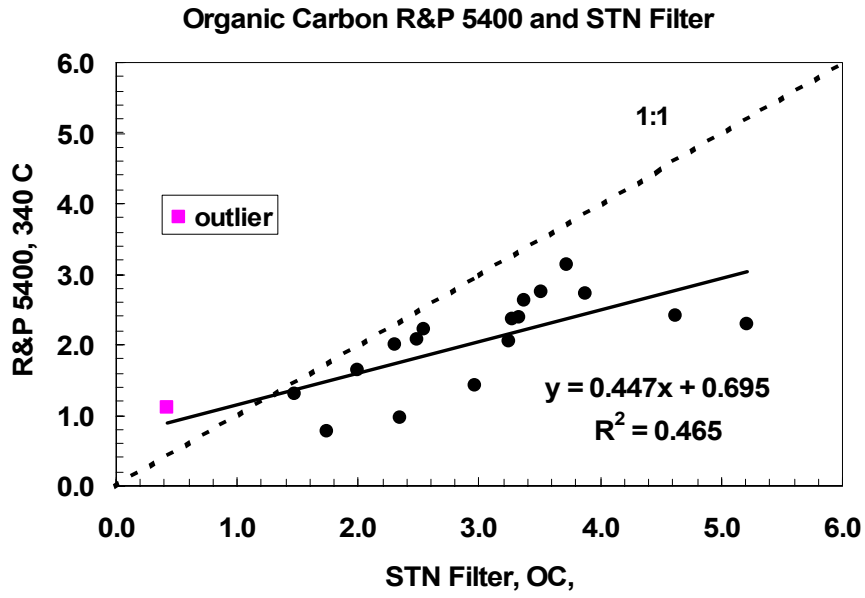

Figure III.42. Comparison of 24 hr average Organic Carbon (μg/m^3) from the R&P 5400 and EPA Speciation Filter Sampler. The solid line is the least squares fit not including the outliers (solid squares). Data has not been blank corrected.

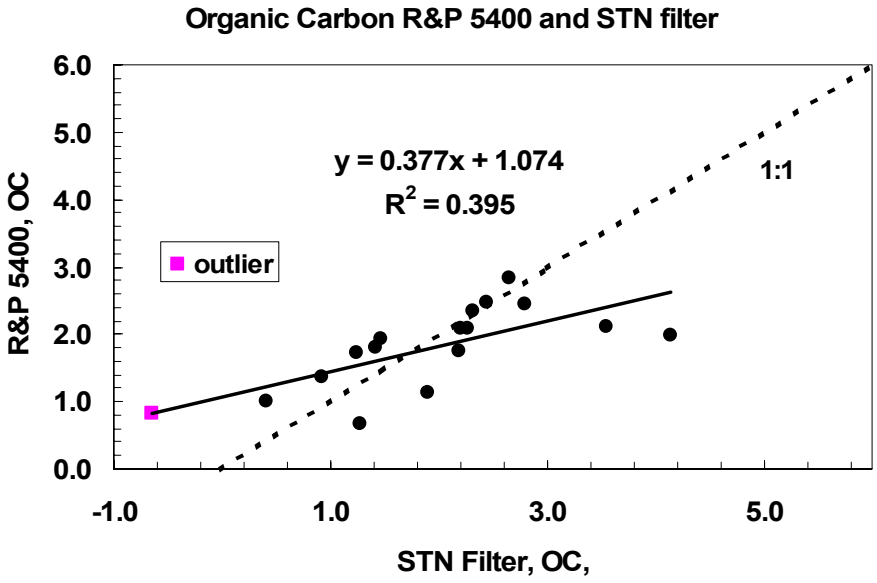

Figure III.43. Comparison of blank corrected Organic carbon(μg/m^3) from the R&P 5400 and the EPA Speciation Filter Sampler. The solid line is the least squares fit to the data not including the outliers (solid squares).

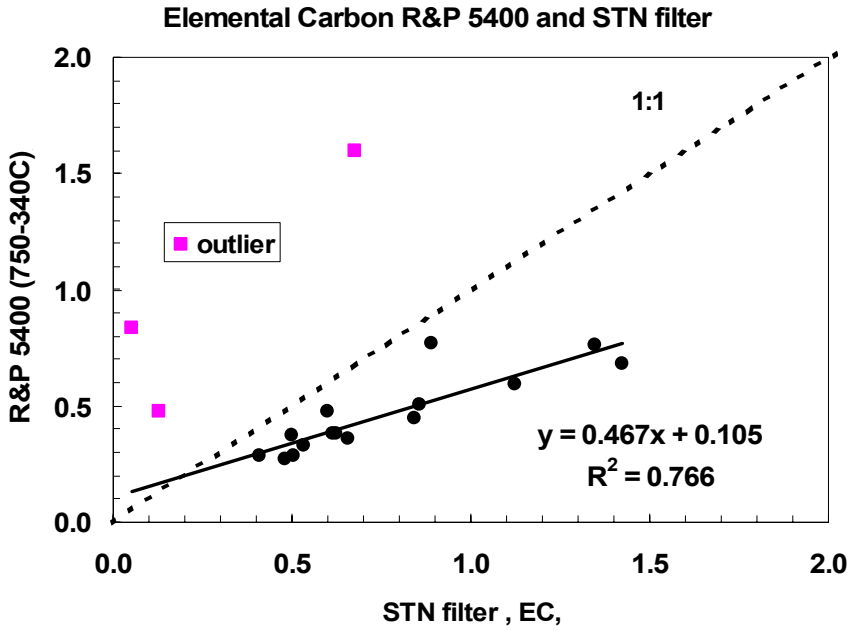

Figure III.44. Comparison of Elemental Carbon (μg/m^3) from the R&P 5400 and EPA Speciation Filter Sampler. The solid line is the least squares fit not including the outliers (solid squares). Data is not blank corrected.

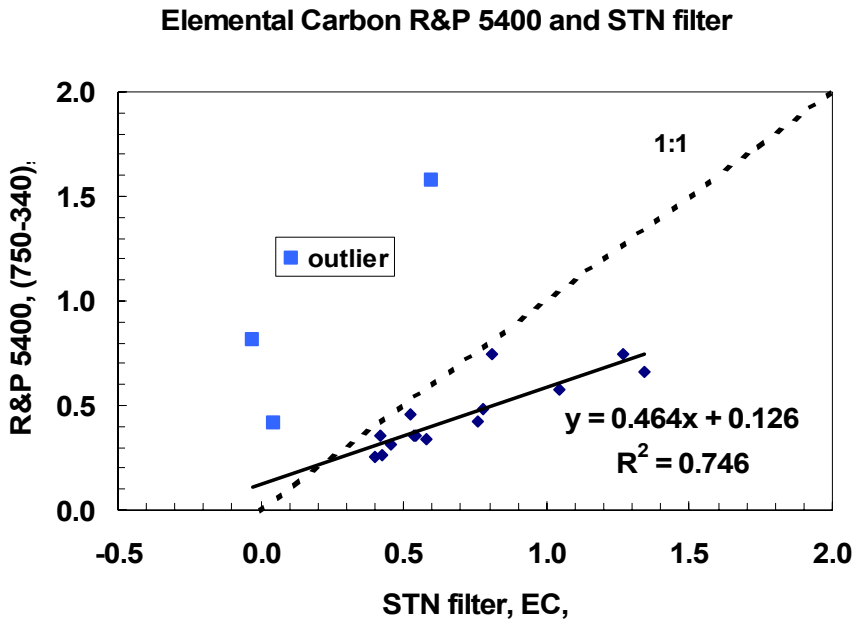

Figure III.45. Comparison of blank corrected Elemental Carbon (μg/m^3) from the R&P 5400 and EPA Speciation Filter Sampler. The solid line is the least squares fit not including the outliers (solid squares).

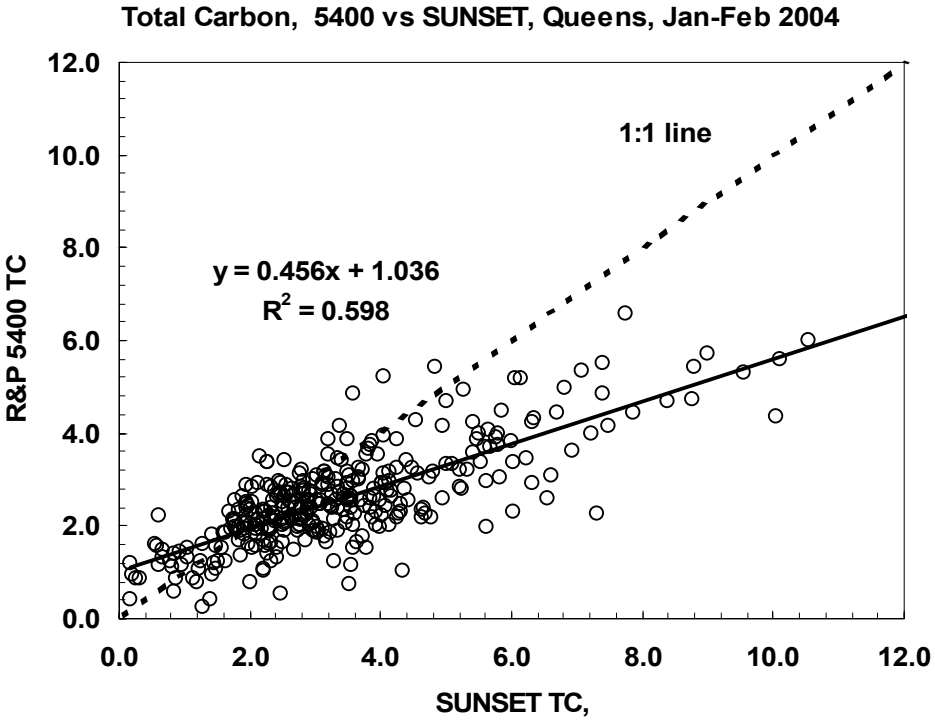

Figure III.46. Comparison of hourly total carbon data (μg/m^3) from the Sunset OCEC Analyzer and R&P 5400 750^{o}C burn. The solid line is the least squares fit to the data. Data is not blank corrected.

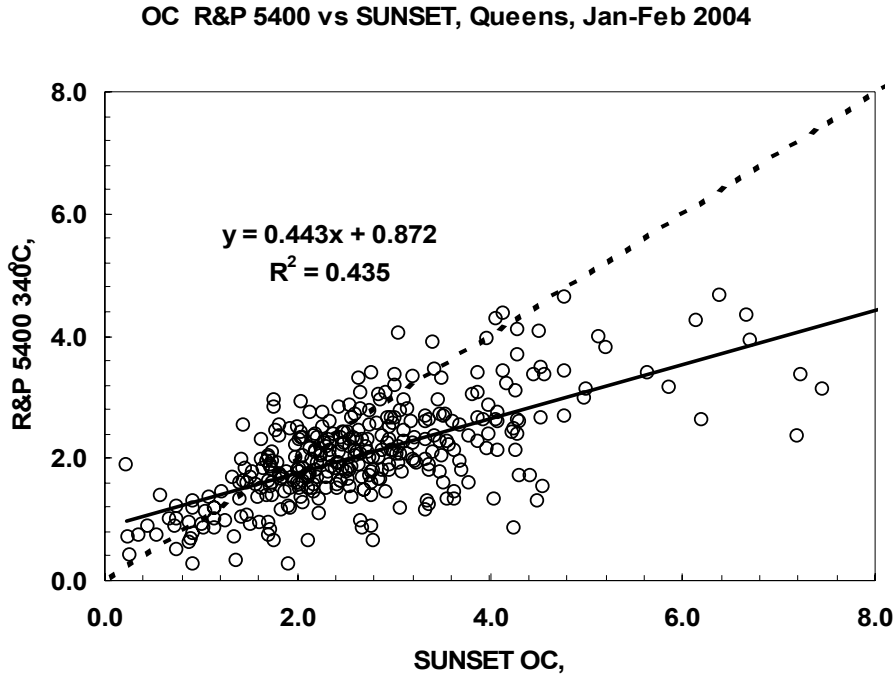

Figure III.47. Comparison of hourly organic carbon (μg/m^3) from the SUNSET OCEC Analyzer and the R&P 5400 340^{o}C burn. The solid line is the least squares fit to the data. Data is not blank corrected.

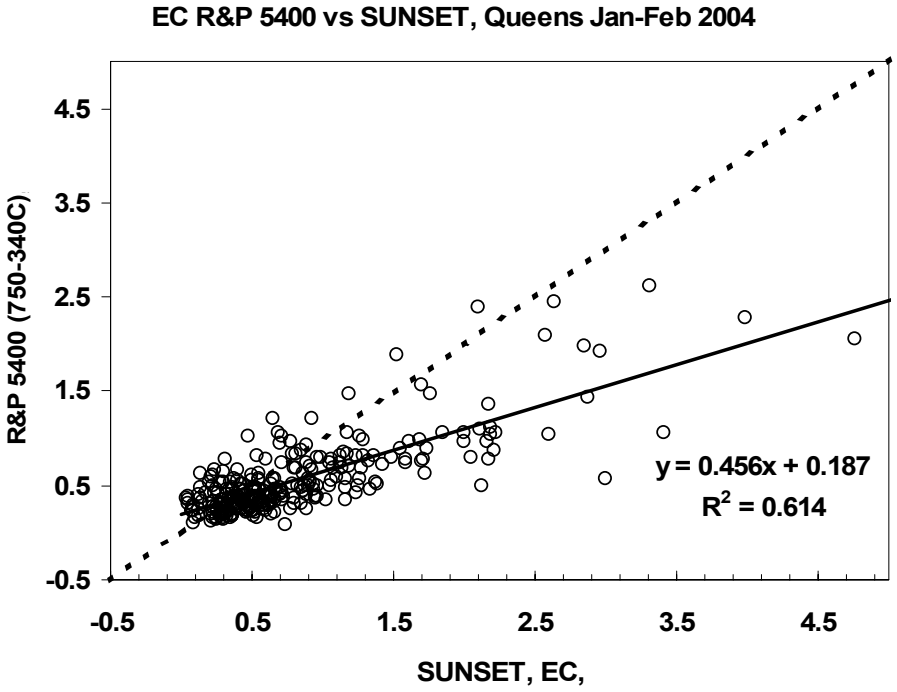

Figure III.48. Comparison of hourly Elemental Carbon (μg/m^3) from the SUNSET OCEC Analyzer and the difference between the 750^{o}C and 340^{o}C burns for the R&P 5400. The solid line is the least squares fit to the data. Data is not blank corrected.

III.10 NYS Department of Health HONO/HNO_3 Analyzer

The gaseous analytes are sampled by two coil samplers. The scrubbed nitric acid in channel 2 is converted to nitrite using a Cd-reductor: $NO_3^- + Cd_{(s)} + 2H^+ \rightarrow NO_2^- + Cd^{++} + H_2O$. The nitrite in the two channels is converted to a highly light-absorbing azo dye by a two step derivatization with sulfanilamide (SA) and N-(1-naphthyl)-ethylenediamine (NED), which proceeds in on-line derivatization coils with 5 min, The derivative azo dye is preconcentrated on two on-line C_{18} reversed-phase cartridges on a 10-port injection valve, and is separated with a reversed-phase C_{18} HPLC column and detected with an absorbance detector at 540 nm. The auto-injection valve is controlled by a PC-based HPLC software and the valve position is switched every 5 min, resulting in a 10-min sampling cycle with a 5-min sampling integration time for both channels. The method detection limits are 3 ppt and 10 ppt for HONO and nitric acid, respectively.

Winter 2004:

QC of HONO, HNO_3, NH3 and NH_4^+ Measurements in NYC,

	HONO	**HNO_3**	**NH_3**	**NH_4^+**
Precision (SD [a])	1.4%	4.2%	6%	6%
Accuracy [a]	±5%	±10%	±10%	±10%
Bias with FRM	NA	NA	+4% [b]	NA
MDL	3 ppt	100 ppt	100 ppt	30 ppt
Data Completeness	67%	60%	63%	61%

[a] At 1 ppb.

[b] Bias with respect to TDLAS.

III.11 Formaldehyde Alpha-Omega MA100

III.11.1 Introduction

Measurement of formaldehyde with high sensitivity and hourly or sub-hourly time response is important to the scientific and regulatory communities working to understand atmospheric oxidation processes, and in particular, the risks associated with exposure to this toxic air pollutant. Significant work has been done, and is ongoing in at least three major areas related to the topic of gas phase formaldehyde in the atmosphere. First, there is an attempt to increase our understanding of the types and magnitudes of sources of formaldehyde to the atmosphere (Friedfeld et al., 2002; Altshuller, 1993; Possanzini et al., 1996; Kawamura et al., 2000). Second, measurements of the abundance of formaldehyde as a function of location and season are ongoing, as is work aimed at understanding the reactions and transformations of this important species (Fried et al., 2003; Wert et al., 2003; Singh et al., 2000).

Most recent studies show that more than half, and potentially up to 90%, of the gaseous formaldehyde in the atmosphere is from secondary sources (Friedfeld et al., 2002). In this case, outdoor formaldehyde is more similar to ozone than to a primary pollutant like benzene. The atmospheric chemistry of formaldehyde involves its formation as an intermediate product of the oxidation of nearly all VOCs, and its destruction via photolysis and reaction with hydroxyl radical (OH). Formaldehyde can also act as an important source of HO_x radicals in locations where its concentration is elevated and there is sufficient sunlight. Some formaldehyde precursors are hazardous air pollutants themselves, like benzene, butadiene, and acetaldehyde.

Formaldehyde is one of the most intensely studied and scrutinized compounds on the air toxics list because of its large impact in risk assessment studies. Both the 1996 National Scale Assessment and the 1999 NEI found formaldehyde to cause significant risk for both cancer and non-cancer health outcomes(National-Scale Air Toxics Assessment, http://www.epa.gov/ttn/atw/nata (accessed March 2004); 1999 National Emission Inventory Documentation and Data, http://www.epa.gov/ttn/chief/net/1999inventory.html (accessed March 2004)).

Evaluation, characterization and intercomparison of this commercial gas phase formaldehyde analyzer was carried out during a five-week period in Albany, NY. Two identical diffusion scrubber/liquid fluorescence analyzers were run side-by-side to evaluate instrument precision, and these commercial analyzers were compared to a tunable diode laser system to assess absolute accuracy. From the side-by-side evaluation, we conclude that the precision of the analyzers is about 25%. From the comparison with the diode laser absorption instrument, the accuracy of the analyzers is estimated to be between 15-35%. We are concerned that there may be an interfering species which contributes an average signal corresponding to a fraction of a ppbv. Suggestions for improvements to the commercial analyzer include incorporation of a functional automated signal processor; a more precise timer with adjustable sample and zero periods; and a better controller for the air flow rate.

III.11.2 Measurement

Measurements of atmospheric formaldehyde have been made for at least two decades using a variety of techniques. At least three studies have been published in the last eight years comparing different measurement techniques for gaseous formaldehyde (Heikes et al., 1996; Gilpin et al., 1997; Apel et al., 1998; Fried et al., 2002). In spite of this activity, the only technique that can boast widespread and routine measurements is the DNPH (di-nitro-phenyl hydrazine) cartridge method described in Method TO-11a (Compendium of Methods for the Determination of Toxic Organic Compounds in Ambient Air: Second Edition – Compendium Method TO-11A: Determination of Formaldehyde in Ambient Air Using Absorbant Cartridge Followed by High Performance Liquid Chromatography (HPLC) [Active Sampling Methodology*;* Winberry, W.T., Jr., Tejada. S., Lonnenman, W., Kleindienst. T, USEPA Document Number EPA/625/R-96/010b, USEPA, Cincinnati OH, 1999. (Available on the World Wide Web at http://www.epa.gov/ttn/amtic/airtox.html - accessed March 2004)). Unfortunately, this technique has a variety of well-known disadvantages. First, it is prone to interference from ozone and other oxidants (Gilpin et al., 1997). Second, it is an integrated sampling method, so the time resolution of the data is typically 3 hours or longer. Third, it is an "off line" measurement, that is, the samples are collected, stored, and then shipped to a laboratory for analysis. This process can easily add a delay of days to weeks before the data are available for review and analysis.

This final QA report describes a commercial formaldehyde analyzer which makes semi-continuous measurements and is intended to be capable of deployment for routine and long-term monitoring. The instrument is the MA-100 Methanalyzer built under license by Alpha-Omega Power Technologies of Albuquerque. NM, and based on the design of diffusion scrubber/liquid fluorescence instruments fabricated by Dasgupta's research group at Texas Tech University (Dong and Dasgupta, 1987; Fan and Dasgupta, 1994). The instrument is capable of providing a three minute averaged signal every ten minutes continuously, requiring water about once a week and reagents about every two weeks. We tested two of these commercial instruments side-by-side for a one-month period, performing daily span point calibrations of the two systems. We also compared the measurements from these analyzers against (two or three) shorter periods of formaldehyde measurements from a tunable diode laser absorption spectrometer (TDLAS) system. While a five-week study does provide a considerable amount of experience with an instrument, it may not be a long enough period of time to draw conclusion about suitability of this instrument for long-term (i.e., multi-year) deployments.

The Alpha-Omega Power Technologies MA-100 is configured to allow measurement of aqueous or gas phase formaldehyde. In either case, the dissolved HCHO reacts with acetylacetone and ammonium acetate to produce 3,5-diacetyl-1,4-dihydrolutidine, a highly fluorescent product (Dasgupta et al., 1988). The reaction takes place in a zone heated to 70ºC to insure complete conversion of formaldehyde to the dihydrolutidine product. The excitation wavelength is between 400 and 465 nm; and emission of the fluorescent product is detected at 510 nm. The current implementation uses a high power light emitting diode as the light source and a photodiode detector.

A schematic diagram of the liquid flows is shown as Figure III.11.1. There are three liquid flows – acetylacetone, ammonium acetate, and water. Highly purified water, such as HPLC grade,

works best; but any reasonably pure water can be used as long as its purity is consistent. We purified water in our laboratory by passing tap water through a pretreatment cartridge, then distilling it, and finally finishing it using activated charcoal, organic extraction and deionization cartridges. The front panel of the instrument has two manually actuated multi-port valves which control the measurement mode of the instrument and injection of liquid samples. If the liquid/gas valve is set to liquid, the water bypasses the diffusion scrubber assembly and flows through the peristaltic pump to the load/inject valve. For routine operation this valve is in the LOAD position and the water flows straight through the valve, mixes with the reactants and flows to the reactor.

The liquids take about three minutes to pass through the reactor, which is stabilized at a temperature of 70ºC. During passage through the reactor, any formaldehyde in the liquids is converted to the fluorescent reaction product and the dihydrolutidine is carried to the fluorescent cell where it is detected. The flush ports shown in the figure are normally capped – they are used to purge the system of any persistent bubbles in the fluorescence cell, which can produce very large and spurious signals at the detector.

For liquid formaldehyde measurements, a liquid sample is injected into the injection port while the load/inject valve is in the load position. This fills the sample loop with the liquid sample. The load/inject valve is then turned to INJECT, and the sample is pumped out of the sample loop and directed to the reactor followed by the fluorescence cell. For gas phase formaldehyde measurements, the gas/liquid valve is set to GAS. The purified water from the supply bottle then flows through the diffusion scrubber assembly before passing through the peristaltic pump and the load/inject valve. The gas flow schematic is shown as Figure III.11.2. The heart of the diffusion scrubber is a single strand of Nafion™ tubing. The Nafion has an O.D. of 0.838 mm (0.033”) and an I.D. of 0.635 mm (0.025”). This strand of Nafion passes down the center of 30 cm long thin wall 3.2 mm (1/8”) O.D.

Figure III.11.1. Liquid flow schematic for MA-100

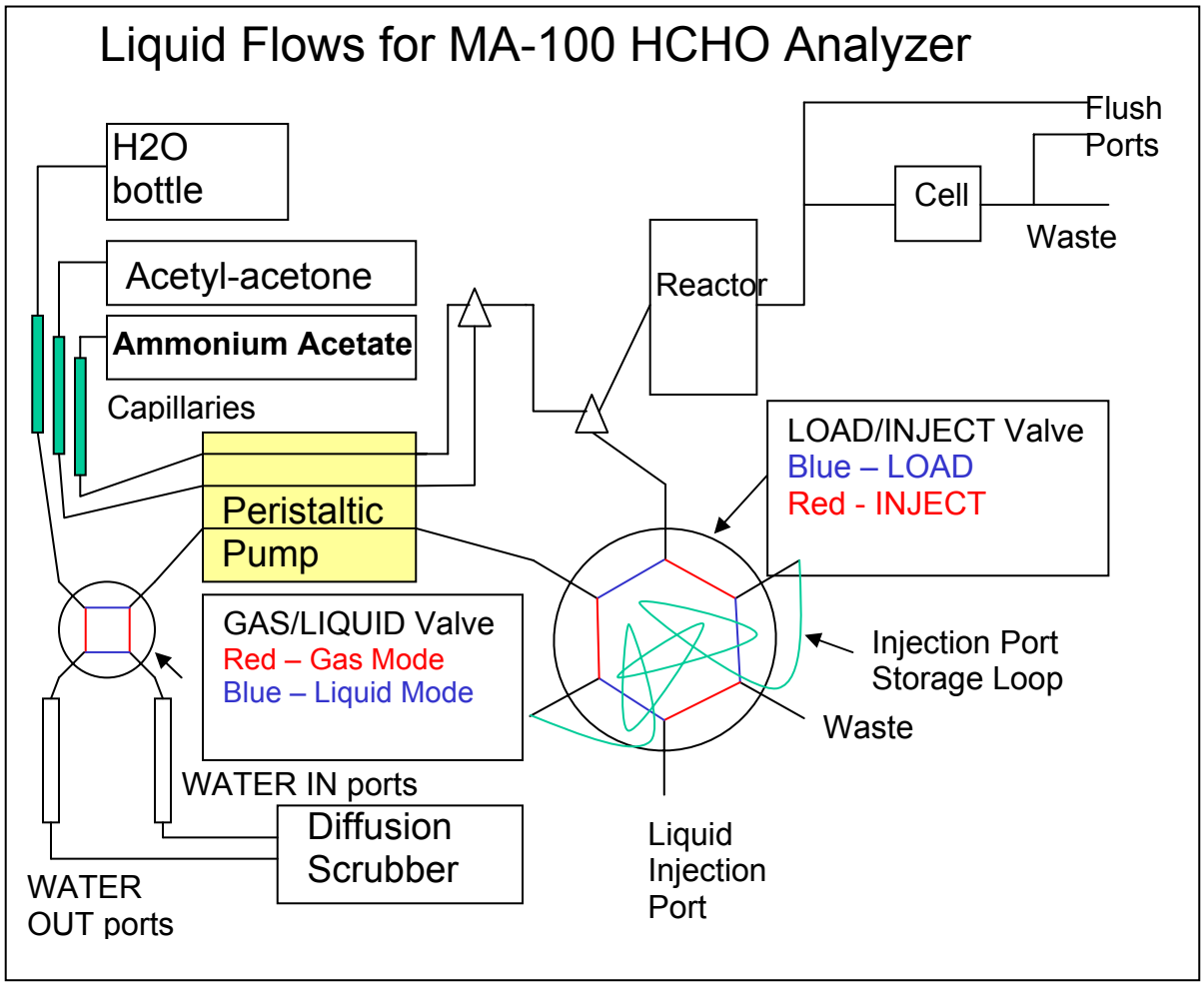

Figure III.11.2. Gas flows for MA-100 HCHO analyzer.

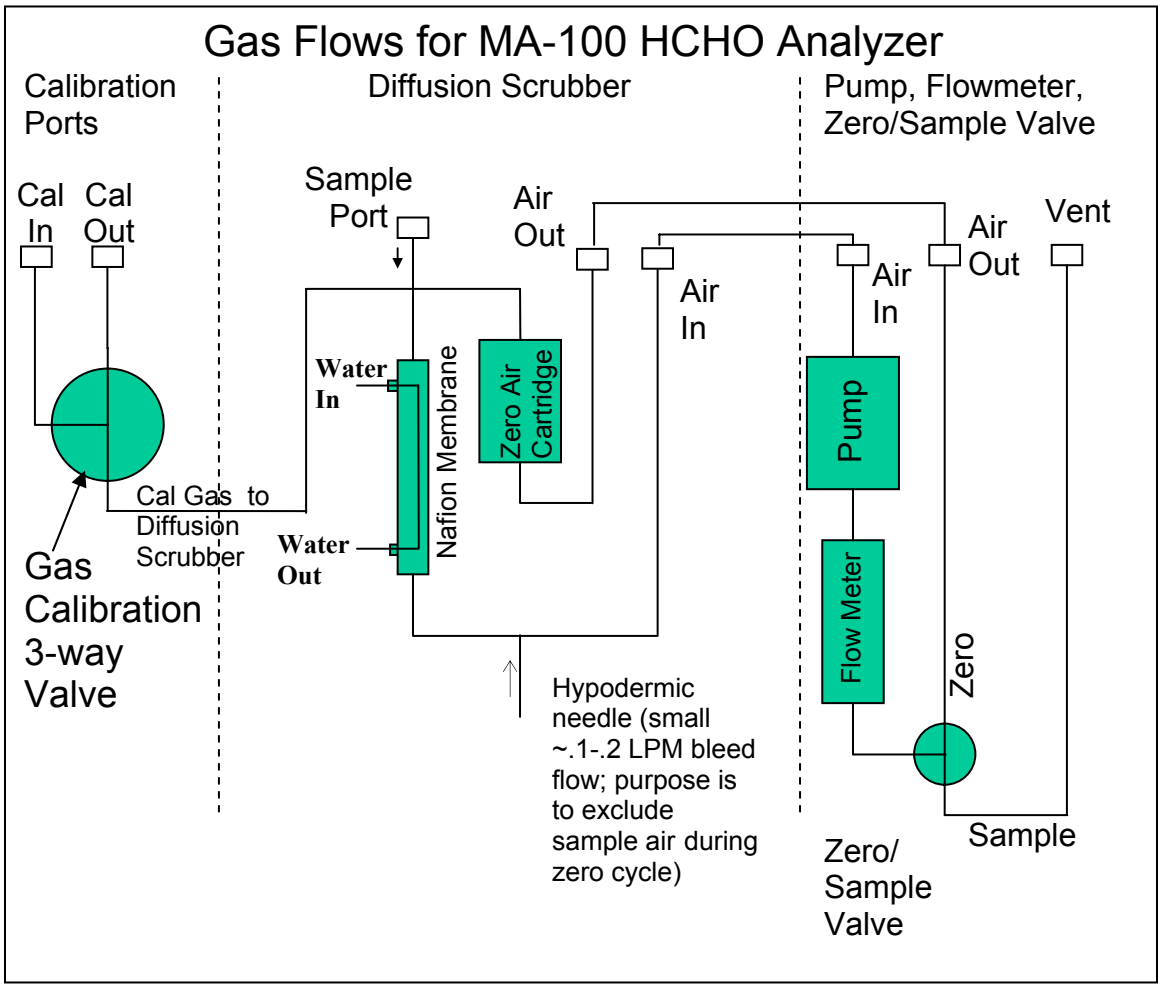

Teflon tube. The water flows through the Nafion tube and the sample air (or zero air) flows through the larger diameter Teflon tube. Nafion is a semi-permeable membrane and gas exchange, particularly of polar gases, occurs across the membrane wall. In this case, formaldehyde from the air flowing in the large diameter Teflon tube exchanges across the membrane wall and is dissolved in the flowing water and carried to the load/inject valve, the reactor and the fluorescence cell.

Each measurement cycle is 10 minutes long and divided into a three-minute sample period and a seven-minute zero period. During the sample period the flow of ambient air (approximately 1.5 LPM) enters the sample port and flows directly into the diffusion scrubber where some fraction of the soluble gases (in particular HCHO) is "scrubbed" into the water flowing through the Nafion tube. After passage through the diffusion scrubber, the sample air is joined by a small bleed flow of 100-200 cc/min before passing through the pump, the flow meter and out the vent port. During the zero period the air which passes through the pump and flow meter is directed through a Carulite chemical scrubber and is subsequently introduced at a cross upstream of the entrance to the diffusion scrubber. Since the total flow is equal to the sample flow plus the bleed flow, this supply of "zero air" is sufficient to meet the sample flow demand and produce a small flow out of the sample port. This small excess flow provides assurance that only zero air passes through the diffusion scrubber during the zero period.

The ambient air was obtained from a "snorkel" port built into the outside wall of our third floor laboratory in Albany, NY. The air is drawn through separate 6.2 mm (1/4") O.D. Teflon lines, one for each analyzer - which have been fed through the port, then ended with an inverted funnel to protect from the intrusion of rain. Once inside the laboratory, the sample lines connect to the two MA-100 instruments.

Calibrations of the instrument may be done manually or programmed to be performed automatically using a potentiometer on the main electronics board and the "CAL" button on the instrument front panel. Manual calibrations are performed by adding calibration gas with a known concentration of HCHO and a total flow of 2 LPM or greater through a "dump tee" into the sample port. Automatic calibrations can be programmed to run in sets of "N" ($0 < N < 15$) calibrations every "M" ($0 < M < 999$) measurement cycles. The potentiometer on the main electronics board sets "N" value. When "N" is 0, there are no automatic calibrations (i.e., the gas calibration valve always remains in its normally open state). The "CAL" button on the front panel sets "M". For this study, "N" was set to one and "M" was set to 24, which resulted in one calibration cycle every four hours. During the automatic calibration cycle, the three way calibration valve switches the calibration gas flow so that it is introduced at the cross fitting upstream of the diffusion scrubber. As during the zero period of the measurement cycle, the excess calibration gas flows out the sample port.

For gas phase measurement, the continuous cycling between sample and zero air produces an output signal with a 10 minute period exhibiting a peak signal due to the sample period and a minimum signal due to the zero period. Figure III.11.3 shows raw signals plotted for a 6 hour period during the study period. There are two calibration periods shown in Figure III.11.3; at 13:00 and 17:00. Small baseline jumps like those observed in the figure are common, and highlight the need for measurement of the zero signal frequently.

.

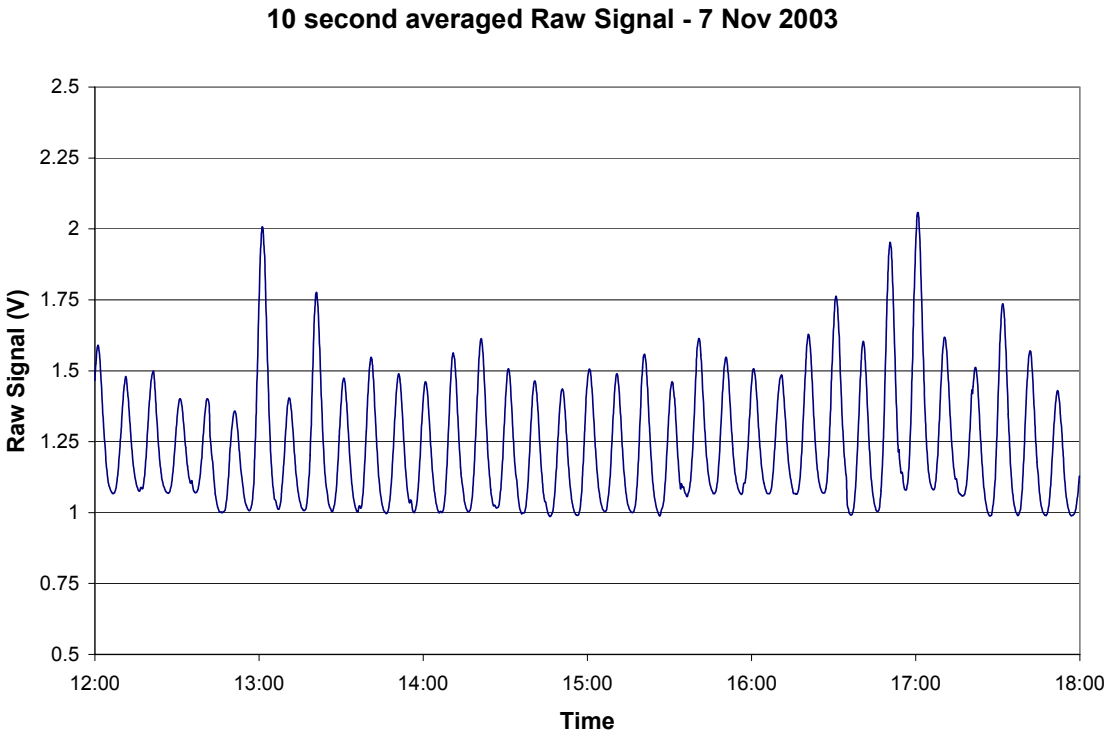

Figure III.11.3. Raw signal showing the peak and valley waveform of data produced by the instrument

The raw signal output data was recorded by an ESC 8816 data logger configured to store 10 second averaged values. Since the sample period is only three minutes long, we determined that sub-minute time resolution for the data was required. These 10-second averaged data were downloaded to a computer for storage and analysis every hour. Referring again to Figure III.11.3, the difference signal in volts between the maximum and minimum signals is the quantity that is proportional to the HCHO concentration in the liquid sample passing through the reactor and the fluorescence cell. We developed a spreadsheet algorithm to calculate difference signals by choosing maximum signals and minimum signals on either side of each maximum. These difference signals were converted to formaldehyde concentrations using the known formaldehyde concentrations and the measured difference signals determined during the calibration cycles.

III.11.3 Kintek Model 491M permeation tube calibrator

Concentrations of formaldehyde for calibrations were produced using a paraformaldehyde permeation device installed in Kintek 491M calibrator. The permeation device was obtained from VICI Metroncs, Inc. and was built with a 1.5 cm long active length. When used at a temperature of 50ºC, the device produced a HCHO output of 8.8-9.2 nanograms per minute, determined as described below. This permeation rate of HCHO, when carried in a zero air flow of 1.7 to 4.6 LPM, produced a concentration range of 1.6 to 4.4 ppbv for calibration of the MA-

100 instruments. For example, the two calibration peaks in Figure III.11.3 correspond to formaldehyde concentrations of 3.7 ± 0.4 ppbv. For automatic calibrations as performed in this study, the Kintek calibrator generates a constant output flow at the selected [HCHO], and the flow is sent to an exhaust hood when the calibration cycle is not active.

The permeation rate for the device was determined by comparing liquid standards of aqueous formaldehyde with liquid samples collected by bubbling the output of the Kintek calibrator through water to collect the gaseous formaldehyde into solution. The concentration of the liquid standard is determined by an iodometric titration (Methods of Air Sampling and Analysis: Third Edition, Lodge, J.P., Jr. Editor, Lewis Publishers, Inc., Boca Ratan FL, 1988). The aqueous standard we use is about 30 millimoles per liter, and is diluted in a two-step process to obtain low level liquid standards in the range between 1.5 and 10 micromoles per liter. These calibration standards are introduced to the analyzer in the liquid mode to produce a liquid formaldehyde calibration curve. The permeation output samples, which are collected for periods ranging from 24-72 hours, are diluted to exactly 100 or 250 milliliters and injected into the analyzer immediately after the liquid calibration curve has been generated. The liquid formaldehyde concentrations of these samples are determined from the calibration curve; and measured permeation rates are determined using the measured concentrations and the exact sample collection durations and volumes. Ten permeation device output samples collected both before and after the measurement period yielded a permeation rate of 9.0 ± 0.5 nanograms per minute as the permeation rate of the device.

The Aerodyne Research, Inc. TDLAS (Tunable Diode Laser Absorption Spectrometer) is used as reference instrument (see Chapter III.14).

III.11.4 Results

III.11.4.1 Instrument precision and performance from side-by-side operation of two MA-100 analyzers

The two AlphaOmega MA-100 analyzers were operated side-by-side for a one month period from October 15 to November 14, 2003. As noted above, the instruments sampled from identical inlets that were fastened to each other to assure identical sample air was introduced into each instrument. On October 23 during a routine maintenance procedure to change pump tubes on the peristaltic pump of one analyzer, the reagent flows were reversed for a short time and acetylacetone and/or ammonium acetate reagents flowed through the Nafion tube and ruined it. The diffusion scrubber for this instrument needed to be rebuilt with a new Nafion tube, and there is not comparable data for the period of October 23 to November 3. Therefore the data for comparison is broken up into two parts; from October 15 to October 23 and from November 3 to November 14.

Figure III.11.4 shows the time series comparison of the two AlphaOmega MA-100 analyzers for the first part of the comparison. The two instruments are identified by their serial

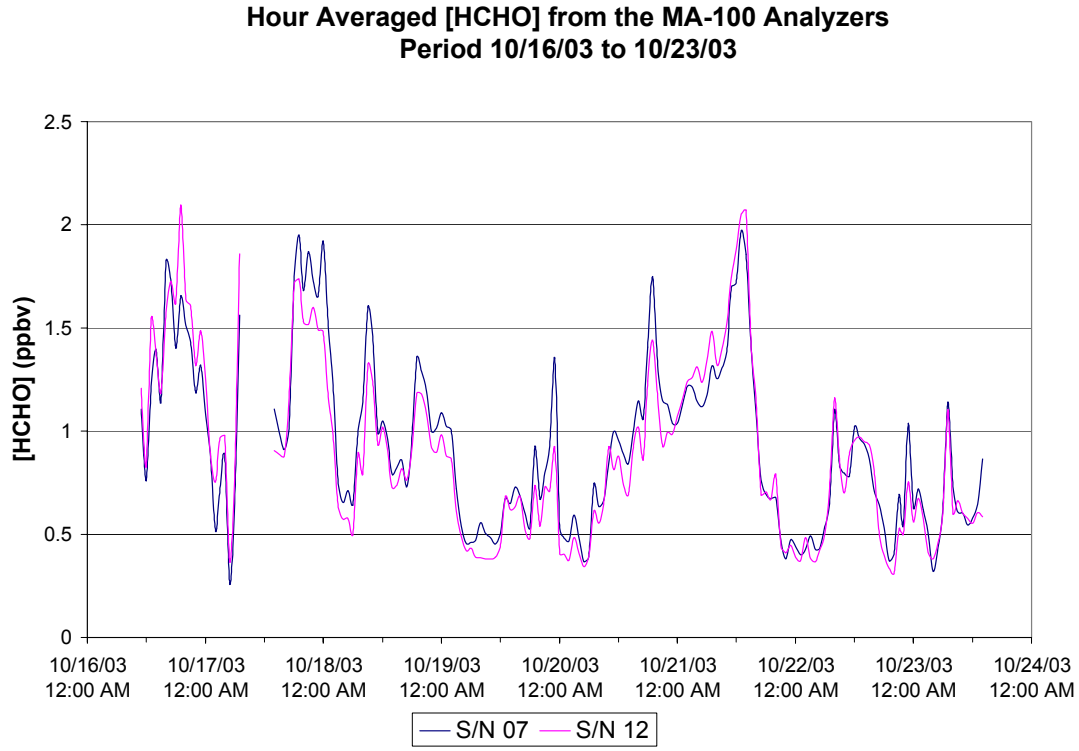

Figure III.11.4. Time series plot of the HCHO concentrations from the two AlphaOmega semi-continuous analyzers for the first part of the study.

numbers, S/N 07 and S/N 12. As the figure shows, the two instruments track each other quite well, but not perfectly. Sometimes one analyzer reports values 10-20% higher than the other, but for this period there is no systematic difference. A correlation scatter plot of these hour averaged data points is presented as Figure III.11.5. The slope is very close to one and the intercept is very close to zero, indicating a high degree of agreement between the two instruments. The correlation R^2 is also high, nearly 0.9, indicating a high degree of correlation. The scatter about the regression lines is consistent with an uncertainty or error estimate of about 20% for this data.

Figure III.11.6 presents a time series comparison of the hour averaged HCHO concentrations from the second part of the study. During this period, some higher formaldehyde concentrations were measured by the analyzers, particularly on November 3 and overnight between November 10 and 11. Once again the analyzers track fairly well, only

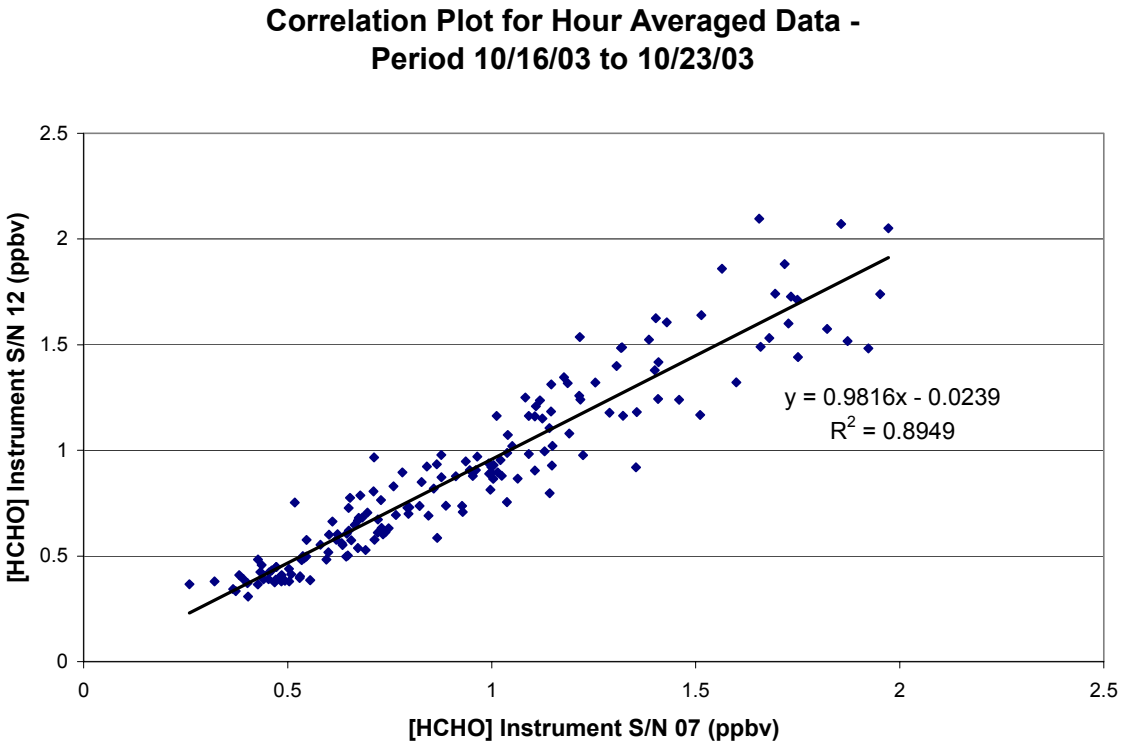

Figure III.11.5. Correlation scatter plot for the hour averaged data from the two AlphaOmega HCHO analyzers. The coefficients and line from a linear regression fit to the data are also shown.

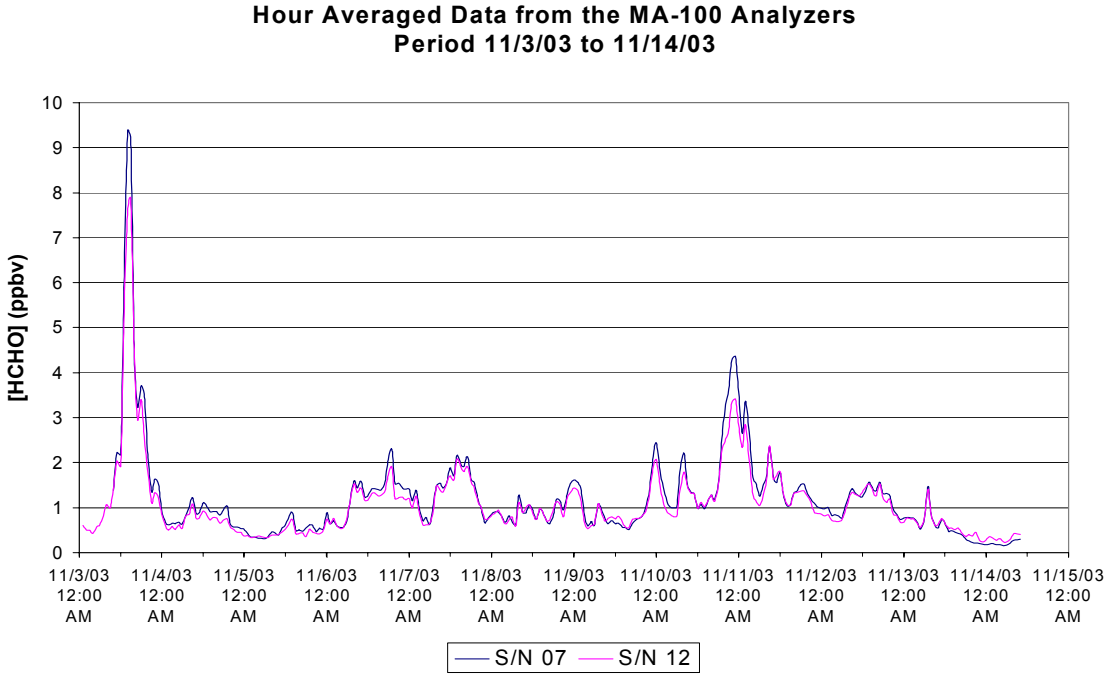

Figure III.11.6. Time series plot of the HCHO concentrations from the two AlphaOmega semi-continuous analyzers for the second part of the study.

for this period there is a clear systematic difference, with instrument S/N 12 consistently lower than instrument S/N 07. Instrument S/N 07 had a newly refurbished diffusion scrubber tube for this period, but it is not clear why this would cause a systematic difference – especially since both instrument calibrations were tied to the ongoing gas phase calibrations from the Kintek calibrator. The timing and structure of the peaks and features in the reported HCHO concentrations are very consistent between the two analyzers. The correlation scatter plot of these hour averaged data points is presented as Figure III.11.7. The slope of the fitted regression line is about 18% below one, but the correlation R^2 is much higher – above .98. If the two highest points in Figure III.11.7 are removed, the regression line coefficients change only slightly, to 0.8303 for the slope and 0.100 for the intercept.

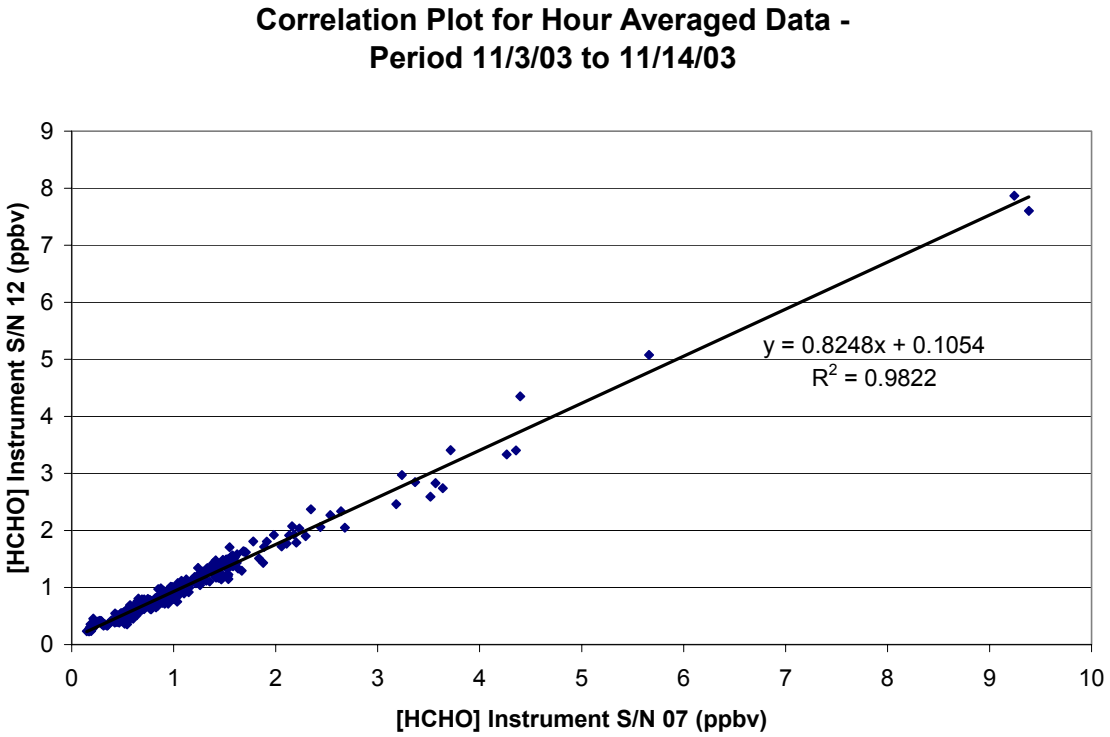

Figure III.11.7. Correlation scatter plot for the hour averaged data from the two AlphaOmega HCHO analyzers. The coefficients and line from a linear regression fit to the data are also shown.

Two things that are different between the data shown in Figures III.11.4 and III.11.5 and the data shown in Figures III.11.6 and III.11.7 are the measured levels of HCHO and the new Nafion tube in the diffusion scrubber of instrument S/N 07. In particular, all the data in Figures III.11.4 and III.11.5 is below 2 ppbv, with the exception of four values reported by instrument S/N 12 between 2 and 2.2 ppbv. If the difference in correlation slopes is due to the higher concentration points, then selecting only data with reported [HCHO] less than 2 ppbv from the second period should show a significantly different slope. When the data is culled and selected in this way, the slope does increase, but only slightly, to 0.854. This "concentration effect" does not seem to explain the difference. To explore the difference due to the new Nafion tube, the calibration

factors for the whole study period are shown in Figure III.11.8. The calibration factor is determined by dividing the calibration concentration of HCHO from the Kintek calibrator by the computed difference signal reported by the analyzer. There were no major changes to the S/N 12 instrument during the study period and the figure shows that the calibration factor changed only slowly over the one-month period of the study. On the other hand, the calibration factor for the S/N 07 instrument changed dramatically after the installation of the new Nafion tube in the diffusion scrubber. The refurbished diffusion scrubber was about 1.5 times more efficient at "scrubbing" the gaseous formaldehyde from the gas phase into the liquid phase. (The scrubber efficiency can be determined from the liquid calibration, the gas calibration, and the water and sample air flow rates. Measured scrubber efficiencies for the two instruments were in the range of 30-60% for the measurement period.) The change in correlation slope occurs simultaneously with the change in calibration factor (and scrubber efficiency), but as noted above, both instruments are calibrated by and tied to the output of the same calibrator; and we have no explanation for this change in slope.

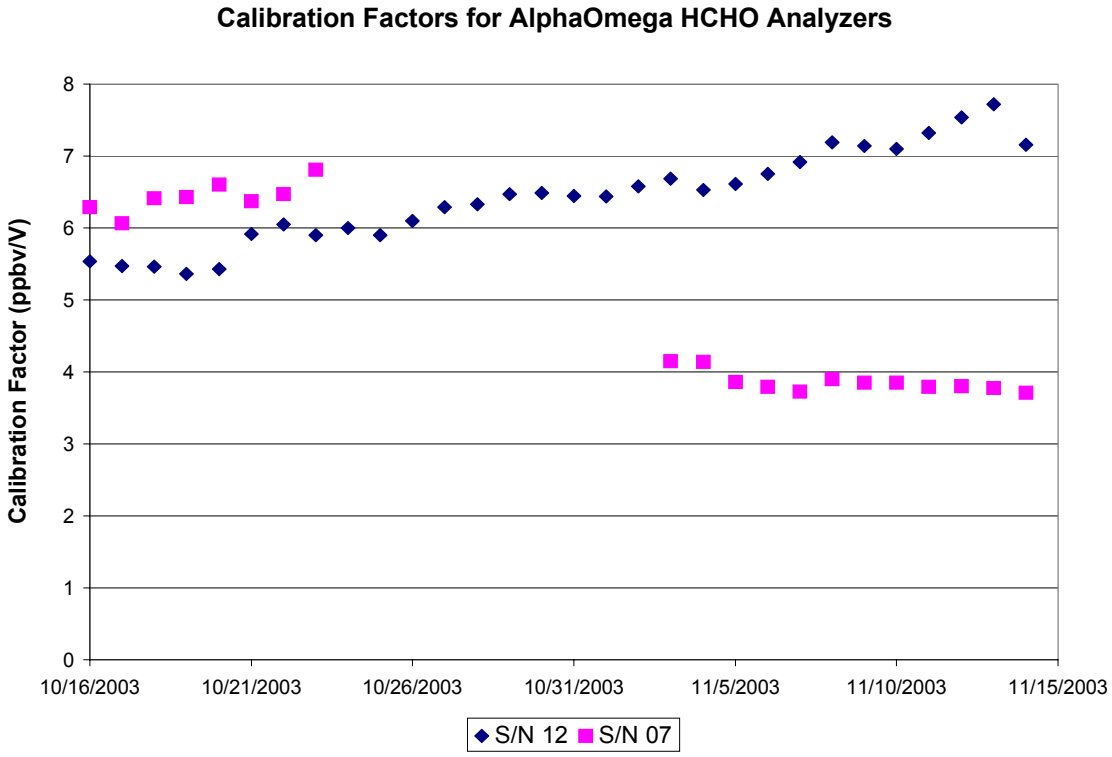

Figure III.11.8. Calibration factors for the study period determined from a permeation tube calibrator.

III.11.4.2 Comparison of the MA-100 instruments with the TDLAS system

As noted above, infrared tunable diode laser measurements of formaldehyde are quantified using tabulated absorption line parameters, and for this reason such measurements are considered to have a high degree of accuracy. We undertook a comparison of the HCHO measurements from the Alpha Omega analyzers and the TDLAS system to further check the accuracy of the diffusion scrubber/liquid fluorescence instruments. The data from the TDLAS system, while

recorded and available every second, was averaged to one hour for the comparison. It is worth noting that the duty cycles of the instruments are both significantly less than one, and they are different from each other. The diffusion scrubber/liquid fluorescence analyzer measures sample air for 3 minutes out of every 10, so its duty cycle is 30% for hours without a calibration cycle, and 25% for hours with a calibration cycle. The TDLAS system spends exactly half the time measuring an absorption spectrum from sample air, and half the time measuring a background spectrum for subtraction; so its duty cycle for normal measurement conditions is 50%.

A comparison of the HCHO concentrations measured by the TDLAS and the two diffusion scrubber/liquid fluorescence (DS/LF) analyzers over a four and a half day period is shown as Figure III.11.9. There is a high degree of correlation between the TDLAS

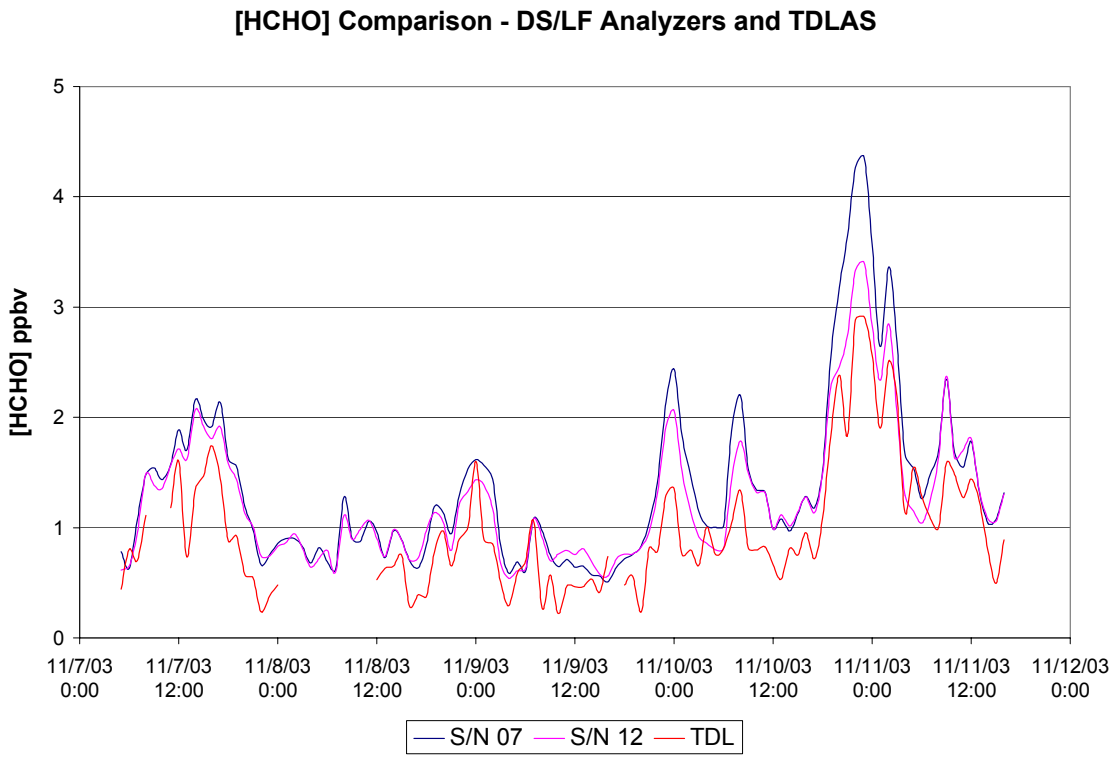

.

Figure III.11.9. Time series comparison of the HCHO hour averaged measurements from the TDLAS and the DS/LF analyzers over the period from November 7 to November 11, 2003

and the DS/LF analyzers, but a systematic difference is also evident. The TDL measurements are systematically lower, and also exhibit a number of downward excursions in concentration not seen by the DS/LF analyzers. There are also roughly six examples of dips in [HCHO] observed by both instruments where the dip reported by the TDL is much lower than the dip reported by the DS/LF analyzers. This could be due to an interfering species (perhaps a higher aldehyde) producing signals that are too high from the DS/LF analyzers; or optical fringe noise from the TDLAS system; or some other unknown cause.

The correlation plot of the data shown in Figure III.11.9 is displayed in Figure III.11.10. There is a high degree of correlation, as could be inferred from Figure III.11.9, but the correlation R^2 values are only in the range 0.82 to 0.85. Likely causes of the scatter are as mentioned above, the possibility of interfering species in the DS/LF analyzers, and/or the optical fringe noise of the TDL system. One indication of the possible interference may be the positive intercept of the unconstrained regression line in Figure III.11.10. The data does have quite a bit of scatter, so we will not use this intercept as proof positive of an interference nor as a quantitative measure of the magnitude of any potential interference. Additional data, or data with much higher correlation would add credence to such a theory. In any case, the DS/LF analyzers report higher HCHO

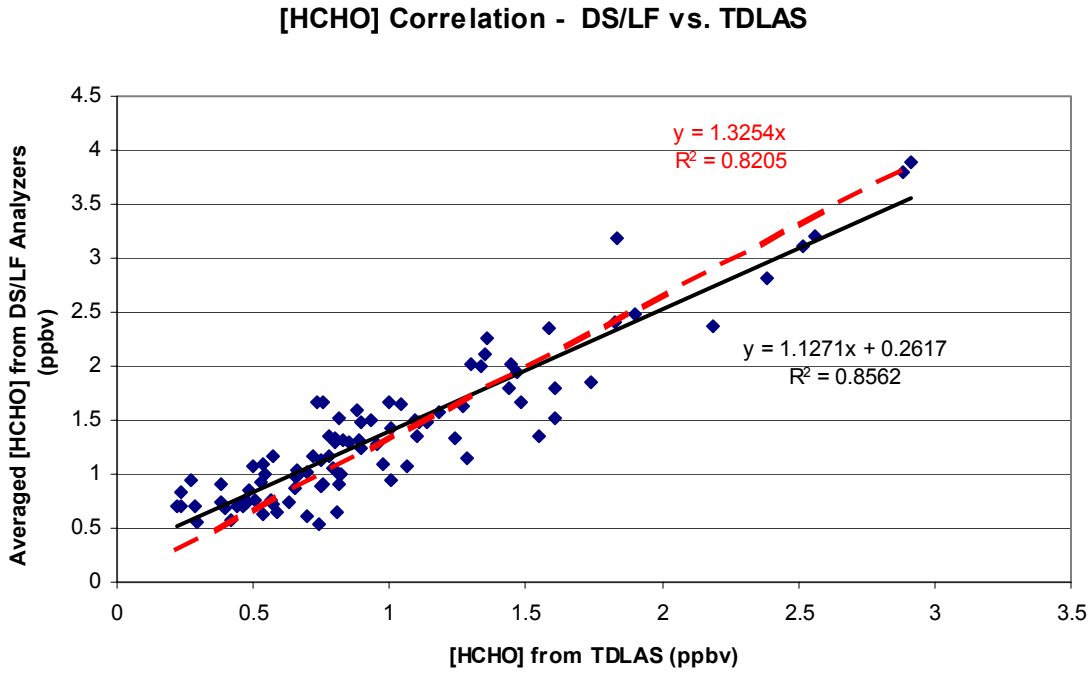

Figure III.11.10. Correlation scatter plot of the hour averaged data for the TDLAS and the DS/LF analyzers. The solid line and the regression equation to the right of the line are from a full unconstrained least squares fit to the data. The dashed line and the equation to the left of the line are from a least squares fit constrained to pass through (0,0).

concentrations than the TDLAS system. The TDLAS and the Kintek calibrator were checked against each other for a period of more than 6 hours on November 6, 2003. Using the permeation rate determined as described above and the calibrated gas flow rate, the calculated output concentration from the calibrator was 2.0 ± 0.2 ppbv. The TDLAS measured [HCHO] equal to 1.77 ± 0.38 ppbv for the comparison period. These values easily agree within the error limits, but show the same systematic difference observed in the comparison of the TDLAS and the DS/LF analyzers.

III.11.5 Summary

A commercially available semi-continuous formaldehyde analyzer (MA-100 Methanalyzer, AlphaOmega Power Technologies, Albuquerque, NM) was evaluated in a month long series of

tests at our laboratory in Albany, NY. The instrument precision was tested by operating two identical analyzers side-by-side for this period. The analyzers were calibrated using a formaldehyde permeation device installed into a permeation oven gas calibration instrument. An additional check of the calibration and accuracy of the analyzers was provided by comparison with gaseous formaldehyde measurements from an infrared tunable diode laser instrument. The month long precision test was interrupted by a problem with the instrument due to an operator error which ruined the diffusion scrubber of one instrument. This resulted in two periods of side-by-side measurements, the first lasting seven days, and the second twelve days. During the first period the correlation R^2 was reasonably high (almost 0.9) and the slope of the regression line was nearly one (0.982). During the second period the correlation was much higher, but the slope of the regression line was only 0.825. Some possible causes for this change in behavior were proposed, but the true cause remains unknown. We conclude that the relative precision for this instrument is on the order of 25%.

The comparison tests with the TDLAS system showed good correlation and a level of agreement within the combined error limits of the two techniques. There are some indications that there may be an interference signal in the DS/LF technique, causing the observed systematic difference. The observed systematic difference for the ambient measurements is consistent with the fact that the TDLAS also reported [HCHO] about 11-12% lower than the expected value while measuring the output of the permeation calibrator. Our tests were not extensive enough to confirm the existence nor identify any interfering species. Depending on whether there is a systematic interference or not, the accuracy of the DS/LF analyzers with respect to the TDLAS system is approximately 15-35%.

The AlphaOmega MA-100 analyzer is a very sensitive, fairly robust instrument which ran well during the study period. The reagent consumption is quite modest and maintenance is straightforward. There are some improvements which would make the analyzer considerably more attractive for routine operation. First, and most important, a reliable on-board data differencing and signal processing scheme needs to be implemented. We needed to download data in 24 hour increments and perform time consuming manual analysis to obtain the data used in this paper. Second, the air flow rate is determined by the pump capacity and not by any active or passive flow control device. This leads to rather different flow rates for different instruments (for our two instruments the air flow rates were roughly 1.35 and 1.65 LPM). These flow rates are susceptible to change as the pump get less efficient. The air flow rate will affect the efficiency of the diffusion scrubber and needs to be stable. Third, the cycle timer should be more precise and be adjustable by the user. External data reduction would be simpler if the ten-minute period was precisely ten minutes, but it is not. Instead of exactly 144 cycles in a day, we observed closer to 144.15. In addition to more precision in the timer, it would be useful if the user could choose the duration of the sample and zero periods within the 10-minute measurement cycle.

- Instrument deployment period during the winter 2004 field campaign: 1/12/04 – 2/6/04
- Air was sampled from a glass manifold. The inlet tube to the manifold was a 3 meter long, 0.5 inch O.D. PFA Teflon tube. A blower produced a residence time in the manifold and inlet tube of less than 0.1 seconds. The instrument was connected to the manifold with a roughly 1.5 m long, 0.25 inch O.D. black PFA Teflon tube.

- In field QA procedures and checks included daily checks of operation parameters, and frequent checks of instrument calibration and zero as described below.
- Perastaltic pump tubes were changed once during the campaign.
- Zero air from a cylinder was further scrubbed with columns of drierite, purafil and activated charcoal for use in measuring instrument zero response.
- The instrument detection limit (calculated as 3*SD of a blank series) is 0.03 ppbv.
- Accuracy (determined ultimately from liquid titrations of an aqueous HCHO standard) is estimated to be ± 30%.
- Precision (determined from repeatability of measured difference signals for calibration points) is approximately 10%.
- Data completeness (ratio of valid data points to maximum possible data points from 1/12/04 14:45 to 2/6/04 12:15) is 97%.
- Data summaries are presented in Table III.11.1.

Table III.11.1. Data Summary (10-min data). All concentrations in ppbv

	MA100
Minimum	0.061
Median	0.757
Mean	0.880
Maximum	5.797

III.12 Penn State University Ground-based Tropospheric Hydrogen Oxides Sensor (GTHOS)

GTHOS uses laser-induced fluorescence (LIF) to measure OH and HO_2 simultaneously (Mather et al., 1997). OH is both excited and detected with the $A^2\Sigma^+$ (v'=0)$\rightarrow X^2\Pi$ (v"=0) transition near 308 nm. HO_2 is first reacted with reagent NO to form OH and is then detected with LIF. The ambient air is pulled by a vacuum pump through a small upward facing inlet (1mm diameter), down a short, sampling tube, and into two low-pressure multipass White cell detection cells. The first cell is for OH and the second for HO_2. Detection occurs in each detection cell at the intersection of the airflow, the laser beam, and the detector field-of-view. The pulsed laser has a 3 kHz repetition frequency, 28 ns long pulses, and produces about 10-20 mW of tunable UV near 308 nm. The laser is tuned on and off resonance with the OH transition in a 20-second cycle; the OH fluorescence is the difference between the signal on resonance and the signal off resonance. The detector is gated to detect the OH fluorescence after each laser pulse has cleared the detection cell. A reference cell containing OH indicates when the laser is on and off resonance with the OH transition

III.12.1 Data summary

Summer 2001:

During this field campaign GTHOS produced ~ 600 hours 1-minute averaged OH and HO_2 data. The percentage of the valid data was about 88% for both OH and HO_2 (Table III.12.1). The reasons for the 12% downtime are primarily calibrations and interference testing (Figure III.41).

The mean OH concentration was 0.125 ppt (~ $3.0x10^6$ molecules/cm^3) and the maximum during midday was 0.2-0.4 ppt. For HO_2, the mean value was 1.33 ppt (~ $3.2x10^7$ molecules/cm^3) and the maximum was about 3-6 ppt during midday. The frequency distributions of OH and HO_2 are shown in Figure III.40. Most OH mixing ratios were less than 0.3 ppt and most HO_2 mixing ratios were less than 4 ppt.

Table III.12.1a Completeness of OH/HO_2 measurement during PMTACS-NY2001

Species	OH	HO_2
Period of operation	June30—August 2, 2001	July 2—August 2, 2001
Sampling frequency	5 Hz	5 Hz
Average time	1 min	1 min
Percentage of valid data	87.5%	88.0%
Mean	0.125 ppt	1.33 ppt
Median	0.094 ppt	0.921 ppt
Minimum value	-0.010 ppt	-0.11 ppt
Maximum value	0.835 ppt	18.40 ppt

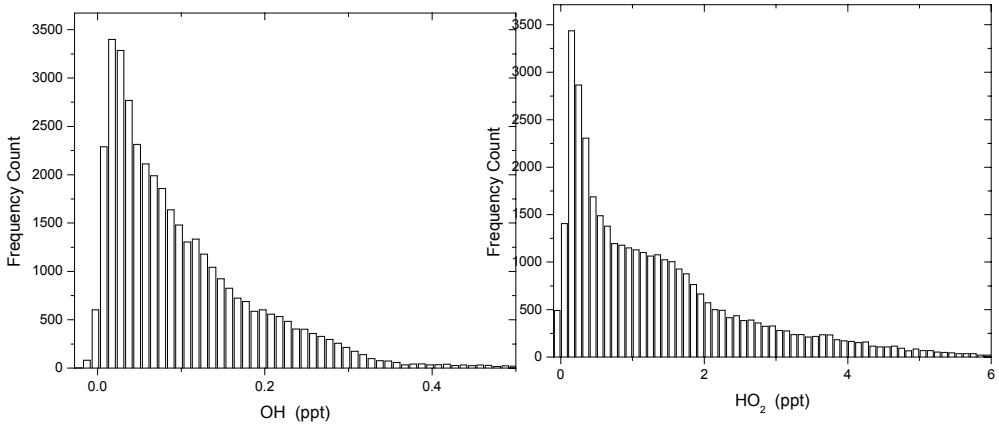

Figure III.40 Frequency distribution of OH and HO_2 data

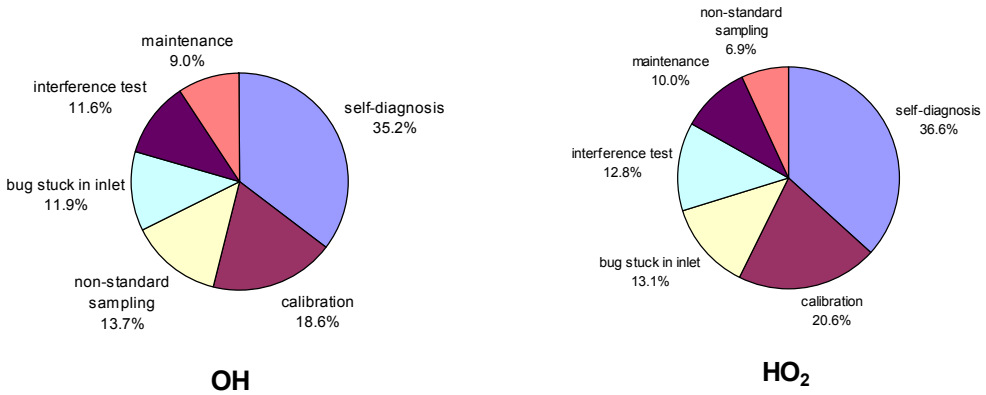

Figure III.41 Reasons for the 12% downtime for OH and HO_2 measurements

<u>Winter 2004</u>:

OH was measured between 10 January and 6 February and HO_2 was measured between 13 January and 6 February during the PMTACS-NY winter 2004 campaign. 1-minute averaged OH and HO_2 data were continuously collected throughout the campaign. The percentage of the valid data was about 90% for both OH and HO_2 (Table III.12.1b). The reasons for the 10% downtime are primarily due to routine interference tests that happened every hour for about 5 minutes.

The mean OH concentration was 0.013 ppt (~ $3.6x10^5$ molecules/cm^3) and the maximum during midday was 0.02-0.15 ppt (Figure III.12.1). For HO_2, the mean value was 0.33 ppt (~ $9x10^6$ molecules/cm^3) and the maximum was about 0.4-2.5 ppt during midday (Figure III.12.1).

Diurnal profiles of measured OH and HO_2 show that the maximum OH mixing ratio was about 0.05 pptv and for HO_2 the maximum value is about 0.8 pptv (Figure III.12.1). Both OH and HO_2 peaks appeared around noon, which indicates that the radical production during daytime was dominated by photolysis processes. Both OH and HO_2 during winter were lower by a factor of 5-6 than in summer in New York City.

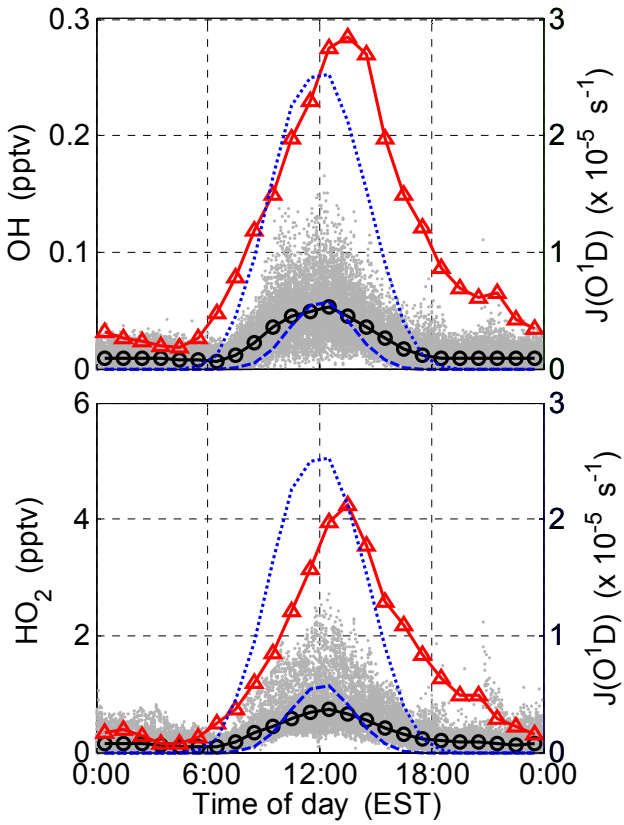

Figure III.12.1 Median diurnal profiles of OH (top) and HO_2 (bottom) during the summer and winter campaigns in New York City, together with O3 photolysis frequency, $J(O^1D)$. Small dots represent 1-minute data measured in the winter 2004 campaign. The linked circles show the average of winter values recorded during one hour time intervals and the linked triangles show the average of summer values recorded during one hour time intervals. The dashed line shows the winter $J(O^1D)$ and the dotted line shows the summer $J(O^1D)$.

Table III.12.1b Completeness of OH/HO_2 measurement during PMTACS-NY winter 2004

Species	OH	HO_2
Period of operation	January 10—February 6, 2004	January 13—February 6, 2004
Sampling frequency	5 Hz	5 Hz
Average time	1 min	1 min
Percentage of valid data	90.0%	90.0%
Mean	0.020 ppt	0.33 ppt
Median	0.013 ppt	0.23 ppt
Minimum value	-0.010 ppt	-0.02 ppt
Maximum value	0.165 ppt	2.72 ppt

For flagging of the OH/HO_2 data the NARSTO Data Qualification Flag set was used. The following flags have been used in the PMTACS-NY 2001 and PMTACS-NY 2004 datasets:

V0	Valid Value	All valid 1-min averaged data, that are not qualified in any way
V1	Valid Value, but wholly or partially below detection limit	For all valid 1-min data, where the average during this interval is below the detection limit
M2	Missing Value, because invalidated by Originator	Value invalidated, because instrument was sampling under non-standard conditions or during maintenance, calibrations and QA tests.

Detection Limit (V1): The detection limit was determined for every 1 min interval for which data are available. The detection limit was calculated as DL = 2 * standard deviation of the background (see below—instrument calibration). All data values below the corresponding detection limits were left as they are and flagged with V1.

Invalidated values (M2*):* Data were recorded when the instrument was sampling under non-standard conditions or during maintenance, calibrations and QA tests. They were flagged as 'M2' and the values are marked as (-999.99).

III.12.2 Quality assurance

III.12.2.1 Field campaign quality assurance

We did quality assurance during the campaign by testing the background signal and by calibrating the HO_x instrument every week.

- Instrument self-diagnosis

Every hour on the half-hour the control system initiated an automatic diagnostic sequence in which various facets of instrument performance were evaluated. During this five minute interval, the spectrum of the OH fluorescence was scanned in the reference cell and in ambient air to ensure proper alignment of the laser system. Spectral scans showed that there was little spectral interference from other atmospheric species and that the laser was alternating wavelengths properly between the on-line and off-line positions. Possible interferences were tested by injecting C_3F_6 upstream of the detection chambers to selectively remove the OH from the sample and thereby establish an instrumental baseline. In addition, the laser was momentarily shut off to keep track of the offsets on the photodiodes that monitor the laser power at various positions in the detection system. For HO_2, the reagent NO flows were varied to ensure that the peak OH signal was obtained from the NO addition. These tests showed that the instrument performance was stable for the entire field campaign.

- Background signal tests

We tested the background signal by internal addition of perfluoropropylene (C_3F_6) and adding a glass-wool filter in front of the inlet to remove OH radicals. Results indicated the lack of interferences. External addition of C_3F_6 or CO decreased the OH signal about twice as much as did internal addition for both the ambient nighttime OH signal and for the OH signal that was produced by the photolysis of water vapor in zero air. All of these tests indicate that the observed OH signal is not generated internally and is not produced by the laser beam.

A simple test determines if the interference signals are due to photolysis by the laser beam. Because one photon is required to initiate OH or HO_2 production and another to detect OH, any background signal that is laser-generated has a quadratic dependence on laser power. As shown in Table III.12.2, we see this quadratic dependence for excessively high levels of acetone (in OH only) and formaldehyde (in HO_2 only), but not for other background signals in the laboratory or in the atmosphere.

- Instrument calibration

The HO_x instrument was calibrated once a week during the campaign by using photolysis of H_2O to produce equal amount of OH and HO_2. The minimum detectable [OH] we define as the OH derived from twice the standard deviation of the background signal:

$$[OH]_{min} = \frac{(S/N)}{C}\sqrt{\frac{2\sigma_b}{t}}$$

where, S/N is the ratio of signal to noise, C is the OH sensitivity (counts/sec/ppt), σ_b is the standard deviation in the background count rate (counts/sec) and t is the integration time (sec). The detection limits (with 2σ confidence and 1min integration time) were 0.012 ppt (~ $3x10^5$ molecules/cm^3) for OH and 0.1 ppt (~ $2.5x10^6$ molecules/cm^3) for HO_2. These detection limits are consistent with the results of 60-minute laboratory measurements when cleaned zero air is added to the GTHOS inlet.

III.12.2.2 Post field campaign quality assurance

After the field campaign, we carried out the interference studies in the laboratory (Table III.12.2). Many chemical species produce no observable signal. OH and HO_2 signals that are observed when O_3 is added in the laboratory may come from contaminants in system used to produce O_3 and deliver it to the GTHOS inlet, as suggested by the much smaller interference signals that were seen in the lower stratosphere.

Table III.12.2 Laboratory tests of potential interference signals in OH and HO_2 measurements

Gas (X)	$\partial OH/\partial X$ [1] (pptv $ppbv^{-1}$)	$\partial HO_2/\partial X$ [1] (pptv $ppbv^{-1}$)	maximum X in study	Comments
O_3	$1\text{-}15\times10^{-5}$	$2\text{-}40\times10^{-4}$	4 ppmv	higher values observed in lab; Lower values in the stratosphere; produced in the UV laser beam with water vapor present
H_2O_2	~ 0	~ 0	~120 ppbv	
HONO	~ 0	~ 0	~ 5 ppbv	
HCHO	~ 0	5×10^{-4}	250 ppbv	produced in the UV laser beam
SO_2	~ 0	~ 0	4 ppmv	
HNO_3	~ 0	~ 0	~ 50 ppbv	
Acetone	2×10^{-4}	~ 0	200 ppmv	produced in the UV laser beam
Alcohols	~ 0	~ 0	~ 100 ppmv	methanol, ethanol, isopropanol
Alkanes	~ 0	~ 0	200 ppbv	ethane, propane, n-butane
Propene	~ 0	~ 0	20 ppbv	
Isoprene	~ 0	~ 0	20 ppbv	
O_3+alkenes	$<1.5\times10^{-4}$	< 0.015	O_3: 600 ppbv HC:400 ppmv	reaction time: 0.02–0.1 sec

[1] ~ 0 means that the upper limits for maximum X were OH < 0.005 pptv, or HO_2 < 0.1 pptv

III.13 Aerodyne Research, Inc. Mobile Laboratory

The mobile laboratory (operated by Aerodyne Research, Inc. only during the summer 2001 field study) has deployed a series of sensitive, specific, real-time (~1 second response) sensors for aerosol and ozone precursor trace gases and fine particulates; a global positioning system (GPS) ; and a central data logging computer. Specifically, the sensors include: an ARI two-color tunable infrared laser differential absorption spectrometer (TILDAS), capable of measuring between 2 and 4 trace gases simultaneously, such as carbon monoxide (CO), nitrogen oxides (NO, NO_2), nitrous acid (HONO), formaldehyde(CH_2O), and sulfur dioxide (SO_2).; a Licor NDIR instrument to measure carbon dioxide (CO_2); a aerosol mass spectrometer (AMS) to measure particulate number densities, size distributions (0.05 to ~2.5 μm), and volatile and semi-volatile chemical composition as a function of particle size. CN counter to measure particulate number densities (0.003 to 1). Data from the individual instruments are logged on a central computer, enabling all data streams to be stored synchronously. A Trimble GPS system with real-time differential correction collects position information at 1 Hz.

The instruments that are covered by an FRM passed audits prior and after their deployment in the summer 2001 intensive initiated by the company. The remaining instruments were operated under a research method protocol. The QA responsibility for data generated by the mobile laboratory rests with Aerodyne Research, Inc.

The TDLAS uses rapidly tuned infrared diode lasers, coupled to a low pressure, high flow multi-pass absorption cell to measure low level concentrations of atmospheric trace gases with high time resolution. The instrument is described in detail in a series of recent papers. A brief description of the sample handling, the optics, and the data collection modules of the instrument is presented here.

The TDLAS system used a 9.5 mm (3/8") O.D. Teflon tube as its inlet. This inlet was tied together with the two inlets for the MA-100 analyzers. The TDLAS sample flow rate was 10 SLPM, which corresponds to an ~ 1 second residence time for sample gas in the multi-pass absorption cell. The sample flow enters the absorption cell through a small orifice and the pressure in the absorption cell is maintained at around 3300 N/m^2 (25 Torr). The reduced pressure is necessary to maintain sharp and distinct absorption lines.

The optical portion of the TDLAS system forms the light from the output of the infrared diode laser in two beams for each laser – a main beam and a reference beam. The reference beam is sent through a reference cell containing a high concentration of HCHO (bus also at a low pressure). The high contrast absorption signals from the reference beam are used to lock the laser frequency to the absorption line. The main beam is directed into an astigmatic Herriott-type multi-pass absorption cell, then out of the cell and back to a liquid nitrogen cooled detector. The cell's mirrors are aligned such that there are 174 passes of the light beam before it exits the cell; with a mirror spacing of 0.882 meters the total absorption path length for the cell is 153.5 m.

The electronics module controls the laser diode frequency, and processes the detected absorption signals to return HCHO concentrations. The instrument computer sends commands to the laser controller, which in turn adjusts the laser diode temperature and current to tune the laser frequency to "on line" or "off line" with respect to the HCHO absorption feature. The controller also superimposes a fast ramp to the current to sweep the laser across the absorption feature at rate of 100 kHz. The light from the absorption cell is detected by a high-speed photodiode whose signals are digitized by a fast data acquisition board. The analysis program calculates the absorption due to the HCHO gas as the laser frequency is swept across the HCHO absorption line at 2826.7102 cm^{-1}. The absorbance is fit to a calculated line shape based on tabulated spectral parameters to determine the optical depth (or equivalent width) of the HCHO spectral feature. This information, combined with the path length and the measured sample temperature and pressure in the multi-pass cell, yield the absolute concentration of HCHO. From a previous study the measurement precision for HCHO (1 minute averaged data, 1σ) with the TDLAS is 0.08 ppbv.

III.14 Tunable Diode Laser System (TDLAS) Reference Instrument

III.14.1 Instrument overview

The Aerodyne Dual Tunable Diode Laser is based on high-resolution infrared spectroscopy of gas phase molecules. Ambient air is sampled through an inlet into a 5-liter multipass sampling cell with 153 m total path length. The sample is maintained at reduced pressure (typically 20 – 40 Torr) by a Busch vacuum pump with a flow rate of ~ 5l/sec. This results in a residence time

of ~ 1 second in the cell. The TDLAS system utilizes infrared radiation from two individually operated lead-salt tunable diode lasers. The lasers follow independent paths through the sample in the multipass cell and then on to separate infrared detectors. The amount of light absorbed by the trace gases in the sample cell is monitored. The light from the two lasers detected at the infrared detectors is monitored with a well-developed data acquisition system. The data acquisition method is an advanced form of sweep integration that is carried out by a software package. The program sweeps over the full infrared transition or group of transitions, and then integrates the areas under the transitions using nonlinear least square fitting to the known spectral line shapes and positions. Absolute species concentrations are obtained directly, tied to the absolute data found in available database such as the HITRAN database. Calibration gas is not required. The concentrations of monitored trace gases are reported and stored by the data acquisition and controlled computer. The data system provides a real-time display of the collected data. The instrument was not deployed during the summer 2001 intensive.

III.14.2 Absorption features and selectivity

The TDLAS was configured to measure HCHO and SO_2 from July 10 to July 21, 2002 and HCHO and NO_2 from July 21 to August 7, 2002. The strong HCHO absorption feature at 2826.7 cm^{-1} was employed to measure HCHO concentration in the field campaign. The strongest line of 2826.7102 cm^{-1} has an integrated absorption cross section of 3.52×10^{-20} cm^2 $molecule^{-1}$ cm^{-1}. The mode purity for this absorption feature is better than 95%. The NO_2 absorption feature at 1593.3 cm^{-1} was employed. In this region, two strong absorption lines at 1593.2804 cm^{-1} and 1593.3120 cm^{-1} have similar line strengths, 7.466×10^{-20} cm^2 $molecule^{-1}$ cm^{-1} and 8.172×10^{-20} cm^2 $molecule^{-1}$ cm^{-1}, forming a distinctive doublet. Near the NO_2 doublet, there are other six weaker NO_2 lines, among which only 1593.225 cm^{-1} line has a comparable absorption feature. In the data analysis, all of the NO_2 absorption features in the monitored region were included in the fitting procedure. Better than 95% mode purity was measured during the laser characterization study. The SO_2 absorption spectral feature used in this study is also composed of two strong absorption lines, 1353.2537cm^{-1} and 1353.2918cm^{-1}. The line strength of 1353.2537cm^{-1} is 7.466×10^{-20} cm^2 $molecule^{-1}$ cm^{-1}. The absorption feature is clear of any interference in the laboratory and none was detected during the field campaign. Near the SO_2 double lines, there is a strong CH_4 absorption feature, 0.0947 cm^{-1} lower in frequency. This CH_4 absorption feature does not interfere with SO_2 measurement, but it does provide a good marker for locating this desired SO_2 absorption feature among the rich SO_2 absorption spectrum. The mode purity for the employed SO_2 absorption feature was characterized to be more than 99%. The absorption features and mode purity are summarized in the following table.

Table III.14.1: HCHO, NO_2 and SO_2 absorption features employed in the field campaign

	HCHO	NO_2	SO_2
Frequency lock position	2826.7102 cm^{-1}	1593.3120 cm^{-1}	1353.2537cm^{-1}
Line strength	3.52×10^{-20} cm^2 $molecule^{-1}$ cm^{-1}.	8.172×10^{-20} cm^2 $molecule^{-1}$ cm^{-1}	7.466×10^{-20} cm^2 $molecule^{-1}$ cm^{-1}
Mode purity	95%	95%	99%

Measurement accuracy

The absolute accuracy of concentration measurements performed using tunable diode laser differential absorption spectroscopy is fundamentally determined by how well the line strengths used in the spectral fitting procedure are known. Additional factors which contribute to a systematic error in these measurements are as follows: path length, pressure, temperature, the line shape model used in the fitting procedure and diode mode purity. These factors for the overall instrument will be discussed first, and then the specific line strength uncertainty will be detailed. The uncertainty in the path length for the 174 spot /153.5 meter astigmatic Herriot cell is estimated to be less than 0.1% or 15 cm (McManus et al., 1995*;* Herndon et al., 2004). The derived quantity from the spectral fitting is a number density measurement, however for convenience, this is immediately converted to a mixing ratio, which requires an accurate measurement of both pressure and temperature. The systematic uncertainty in the pressure and temperature measurements directly contribute to the accuracy of the measurement, however both pressure and temperature play a subtler role in the spectral fitting. A Voigt line shape model (Humlicek*,* 1979*;* Armstrong*,* 1967) is used to fit the spectral data and extract concentrations for each of the species specified in a HITRAN style (Rothman et al., 1998) input file. With a 'well behaved' diode the uncertainty associated with the fitting procedure can be shown to be less than 1% (Herndon et al., 2004). This occurs when the operator has performed the experiments needed to demonstrate that the diode characteristics are within certain specifications; apparent laser line width < 0.005 cm^{-1} and high mode purity > 98%. If the diode is operating outside of these typical limits, the potential systematic error in the fit concentration increases. However, these arguments also assume that the concentration and path length are such that the minimum transmission is greater than 50% or that "optically thin". The line strengths present in the HITRAN database for the 3.5 μm band of H_2CO ($\nu_1 + \nu_5$) come largely from the determination of Brown et al. (1979) who estimate the individual line strength assignments to be good to 5%. For SO_2 in the 8 μm band ($\nu_1 + \nu_3$) the most recent work which the HITRAN line listings are based on the uncertainty estimate at 10% (Chu et al., 1998). In the case of the 6.2 μm,ν_3 band of NO_2 the current estimate of the uncertainty in the band strength is 4% (Smith et al., 1985), however the most recent update to the HITRAN is based on the work that estimates the uncertainty of the line intensities to be 5% (Mandin et al., 1997).

III.14.3 Data summary

Data summary for HCHO, NO_2 and SO_2 measurements in the field campaign is given in Table III.14.2.

HCHO: In the study, one channel of the dual TDLAS was exclusively set to measure HCHO over the entire campaign from July 10 to August 7, 2002. Data coverage during this interval was greater than 90 %. The missing data are due to the data dropouts during the liquid nitrogen refill, routine optical alignment optimization, line position locking failure, power surges and laser diode switching on the other channel in the middle of campaign. Figure III.14.1 presents the HCHO time series in 30-minute time resolution. As can been seen, the HCHO concentration shows a high variability from below the detection limit to a highest value of 4.7 ppb during the

campaign. The lowest value was observed at 5pm, July 27, and the highest value occurred at 5:30 am, August 5. The average HCHO concentration is 1.4 ± 0.8 ppb over the entire campaign.

NO_2: Measurements of NO_2 were made from July 23 to August 7, 2002, until the end of the campaign. The measurement results with 91 % data coverage were obtained in original 1-second time interval. During the measurement period, the measurement precision level upon sampling relatively constant ambient air was consistent with the laboratory-measured value. The measured NO_2 concentrations varied from below the detection limit to the maximum of 24 ppb. The average concentration was 0.73 ± 0.59 ppb (1σ).

SO_2: Measurements of ambient SO_2 were carried out from July 10 to July 21, 2002. Over the entire measurement period, the data coverage for SO_2 measurements is more than 90%. The data dropouts during the liquid nitrogen fill and routine optical alignment during the campaign mainly account for the missing data. SO_2 concentrations varied from the maximum value of 9 ppb to below the detection limit, and the average concentration over the entire campaign was 0.75 ± 0.95 ppb (1σ).

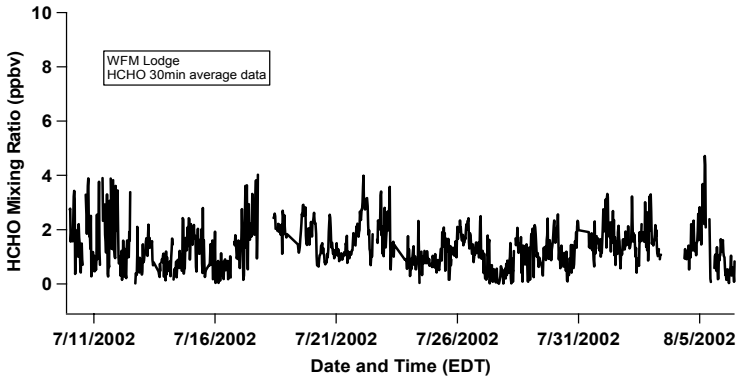

Figure III.14.1. HCHO time series in 30-minute time resolution.

Table III.14.2: Data summary for HCHO, NO_2 and SO_2 in 2002 field campaign

	HCHO	NO2	SO2
Measurement duration	July 10 to August 7, 2002	July 23 to August 7, 2002	July 10 to July 21, 2002
Data completeness	90 %	91 %	90%
Time resolution	30 min	1 second	1 second
LOD	58 ppt	18 ppt	33 ppt
Minimum	<58 ppt	<18 ppt	<33 ppt
Maximum	4.7 ppb	24 ppb	9 ppb
Mean	1.4 ppb	0.73 ppb	0.75 ppb

III.14.4 Quality assurance experiments

HCHO: The TDLAS system employed in the study is an absolute measurement technique, which does not require the calibration, eliminating the need for calibration gas mixtures in the field. To ensure the data quality, this was confirmed in the laboratory experiment by measuring a certified HCHO from a permeation tube (VICI Metrics).

Figure III.14.2: 1-second HCHO average spectrum

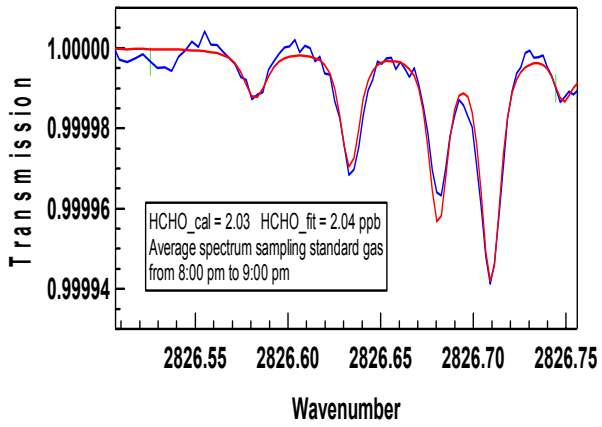

Figure III.14.3: Calibration of TDLAS

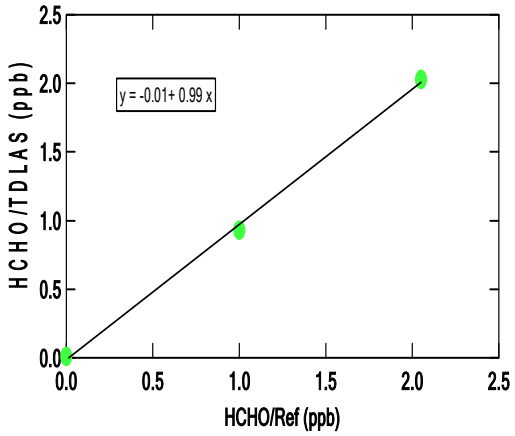

As indicated in figure III.14.2, a fitting result (HCHO=2.04 ppbv) from a retrieval 1-second average spectrum is consistent with the calculated value (HCHO = 2.03 ppbv) based on the permeation flow rate. Figure III.14.3 shows a linear response up to 2 ppbv. A R^2 (equal to 0.99) obtained from the least regression fit suggested a one to one response, relative to the calculation value.

An instrument comparison experiment was also performed in the lab. Figure III.14.4 shows the HCHO measurement comparison between TDLAS system and DSLF (Diffusion Scrubber-Liquid Fluorescence) technique by sampling ambient air. A good R^2 was obtained from the corresponding scatter plot given in Figure III.14.5. The positive intercept might be due to the interference to the DSLF method.

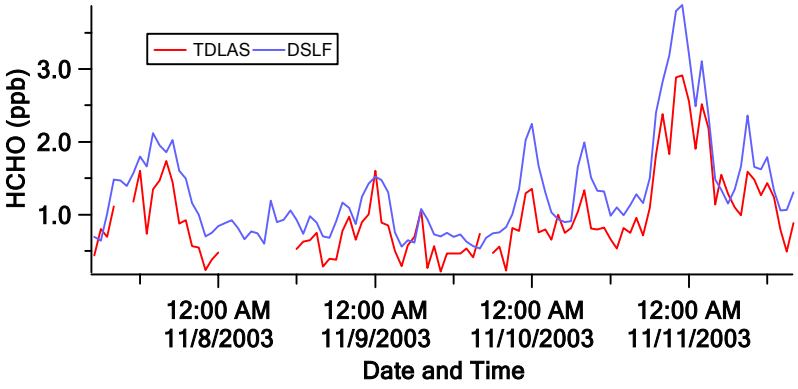

Figure III.14.4: Time series data of HCHO measurements with TDLAS and DSLF

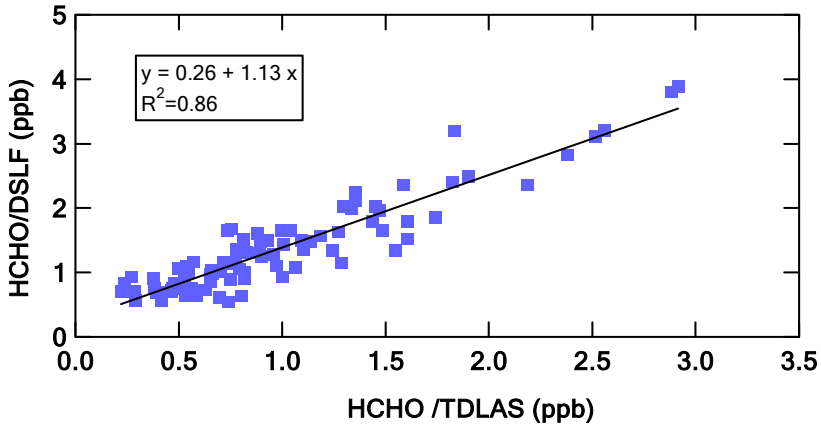

Figure III.14.5. Scatter plot of DSLF measurements versus TDLAS measurements.

NO_2: The calibration of TDLAS with certified source was not performed for NO_2 measurements. In the field campaign, an instrument comparison between TDLAS and a photolysis NO_2 analyzer as well as TEI 42C NO-NO_x analyzer was carried out.

In the study, the high NO_2 spikes associated with the pump contamination, to different extent, were seen by three measurement techniques. This can be explained by the different sampling locations where the measurement techniques were located. The DEC trailer # 1 housing the photolysis NO-NO_x analyzer was almost located downwind of the vacuum pump when the dominant wind was westerly during the field campaign. Relatively, the photolysis NO-NO_x analyzer measurements were more affected by the pump contamination. The contamination data were flagged and removed from the regression analysis.

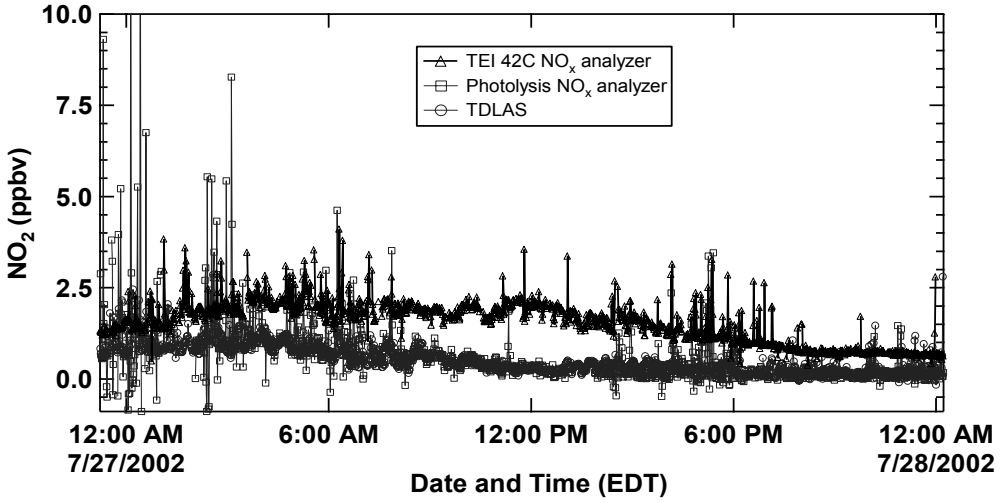

Figure III.14.6: Instrument comparison of NO_2 time series data obtained with three methods

From the time series data, average diurnal patterns and corresponding regression analysis, the NO_2 measurements with TEI 42C NO-NO_x analyzer demonstrated a higher bias, with respect to TDLAS measurements. Such a significant measurement difference can be attributed to the instrument operation principle. The applied TEI 42C NO-NO_x analyzer is a commercial instrument equipped with a heated catalyst (molybdenum). The NO_2 concentration is not directly measured but derived by subtracting the NO concentration measurement from the NO_x concentration measurements. The reduction of NO_2 to NO by this method is not specific and a number of other nitrogen-containing species are reduced to NO that can interfere with the measurement of NO_2 (e.g., HNO_3, PAN, N_2O_5, HONO, and NO_3). Therefore, it is reasonable to expect that the TEI 42C NO-NO_x analyzer would be biased to always measure higher NO_2 concentrations than TDLAS and the photolysis NO-NO_x analyzer. This can be further evidenced by the time series of three instrument measurements shown in Figure III.14.6, where the maximum discrepancy occurring at noon was about 1.8 ppb. Meanwhile, the corresponding HNO_3 and HONO concentrations obtained by NYSDEH group were up to 0.8 ppb and 0.6 ppb, respectively. At this point, the observed measurement discrepancy between TEI 42C NO-NO_x analyzer and TDLAS may indirectly suggests the concentration levels of these reactive nitrogen oxides at the sampling site. From the linear regression fit of the photolysis NO-NO_x analyzer vs TDLAS, the obtained recovery appears to indicate that the photolysis NO-NO_x analyzer measurements were lower than TDLAS measurements by approximately 36%. Comparably, the obtained recovery from the July 27th data pair demonstrates the better agreement between two measurement techniques within 11%. It is unclear what caused the low biased measurements with the photolysis NO-NO_x analyzer.

SO_2: The instrument comparison for SO_2 measurements in the field campaign was also performed. A TEI Model 43C pulsed fluorescence SO_2 analyzer, together with the TDLAS system, was deployed to measure ambient SO_2. For the data comparison analysis, two 1-minute data sets were generated from two methods. A scatter plot of PF (pulse fluorescence) vs. TDLAS is shown in Figure III.14.7. The linear fit yielded the intercept (0.0 ± 0.03 (95% cl.)),

slope (1.09 ± 0.01 (95% cl.)) and recovery (0.99 ± 0.01 (95% cl.)), which suggest almost a one to one response of the two measurement techniques. A multiple R^2 of 0.72, indicating that 72% of the variation is explained by the linear relationship. Given the larger SO_2 variability shown from one pollution event, a compare of two instrument measurements during this sampling period was also performed. Figure III.14.8 displays the corresponding regression fit, which yielded the much improved multiple R^2 (0.92).

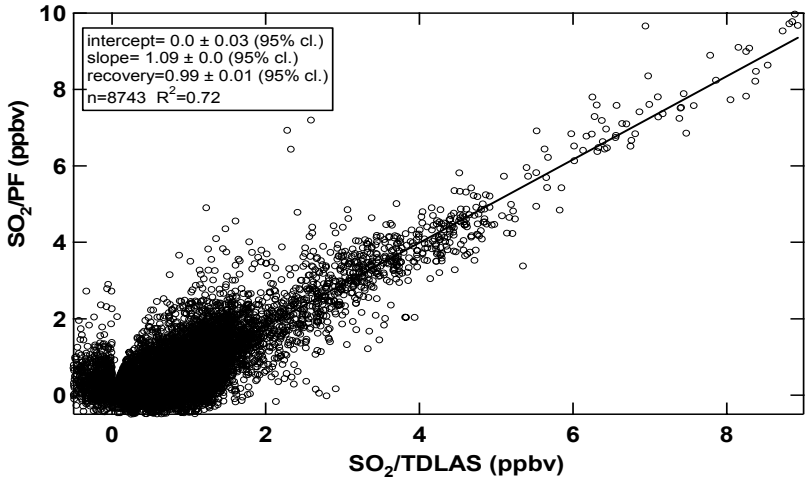

Figure III.14.7: SO_2 scatter plot of PF (pulse fluorescence) vs TDLAS

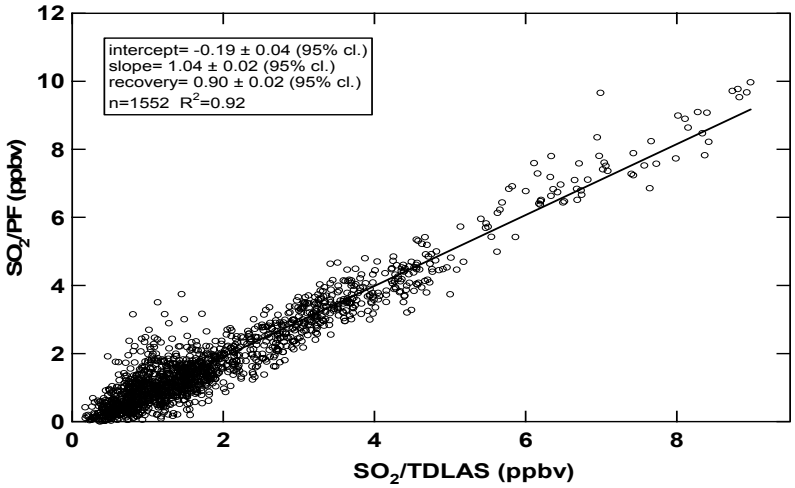

Figure III.14.8: The scatter plot of SO_2 measurements obtained from the pollution event on July 15, 2002.

Winter 2004:

In winter 2004 field campaign, NH_3 and HNO_3 were measured with the TDLAS system. The measurements were performed from January 10 to February 6.

Absorption features and selectivity:
The strong NH_3 absorption feature at 1065.5654cm^{-1} was employed to measure NH_3 concentrations in the field campaign. In this region, three strong absorption lines at 1065.5654 cm^{-1}, 1065.5817 cm^{-1} and 1065.5943 cm^{-1} compose a distinctive triplet. The strongest line at 1065.5654cm^{-1} has an integrated cross section of 2.60 x 10^{-19} cm^2 $molecule^{-1}$ cm^{-1}. In the HITRAN database spectroscopic simulation, O_3 is the only interference species near the NH_3 absorption feature. The nearest strong O_3 line is 1065.6369 cm^{-1}, and its line strength is weaker than the NH_3 absorption feature by two orders of magnitude. In the spectrum fitting procedure, the O_3 absorption feature was also fit as a second species to eliminate its potential interference to the NH_3 measurement. The mode purity for the absorption feature was measured to be better than 99%. The absorption feature at 1722.0012 cm^{-1} was employed for measuring HNO_3. In this region, multiple lines comprise a unique HNO_3 absorption structure, indicated in Figure III.14.9, acquired by sampling a high concentration HNO_3 in a reference cell.

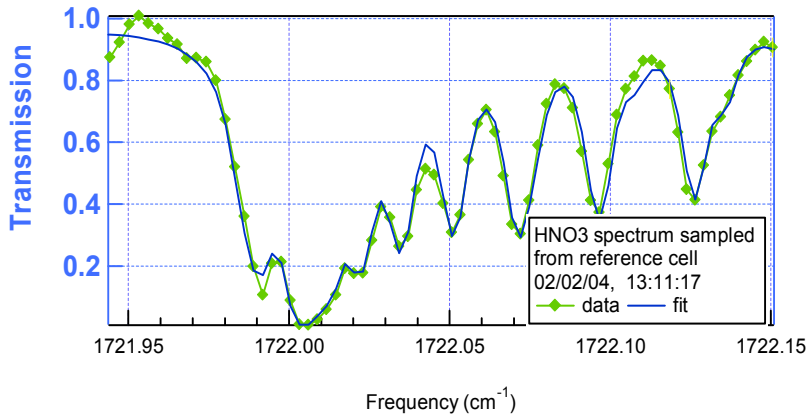

Figure III.14.9. HNO_3 spectrum sampled from the reference cell.

The line strength of 1722.0012 cm^{-1} is 2.60 x 10^{-19} cm^2 $molecule^{-1}$ cm^{-1}. A mode purity of better than 95% was characterized for this laser.

III.14.5 Data summary

The measurements of NH_3 and HNO_3 were made with 1σ precisions of 0.07, 0.6ppb. Data completeness for NH_3 and HNO_3 are 92% and 66%. Over the measurement period, the measured NH_3 ranged from below the detection limit to a maximum of 192ppb. 70% NH_3 data are less than 1ppb with the mean value of 0.76 ppb. Because of the instrument performance for HNO_3 measurements, an hour average data set was generated. 80% HNO3 data are lower than 0.5ppb, with a maximum of 0.98 ppb through the measurement period. The data summary for NH_3 and HNO_3 measurements in the field campaign is given in Table III.14.3.

Table III.14.3: Data summary for NH_3 and HNO_3 measurements

	NH_3	HNO_3
Measurement duration	January 10 to February 6	January 10 to February 6
Data completeness	92%	66%
Time resolution	1 second	1 hour
LOD (precision)	0.07 ppb	0.6 ppb
Minimum	<0.07 ppb	<0.6 ppb
Maximum	192 ppb	0.98 ppb
Accuracy	> 14%	> 4%

III.14.6 Quality Assurance Experiments

Calibration of the TDLAS system

NH_3: To ensure the data quality, the calibration of TDLAS with a certified NH_3 source purchased from Matheson was performed. The certified 10 ppmv NH_3 was balanced with nitrogen and stored in an aluminum cylinder. In the calibration, four lower concentration mixtures (obtained by diluting the certified source with a zero air) were measured with the TDLAS system under the same conditions as those in the field campaign. As evident in Figure III.14.10, the measurement showed a linear response up to 35 ppbv. A slope of 0.86 obtained from the least regression fit suggested a low bias by 14%, relative to the certified value. We believe that the low bias was due to the ammonia decay in the storage aluminum cylinder since an independent calibration showed the same low bias, but consistent with TDLAS measurements. The test sample used for the independent calibration was prepared by directly bubbling the NH_3 source gas through an acid solution (pH = 1), and then analyzed by a chemical derivative technique coupled with a HPLC detection system.

Instrument comparison between TDLAS system and NYS DOH group's diffusion scrubber system was performed in the lab after the field campaign. By sampling room air, two systems showed a reasonable agreement over 24 hour continuous measurements. The time series data from both systems are presented in Figure III.14.11. A corresponding scatter plot is given in figure III.14.12, yielding a R^2 of 0.74.

HNO_3: The calibration of TDLAS system with a certified HNO_3 source from a permeation tube (VICI Metrics) was performed. One point calibration was carried out. Figure III.14.13 shows a retrieval 20-min average spectrum sampling the certified HNO_3 with a calculation value of 2.54 ppbv. The fitting result from the spectrum gave a value of 2.63, 4% higher than the calculation.

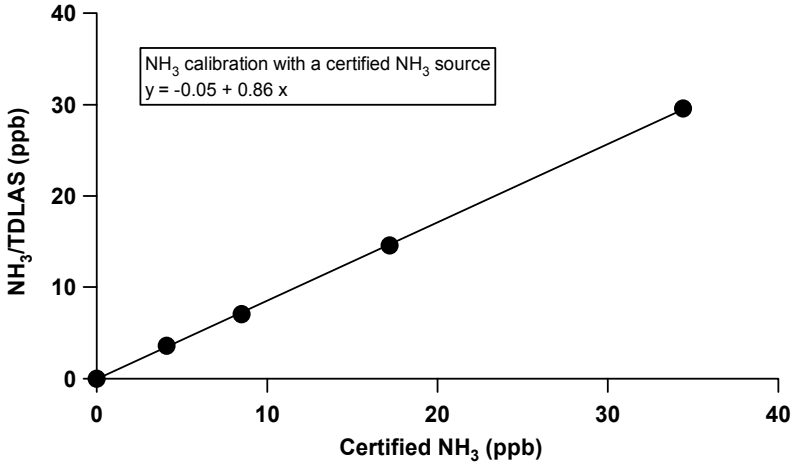

Figure III.14.10: Calibration of TDLAS system with the diluted mixtures prepared from a certified NH_3 source.

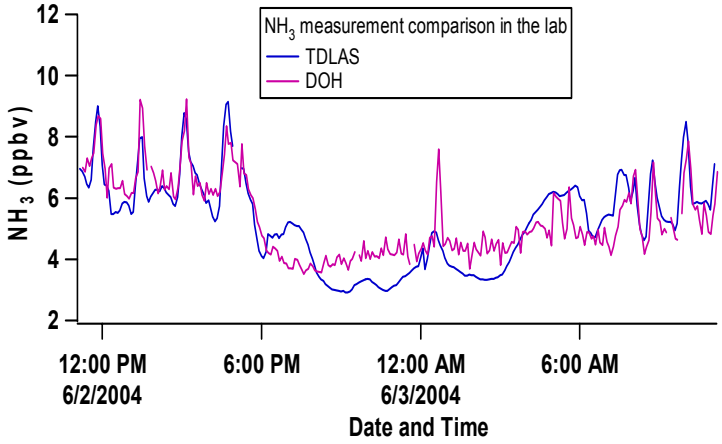

Figure III.14.11: 15-min time NH_3 series data obtained by sampling room air

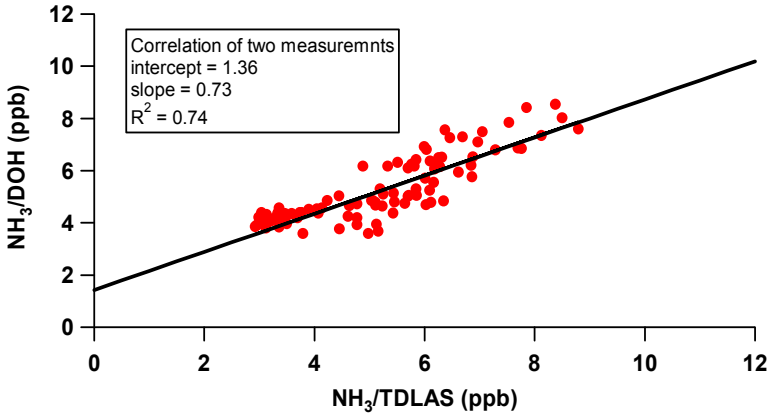

Figure III.14.12: a scatter plot of DOH measurements vs TDLAS system

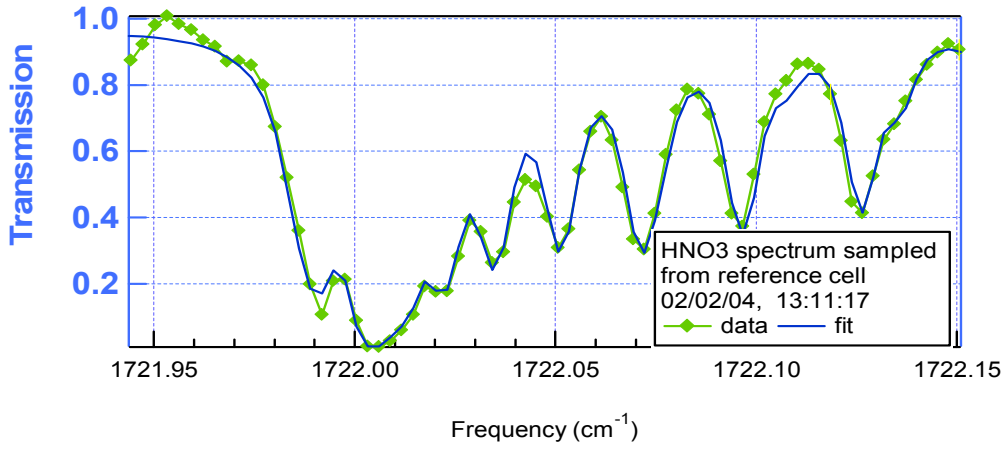

Figure III.14.13: A retrieval 20-min average spectrum sampling the certified HNO_3

III.15 Sizing and Counting Instruments

PMTACS-NY Winter 2004, Data and QA Summary

A variety of aerosol sizing instruments were deployed by the Atmospheric Sciences Research Center, U-Albany and the NYS Department of Environmental Conservation. For the continuous counting and sizing methodologies deployed in PMTACS there exists currently no "officially" recognized reference method or NIST traceable reference materials. The instruments therefore are operated in an "uncalibrated" state and their "accuracy/bias" is unknown. The only available QA parameter is "Precision".

These include the conventional TSI Model 3936 Scanning Mobility Particle Sizer with a Model 3085 Nano Differential Mobility Analyzer and a Model 3025 Condensational Particle Counter (Nano SMPS), an Aerodynamic Particle Sizer (TSI Model 3321, APS) and a stand-alone Condensation Particle Counter (TSI Model 3022, CPC 3022).
The conventional SMPS system measures the number size distribution of ultrafine particles using an electrical mobility detection technique (Wang and Flagan, 1989). The two main components of the conventional SMPS (TSI Model 3936) are an Electrostatic Classifier (ESC) and a Condensation Particle Counter (CPC). In the ESC a polydisperse aerosol is divided into fractions according to their electric mobility size. This is achieved by passing a charged aerosol sample through a Differential Mobility Analyzer (DMA), which consists of two concentric metal cylinders. While the outer cylinder is grounded, a controlled negative voltage is applied to the inner cylinder. Two laminar flows, the one containing a positively charged sample aerosol and the other one containing particle-free sheath air, flow through an annular space between the two cylinders. At each specific voltage, only particles with a specific electrical mobility (which is a product of particle diameter and charge) are capable of escaping the DMA into a butanol-based CPC where the particles are counted. To obtain a full size distribution of an aerosol, the voltage applied to the inner cylinder of the DMA is dynamically scanned. A NanoDMA is used for sizing smaller size aerosol particles (3-100 nm), while a Long DMA is used for sizing larger particles.

- Total number concentration of ambient aerosol particles was measured by a Condensation Particle Counter (TSI Model 3022). In the CPC 3022 particles grow as result of condensation of a supersaturated butanol vapor onto their surfaces and then are counted by an optical detector.
- Particle Sizing Instrumentation included
    - Scanning Mobility Particle Sizer with Nano Differential Mobility Analyzer and CPC 3025 (TSI Model 3936, NanoSMPS)
    - Scanning Mobility Particle Sizer with a long tube Differential Mobility Analyzer and CPC 3010 (TSI Model 3936, LDMA SMPS)
    - Aerodynamic Particle Sizer (TSI Model 3321)

- NanoSMPs, LDMA SMPS and APS measured size distribution over a specified diameter range (see Table III.15.1). In addition particle mean, median and mode diameters as well as total concentration are calculated.
- Instrument deployment period: 01/08/04-02/06/04
- In-field QA procedures and checks included daily checks of operation parameters, necessary adjustments; weekly (or more often if needed) flow audits, dynamic filter blanks, replacement of Drierite in bypass flows of the SMPSs; inlet impactor orifice cleaning; all flow calibrations were performed right after setting instruments up in the field.
- Cycle length, scanned diameter, sample and sheath flows of each instrument are listed in Table III.15.1.
- Bias and MDL are not applicable to these instruments. Accuracy values are given in Table III.15.1.
- % of data capture is the ratio of valid data "samples" to maximum possible data "samples" can be also found in Table III.15.1.
- Time series of Total Number concentrations as measured by the NanoSMPS, LDMA SMPS, APS and CPC 3022 are shown in Fig. III.15.1.
- NanoSMPS data from the ASRC operated instrument were compared to the NYSDEC operated NanoSMPS (see Fig. III.15.2 and III.15.3). Outliers which were removed for comparison are listed on the plots.

Table III.15.1. Operational parameters and data completeness

	NanoSMPS	LDMA SMPS	APS	CPC 3022
Cycle Length, min	5	5	5	5
Inlet Flow, l/min	0.6	0.3	1	1.5
Sheath Flow, l/min	6	3	4	N/A
Diameter Range, nm	4.6–163 nm*	16-626*	542-1980 **	Min particle D 7 nm (50% efficiency detection)
Concentration Accuracy***	±10% up to 9.99 × 10^4/cm^3 (for CPC 3010)	<10% coincidence at 1× 10^4 particles/cm^3	±10% of reading plus variation from counting statistics.	±10% up to 5 × 10^5/cm^3 ±20% from 5 × 105 to 9.99 × 10^6/cm^3
% of data capture	99 ****	88 *****	100	100

* - electrical mobility diameter, corresponds to physical diameter for spherical shape particles;
** - aerodynamic diameter, actual particle diameter can be calculated diving the aerodynamic diameter by a square root of particle density
*** - information is taken from corresponding TSI CPC manual
**** - occasional unusually high values (800, 000 particles/cm^3 or higher) had been recorded by the NanoSMPS. These concentration "spikes" are random, not correlated either with the second NanoSMPS, or with the CPC 3022 measurements, and were considered artifacts. Corresponding samples were removed from the NanoSMPS data set.
***** - lower % of data capture is due to the fact that the SMPS was frequently borrowed for Aerosol Mass Spectrometer size calibrations

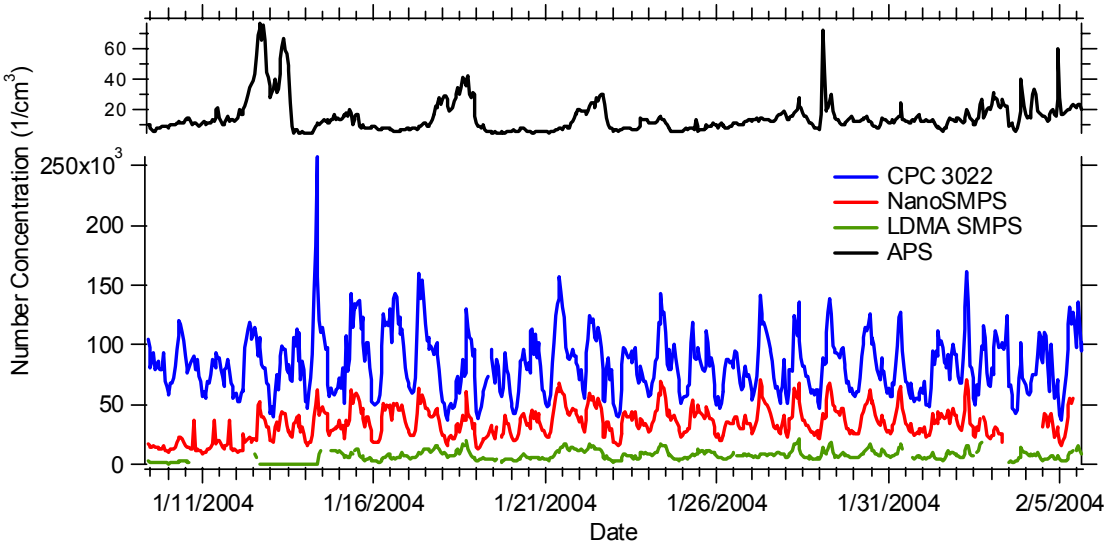

Figure III.15.1. Hourly Time Series of Number Concentrations from Particle Sizing and Counting Instruments Operating by the ASRC during the PMTACS-NY Intensive Winter 2004 Campaign**.**

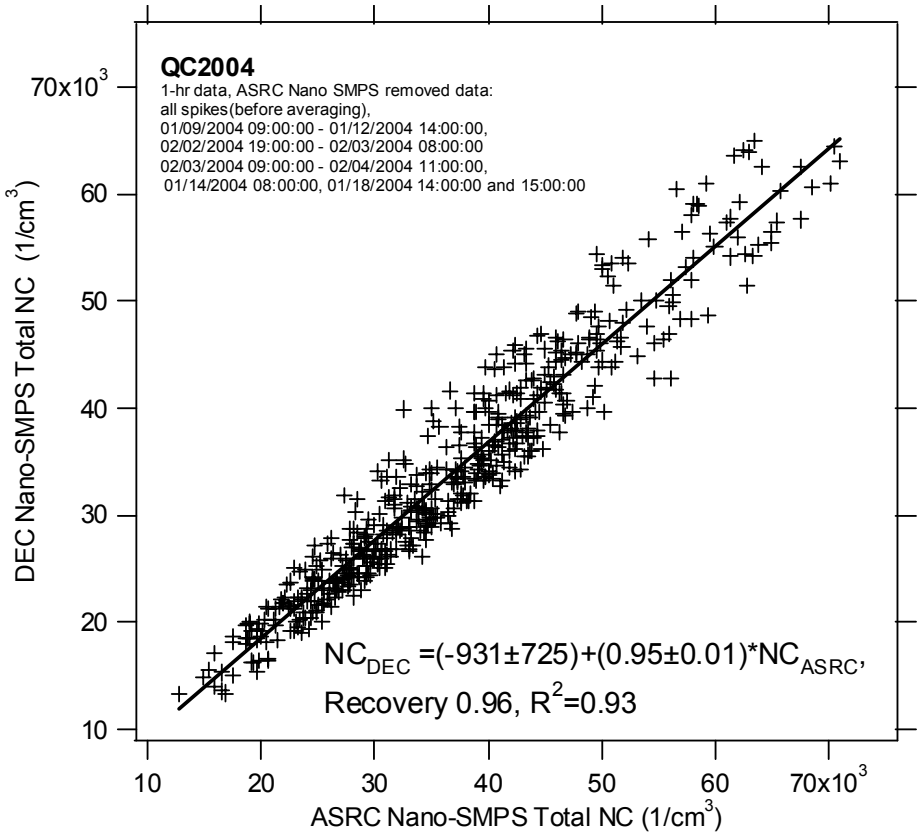

Figure III.15.2. ASRC NanoSMPS total number concentration data (1-hr averages) plotted vs. data from NYSDEC ASRC NanoSMPS**.**

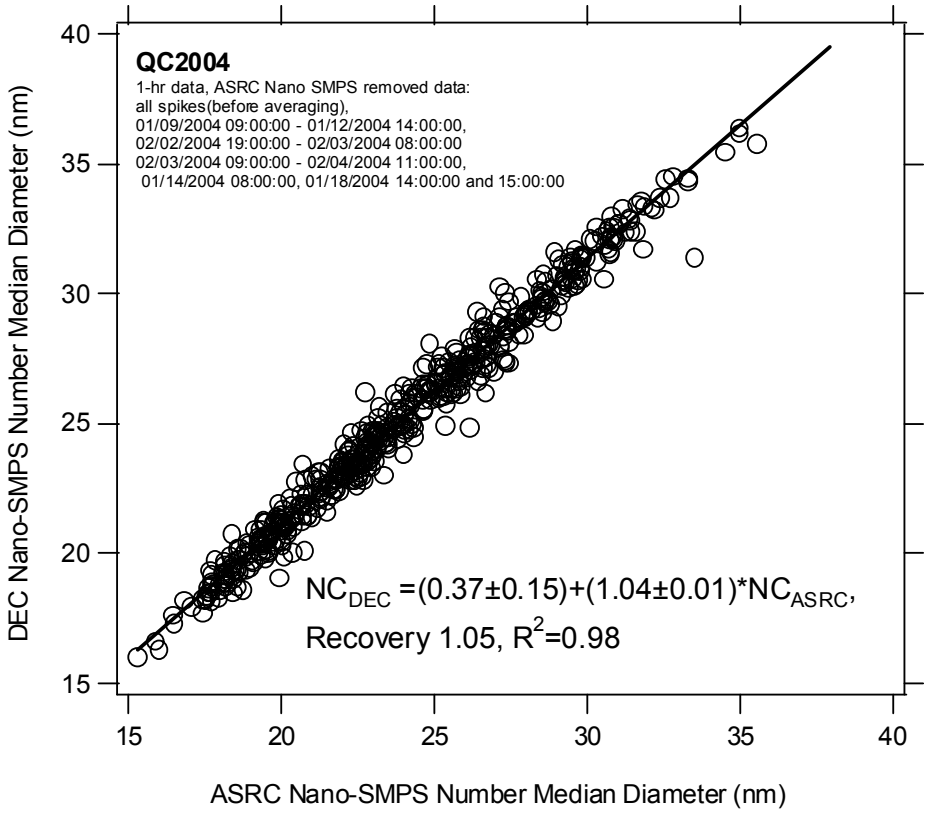

Figure III.15.3. ASRC NanoSMPS median number diameter data (1-hr averages) plotted vs. data from NYSDEC ASRC NanoSMPS.

III.16.Carbon in New York City (Winter 2004)

III.16.1. Introduction

Carbonaceous aerosols are a ubiquitous component of ambient particulate matter (PM), both urban and rural, and are significant contributors to the fine aerosol burden of Urban atmospheres (Gray et al , 1984). Recent chemical speciation measurements of PM2.5 in New York City indicate that close to half the total mass is carbon based (Ito et al , 2004) and the measurements show little seasonal variations. Carbonaceous aerosol is a complex mixture, but may be broadly classified into two major components, organic carbon (OC), which is volatile and elemental carbon (EC) that is non-volatile and strongly light absorbing. The mass related to light absorption is black carbon (BC). Even though BC and EC are often used interchangeably, and are well correlated, studies have shown that they reflect different characteristics of the particles (Jeong et al , 2004)

Measurements of' black carbon were made at two sites in New York City during the winter of 2004 and are compared. Spatial and temporal variability in the black carbon concentrations were explored by examining the diurnal and weekday/weekend trends in black carbon concentrations at these two sites. Associations of black carbon with gaseous pollutants such as CO, NOx, and non-methane hydrocarbons are also explored in an attempt to identify the temporal variations in

their emissions. It was found that the concentrations of black carbon vary in response to the interplay of source activity, meteorological conditions, and spatial factors. The high time resolution measurements were found to yield insights into the spatial scales of emissions that are not possible with longer time scale measurements such as 24 hour averages.

III.16.2 Measurement

Near real-time Black Carbon was measured continuously at two New York City sites maintained by the New York State Department of Environmental Conservation (NYSDEC). The study was conducted during the period of January 12, 2004-Feb 5, 2004, at the New York Super site at Queens College II (7096-15), about 14 kilometers east of Manhattan. The Long Island Expressway (1-495) and the Van Wyck Expressway (I-678) are situated less than 2 kilometers from the site. The companion site used in this study was the IS 52 site in the South Bronx. The South Bronx has a high concentration of diesel trucks and waste transfer facilities. The Bruckner Expressway is less than a kilometer southeast of the site. The South Bronx also has large volumes of heavy vehicle traffic passing through it along several major highways (Inter states I-87, I-95, I-278 and I-895). The distance between the Queens Super site and IS 52 was 9 1 kilometers. An Aethalometer (AE-20, Magee Scientific, Berkeley, CA) was employed to acquit e five minute average BC data at these two sites. This method is based on the optical attenuation from BC in terms of the decrease in light transmission at 880 nm through the filter for a given volume of sampled air The manufacturer's conversion factor of 16.6 m^2 g^{-1} was used to calculate BC concentrations. The principle and working of the Aethalometer are described in detail elsewhere (Hansen et al, 1984). Samples introduced into the Aethalometer were size segregated using a sharp-cut PM2.5 cyclone (Kenny and Gussman, 2000). Since UVBC data was available at the Queens College site, the hourly data were screened for unusual local source influences such as wood smoke by examining the UV-BC data relative to the BC data (Jeong et al,, 2004). The gas phase measurements at the Queens site were made by the NYSDEC monitors situated at the site.

III.16.3. Results

Black carbon concentrations for the 25-day period at the two sites for sample durations ranging from 5 minutes to the entire 25-day period are summarized in Figure III.16.1. Out of the possible 7200 fiveminute average values for the 25 days in this study, 6476 (90%) are valid for the Queens College site and 7069 (98%) are valid for the IS 52 site. Hourly averaged BC concentrations in Queens College varied from 023 microg/m3 to5.87 microg/m^3 with a mean of 1.01 microg/m^3. BC concentrations in IS52 ranged from 0 42 microg/m^3 to 7.67 microg/m^3 with a mean of 1.38 microg/m^3. The BC concentrations were high enough to be measured with reasonable precision in greater than 95% of the valid hourly averages. Very few of the 5 minute and hourly BC averages approached the maximum concentrations, as indicated by the distance between the corresponding 95th and 99th percentile values and the maximum values. The 6 hour and daily averages are better correlated with the maximum concentrations observed, which is to be expected since longer averaging times spread the highest concentrations. However, the downside of using these longer averaging times is that they do not provide good estimates of the frequencies or magnitudes of the high concentrations to which people might be exposed. These statistics seem to indicate the need to initiate studies to assess the response of populations to shorter time resolution maximum concentrations, and to consider their efficacy as an

independent exposure parameter in predicting acute health effects. The regression of BC versus PM2.5 measured at the two sites, shown in Figure III.16.2, indicates that BC tracked PM2.5 well at the Queens College site and contributed about 8 % to the fine particle mass measured at this site. At the IS 52 site, however, BC did not nackPNI2 5 as well, and accounted for a slightly higher 11% of the total fine mass.

The data from monitors in the same geographical area only a few kilometers apart can be substantially different. Variation on this spatial scale is generally presupposed to be driven by local mobile particle source emissions. One of the best indicators of local mobile source aerosol in urban areas is BC, associated with primary diesel and automotive emissions.

Diurnal variations in BC concentrations at the two sites for all days of the week are shown in Figure III.16.3. As expected, a pronounced morning increase in BC concentrations is observed at both sites, peaking between 7 and 9 am, consistent with traffic patterns This increase can be attributed to local mobile sources combined with low mixing heights and consequent poor dispersion conditions at this time of day. The increase in BC concentrations in the morning is observed to be sharper in Queens while it is more gradual at IS 52. This peak is followed by a gradual decrease in BC concentrations at both sites through the afternoon, presumably due to growth of the mixing layer depth and more atmospheric ventilation during the afternoon. An evening peak is observed at both sites consistent with the evening rush how traffic. The fact that the growth in mixing depth does not dilute this rush hour peak seems to indicate that middle scale local sources, i e sources at 0 1-1 km from the receptor site (Watson and Chow, 2001), play a major role in the observed BC concentrations at this time of day BC concentrations from middle scale sources would have insufficient transport time to be strongly affected by changes in mixing height. The BC concentrations drop off at night in Queens due to reduced traffic At IS 52, however, the drop is insignificant, and this might be due to transport from distant urban centers.

During the winter when this study was conducted, strong winds and active frontal passage strongly influenced the concentration variability at the sites with photochemical processes playing a minor role. Therefore, atmospheric concentrations of gas phase pollutants like NO_x., CO, and non-methane hydrocarbons (NMHC) should be largely a function of source characteristics.

Figure III.16.4a-c shows the associations between BC and its gaseous co-pollutants observed at the Queens College site. The comparisons of the diurnal variation of mean NO_x .with BC, CO and NMHC show that NO_x was more closely associated with BC than CO or NMHC. CO and NMHC are observed to have similar temporal variations but different from those exhibited by BC and NO_x.

This plot shows that the early morning peak in BC is accompanied by a dip in CO and NMHC concentrations supporting the hypothesis that this peak was caused by diesel trucks operating at this early hour The concentrations of NO_x, and BC exhibit similar diurnal variations, and the regression plot between BC and NO_x. (Figure III.16.4(b)) confirms that they track each other reasonably well. BC and CO track each other weakly (Figure III.16.4(c)). BC is usually most

abundant in diesel exhaust, wood burning and cold start or high emitting gasoline vehicle emissions (Watson and Chow,2002).

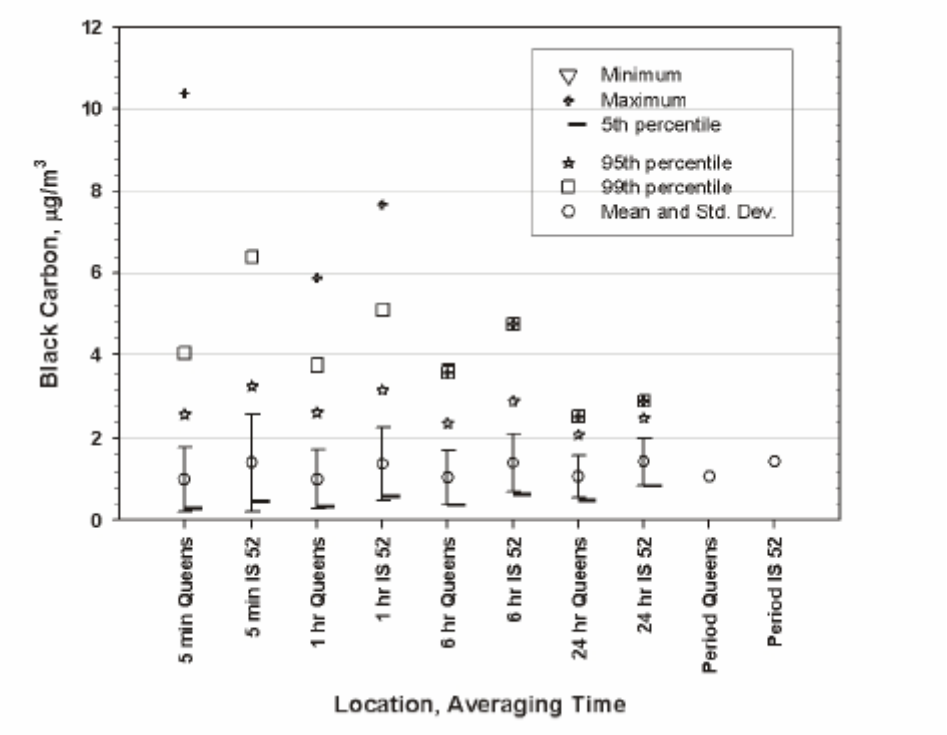

Figure III.16.1. BC Statistics for different averaging times at the Queens and IS 52 sites for January 12, 2004, through February 5, 2004.

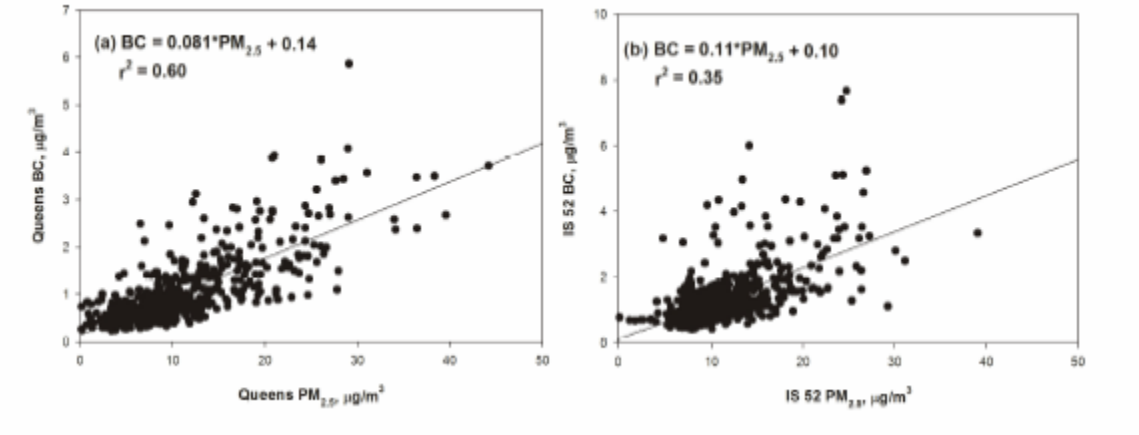

Figure III.16.2. Regression plots of hourly averaged BC versus PM2.5 at the (a) Queens and (b) IS 52 site for January 12, 2004 through February 5, 2004.

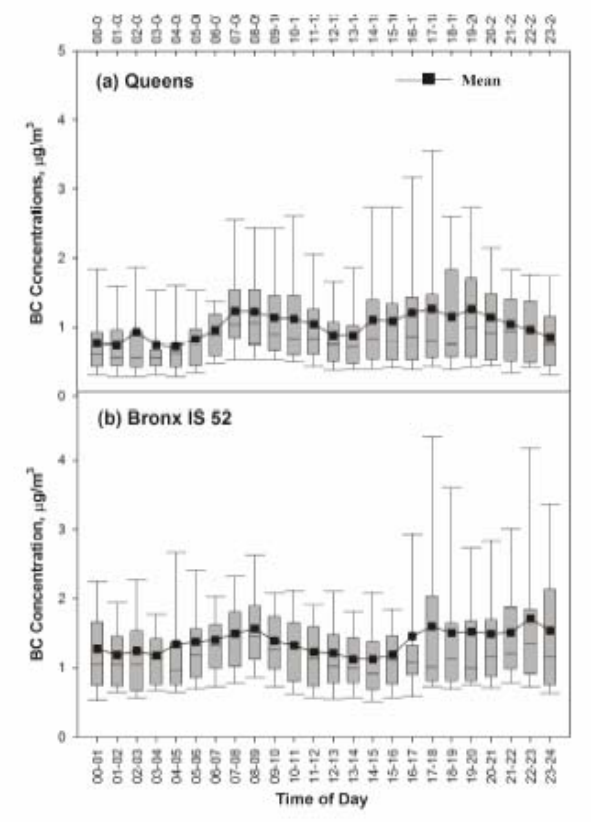

Figure III.16.3. Diurnal variation of BC concentrations for all days of the week at the (a) Queens and (b) IS 52 site for January 12, 2004 through February 5, 2004.

Figure II.16.4.(a) Diurnal covariations of mean BC, CO, NMHC and NO_x concentrations, (b) Regression plot of hourly averaged BC versus NO_x and (c) Regression plot of BC versus CO, at the Queens site for January 12, 2004 through February 5, 2004.

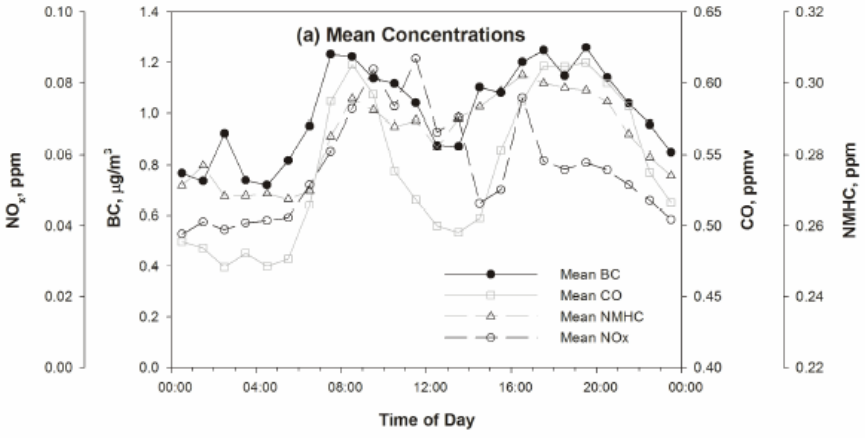

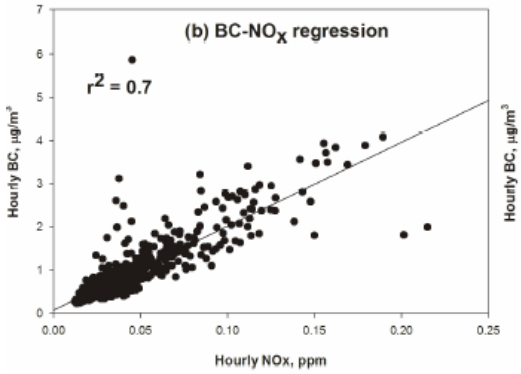

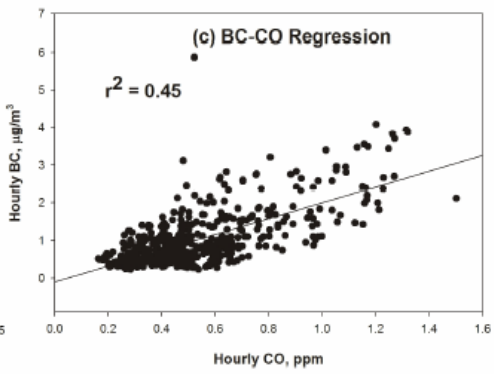

III.17 Assessment of PAMS Instrument During Winter 2004 Intensive

III.17.1 Overview

In accordance with the 1990 Clean Air Act Amendments, EPA has required more extensive monitoring of ozone and its precursors in areas with persistently high ozone levels (mostly large metropolitan areas). In these areas, the States have established ambient air monitoring sites called Photochemical Assessment Monitoring Stations (PAMS), which collect and report detailed data for volatile organic compounds, nitrogen oxides, ozone and meteorological parameters. Analyses of these data are helping the States to better understand the underlying causes of ozone and conceivably PM 2.5 pollution, to devise effective remedies and to measure environmental improvement. A PAMS instrument (Perkin Elmer Ozone Precursor System, Automated Gas Chromatograph) was operated at the Queens College site during the winter 2004 field campaign. The instrument was operated under a Research Method protocol.

III.17.2 Data quality assessment

The winter field campaign began on January 7, 2004; however, because of problems getting the GC set up and functioning, only 159 hourly air (or calibration) samples were obtained, a little less than a week (from 1/30/04 at 1600 to 2/6/04 at 0800). In the case of benzene, it was even lower. The benzene concentration seemed to be too low at the beginning then recover after the Dean switch timing was adjusted. On the other hand, the benzene concentration profile in VOCDat agrees very well with acetylene for most of the time. Since the weather was unusually cold for the first part of the campaign, with wind blowing out of Canada, the air may have been cleaner than normal, and the benzene/ acetylene data may actually be correct.

The baselines of the chromatograms are very noisy, especially from the BP1 column. That may be characteristic of the Queens College site, but the noisy baselines, the sharp rise of the baseline at the end of all the BP1 chromatograms, and the poor shape of some of the peaks don not lend a lot of credibility in the quality of the data. When using the data, the following qualifications should be considered:

- the anomalous behavior of benzene concentration between 2/1/04 at 0400 and2/2/04 at 1600. The concentration is very low during this period. Therefore, that data is not included in the data base.
- the last peak on the PLOT column which may or may not be methylcyclopentane. Since the identity of this peak is in question, that data is not included in the data base.
- the total absence of 2,4-dimethylpentane
- the following peaks are generally of poor quality, with ± 100% uncertainty, in the given time frames. (Their poor quality is probably the result of their low concentration, which is less than 0.4 ppb in every case).

cyclohexane	1/30/04 at 1600 to 1/31 at 0600
2,3-dimethylpentane	1/30 at 1600 to 2/2 at 0500
2-methylheptane	1/30 at 1600 to 2/2 at 0500
3-methylheptane	1/30 at 1600 to 2/2 at 0500
isopropylbenzene	1/30 at 1600 to 2/2 at 1600
n-propylbenzene	1/30 at 1600 to 2/2 at 1600

1,3-diethylbenzene 1/30 at 1600 to 2/2 at 1600
1,4-diethylbenzene 1/30 at 1600 to 2/2 at 1600

Following the hour, February 2 at 1600 (when the timing problem was fixed), all the peaks are generally of much better shape.

Gas chromatographic monitoring of the air began with a visit of a service engineer from Perkin Elmer to set up the auto sampler in one of the temporary buildings at Queens College. Making it work properly proved to be quite a challenge. The cable to connect the 970 interface to the computer was missing, and the mass flow controller wasn't working. The PE engineer ordered the cable, and the mass flow controller from the system at the Bronx Botanical Gardens was brought down and installed. The software keys to allow data acquisition did not work, and the code that could be used as a key was incorrect. Although the set-up was complete, the chromotograms were not usable. A calibration sample would yield peaks, but not in the right place or the right order. An air sample would yield no peaks at all. Two subsequent visits from Perkin Elmer and a visit by DEC staff failed to get the system working properly. Problems were found and corrected each time (helium leaks, air leaks, loose connections, plugged Dean's switch), but still there were no chromatograms of ambient air. After several visits from Perkin Elmer and senior project staff reliable chromatograms were being collected, but the baselines were still very noisy, especially in the BP1 column. The baseline from that column also rose sharply at the end of every chromatogram. The ATD was cycling every 41 or 42 minutes instead of 40. This caused an incorrect labeling of the time of acquisition of the chromatograms. On February 2, the ATD was shut off, the Dean switch timing was adjusted, and the ATD was restarted at 17:57. This caused a one hour skip between #144 and #145; but the ATD cycled regularly thereafter, and there were no further problems with acquisition time. Note, though, that the times in VOCDat, instead of being top of the hour, reflect the times when the samples were actually sent to the GC.

Electronic spikes were a source of another problem. Most were small or occurred between peaks. Two were quite large and occurred just as a compound was eluting: p-ethyltoluene on Jan. 30 at 07:00 (#76) and 3-methylpentane on Feb.4 at 17:00 (#192).

The time of elution of the various compounds kept changing also. From the beginning of the sequence to the end, there is a difference of several seconds, enough that it was necessary to batch the chromatograms in groups in order to accommodate the changing elution time. Beginning with #73 (the first 72 chromatograms of this sequence were unusable), the chromatograms of the PLOT column were batched from:

16:00 on Jan.30 to 02:00 on Feb.1
0300 on Feb.1 to 01:00 on Feb.2
0200 on Feb. 2 to 01:00 on Feb. 4
02:00 on Feb. 4 to 11:00 on Feb. 5
and 12:00 on Feb. 5 to 08:00 on Feb. 6
(chromatograms 73 to 107, 108 to 129, 130 to 176, 177 to 210, and 211 to 231).

The following two groups were sufficient for the BP1 column:

16:00 on Jan. 30 to 02:00 on Feb. 2
and 03:00 on Feb. 2 to 08:00 on Feb. 6 (dividing at chromatograms 130/131). The changing elution times also caused problems in assigning peak identities, especially if there were two peaks close to each other. As bottled air was used instead of an ultra dry air generator, the moisture in the air may have caused the changes in elution time.

Probably the biggest problem with elution time is the first three peaks of the BP1 column. Methylcyclopentane probably came out at the end of the PLOT chromatogram, 2,4-dimethylpentane was lost entirely in the heart cut, and benzene was affected sometimes, too. From Feb. 1 at 04:00 to Feb. 2 at 16:00 (chromatograms 109 to 144), benzene was very low or zero. Even though there is a clear peak at the end of the PLOT column that was identified as methylcyclopentane, its concentration is lower than expected. It should match very closely the concentration of 3-methylpentane but is sometimes noticeably lower. This may be attributable to a heart cut problem as well.

On the positive side, some of the small peaks that are frequently lost from the Botanical Gardens chromatograms showed up clearly in the Queens chromatograms.

IV INTERCOMPARISON: CONTINUOUS PM-2.5 SULFATE IN QUEENS, NY MEASURED USING FOUR DIFFERENT TECHNIQUES

IV.1 Introduction

As the scientific and regulatory communities attempt to understand and solve the problem of fine particulate pollution, measurements of increasing specificity and precision are required. It is widely recognized that sulfate, either acidic or neutralized, is a major component of fine particulate (PM-2.5) mass. In the past three years a number of new techniques for the measurement of this important component have been developed.

The four instruments were: 1) an Aerosol Mass Spectrometer (AMS) built by Aerodyne Research, Inc., and operated by ASRC; 2) a Particle Into Liquid Sampler (PILS) built by Georgia Tech and operated jointly by ASRC and Georgia Tech; 3) a Rupprecht and Patashnick 8400S Particulate Sulfate Monitor owned and operated by ASRC; and 4) a continuous sulfate monitor designed by Harvard School of Public Health and licensed, built and operated by ASRC. The instruments, each described briefly below, used a wide variety of sampling, collection and analysis techniques. Continuous operation and high data recovery were important goals for all of these measurement techniques.

IV.2 Measurement Methods

IV.2.1 Aerodyne aerosol mass spectrometer

In an aerodynamic lens particles are focused to form a narrow beam, which passes through a skimmer into the drift chamber, where it's chopped to measure the particle size distribution. The particle beam impacts on a heated surface, causing volatile and semivolatile species to evaporate. The vapor is electron impact ionized and analyzed using a quadrupole mass spectrometer and subsequent detection with an electron multiplier.

- Sampling inlet: 10 l/min cyclone with 2.5 mm cut; isokinetic sampling of 0.4 l/min for CPC (0.3 l/min) and AMS (0.1 l/min) close to AMS inlet.
- Analysis modes: MS mode for measurement of complete mass spectrum with no size information, fast scanning of the total mass range (1-300 amu); ToF mode for measurement of size distribution at pre-selected masses, typical for different aerosol chemical species, stepwise time-resolved measurement at different masses.
- Operation scheme: Continuous sampling and analysis; change between analysis modes every 20 seconds. Averaging time: 10 minutes.
- Measurement Period: June 30 – August 5, 2001
- Calibration: Frequent multiplier gain calibration; continuous monitoring of multiplier gain; ionization and transmission efficiency calibration using monodisperse NH_4NO_3 particles; continuous monitoring of inlet flow and chamber pressure.

IV.2.2 Particle-into-liquid sampler coupled with ion chromatograph (PILS-IC)

In this technique, the ambient air stream flows first through diffusion denuders to remove potentially interfering gaseous species. The particle-into-liquid sampler (PILS) collects the

particles by passing the aerosol through a steam chamber to produce a concentrated liquid. This liquid is then sent simultaneously to cation and anion ion chromatographs (ICs) for quantitative mass analysis of the ionic species dissolved in the liquid from the PILS.

- Sampling inlet: 10LPM inlet flow rate through PM2.5 cyclone, 5 LPM flows through two concentric cylinder glass denuders coupled in series, 5 LPM flows through a filter for use as internal check.Analysis: collected liquid is sent to computer-controlled anion and cation ICs to measure the major ionic components.Data Collection: data is collected online semi-continuously; chromatographs are produced every 15 minutes; data is reported as 15 minute averages.Measurement Period: July 1 to August 5, 2001Calibration: IC is calibrated using NIST traceable standard solutions (Fisher Scientific). IC calibration is routinely checked using one standard for the cation and anion.

IV.2.3 R&P 8400S Ambient Particulate Sulfate Monitor

R&P 8400S measures the mass concentration of ambient particulate sulfate contained in PM-2.5. Collection of particulate matter on a platinum strip is followed by flash vaporization. Resulting SO_2 is quantified by fluorescence detection.

- Sampling Inlet: rain cap, PM-2.5 sharp cut cyclone, activated carbon denuder (removes gaseous interferences), Nafion™ humidifier (increases collection efficiency). Sample flow rate 5 l/min through cyclone; 1 l/min sample flow through critical orifice onto flash strip; collection by impaction of PM-2.5 on exchangeable platinum strip.
- Major Components: C3 Pulse Generator for aerosol collection, conditioning and flash-vaporization; SO_2 Pulse Analyzer for subsequent quantification of SO_2, produced in the Pulse Generator.
- Operation Scheme: Aerosol collection time 8 min, analysis time 2 min. Flash strip heated to 600^{o}C by passing a high current through it for about 10 msec, resulting in a pulse of SO_2. 10 min data are generated.
- Measurement Period: June 29 – August 5, 2001
- Calibration/QA: Obtained "raw" data adjusted to aqueous standards calibrations, SO_2 Analyzer audits and blank tests.

Continuous Sulfate Monitor (George Allen/ HSPH Design)

In this technique, the ambient air stream, denuded of SO_2 and interferents, but containing PM-2.5 flows through 8-10 foot long coil of SS tubing maintained at 900°C in a tube furnace, then into a pulsed fluorescence SO_2 analyzer. The key concept is that the heated SS tubing acts as a catalytic reduction oven, volatilizing the SO_4 aerosol, then reducing it to SO_2, which is relatively easily detected.

- Sampling inlet: 5 LPM sharp-cut cyclone followed by carbonate denuder to remove SO_2 gas, honeycomb charcoal denuder to remove interferents, and Nafion™ dryer.
- Analysis: about 400 sccm of the sample flow goes into the SS reduction oven at 900°C, then to a TEI Model 43S pulsed fluorescence analyzer.
- Data Collection: data is collected continuously; 10 minute zero period at the beginning of each hour; data is reported as 10 minute averages.
- Measurement Period: July 22 – August 5, 2001

- Calibration: 43S SO_2 analyzer was calibrated using a certified standard and Environics Model S100 calibrator. Lab tests using generated aerosol are planned.

IV.3 Measurements

Measurement Periods:

Summer 2001:

- AMS June 30 – August 5, 2001
- PILS July 1 – August 5, 2001
- R&P 8400S June 29 – August 5, 2001
- Harvard Instrument July 22 – August 5, 2001

Winter 2004:

Inter-comparisons were performed during the winter field campaign between three semi-continuous sulfate measuring instruments and three semi-continuous nitrate instruments. The R&P 8400 S & N data were compared with those from the Aerosol Mass Spectrometer (AMS) and the Particle into Liquid Sampler with IC (PILS-IC).

Measurement Site:
PMTACS NY 2001 Site
Parking Field # 6 of Queens Colle
Queens/New York

Time Series: Sulfate Concentration, measured with all four instruments, June 30 until August 5:

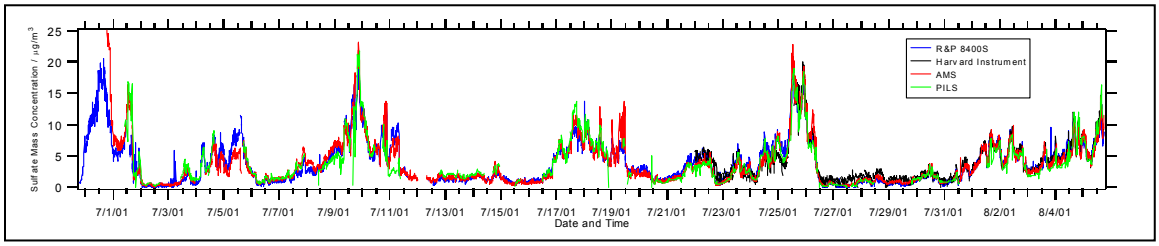

Instrument Comparison, Close-ups for the period July 23 – July 28:

AMS – PILS:

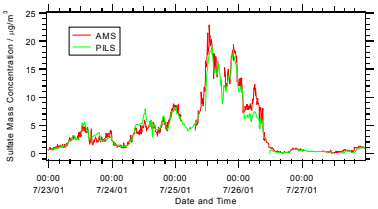

R&P 8400S – PILS:

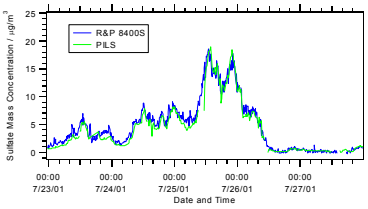

HSPH – PILS:

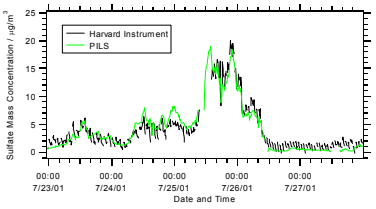

Statistical Comparison, Scatter Plots AMS/R&P 8400S/Harvard versus PILS Sulfate Concentration:

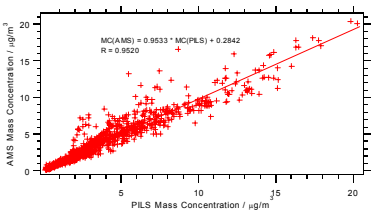

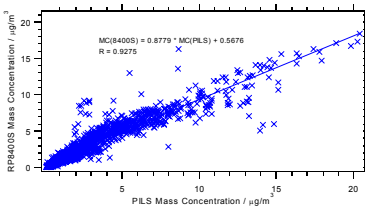

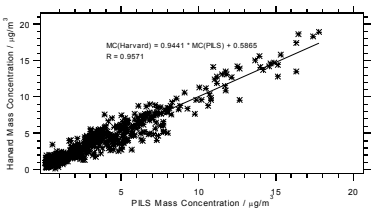

8400N and 8400S Data with Those from Other Semi-Continuous Instruments and with 24-hr STN (or STN-equivalent) Filter Samples

Correlation***	R^2	Slope	Intercept	**Recovery***	N points	8400 MC_{min}-MC_{max}*
8400N vs AMS.	0.75	0.57	1.18	**0.76**	134	1.90 –8.32
8400N vs. PILS-IC (before PILS modifications**)	0.76	0.72	-0.18	**0.69**	68	2.85 – 8.32
8400N vs. PILS-IC (after PILS modifications**)	0.86	0.81	0.47	**0.91**	47	2.05 - 6.21
8400N vs 24-hr Filters	0.95	0.91	-0.94	**0.67**	16	0.04 – 5.96
8400S vs AMS.	0.50	0.94	0.82	**1.18**	322	1.64 – 8.48
8400S vs. PILS-IC (before PILS modifications**)	0.76	0.58	0.16	**0.60**	105	1.85 – 8.53
8400S vs. PILS-IC (after PILS modifications**)	0.65	1.76	1.46	**1.31**	179	1.64 – 8.48
8400S vs 24-hr Filters	0.91	1.27	-0.69	**1.05**	18	0.65 - 6.04

* - (Slope with Intercept set to 0)
** - Several parts of PILS-IC were modified 01/20/04-01/22/04
*** - for semi-continuous instrument comparisons only 1hr MC>LOD were used

IV.4 Conclusions

- Generally all four sulfate measurement instruments show good agreement and meet the stated Data Quality Objective for precision of $\pm$ 10%.
- R&P 8400S appears to be a reliable commercial instrument.
- Field deployment of the Harvard instrument data requires further investigation.
- PILS could be used as reference instrument because of its relatively long record.
- AMS delivered reliable sulfate data. It needed to be calibrated versus PILS once for the whole measurement period.

V EVALUATION: TSI MODEL 3034 SMPS

V.1 Introduction

The last campaign of the PMTACS-NY was conducted in winter of 2004 in Queens, New YorkCity and took place from January 08 to February 06. Evaluating the performance of a "single box" SMPS 3034 was done during this intensive field study.

A new "single box" Scanning Mobility Particle Sizer (TSI SMPS Model 3034) was deployed and operated during a period of four weeks as a part of the PMTACS-NY Winter 2004 intensive study in Queens College, New York City. The SMPS 3034 is an alternative to a conventional multi-component TSI SMPS and houses a Differential Mobility Classifier and butanol-based Condensation Particle Counter in one cabinet. The SMPS 3034 operates at a fixed 1 liter/min sample flow rate (4 l/min sheath flow rate) and measures size distributions within a 10-487 nm size range. One size scan is produced every 3 min. A conventional TSI SMPSs with a Nano Differential Mobility Analyzer, an Aerodynamic Particle Sizer, a stand-alone Condensation Particle Counter, and an R&P Inc. FDMS TEOM mass monitor were operated side-by-side with the SMPS 3034. Results from those measurements were used to evaluate performance of the SMPS 3034.

A scanning mobility particle sizer (SMPS) is a multi-component instrument which measures the size distribution of aerosols, thus providing information about concentration of aerosol particles of various diameters in an analyzed air sample. SMPSs have been used in numerous laboratory and field studies for many years (examples of the most recent field experiments where SMPS was used can be found in Shen et al. (2002), Khlystov et al, (2004), Park et al. (2004), Zhu et al. (2004)). For some studies, e.g., advanced aerosol research or designing new instruments where an SMPS is used as one of the components, a conventional SMPS is the best option for a sizing instrument. However, for many routine field measurements it would be sufficient and more practical to use a particle sizer which (1) combines basic features of the SMPS yet is convenient to transport, deploy and operate in field conditions and (2) operates using a set of fixed parameters and thus produces data which are easy to compare with the data from identical instruments at various locations. The newly developed "single box" Scanning Mobility Particle Sizer, TSI SMPS Model 3034 (SMPS 3034) has a potential to function as such an instrument (Figure V.1).

A conventional TSI Model 3936 Scanning Mobility Particle Sizer with a Model 3085 Nano Differential Mobility Analyzer and a Model 3025 Condensational Particle Counter (Nano SMPS), an Aerodynamic Particle Sizer (TSI Model 3321, APS) and a stand-alone Condensation Particle Counter (TSI Model 3022, CPC 3022) were operated alongside with the new SMPS 3034. A PM2.5 Filter Dynamic Measurement System monitor based on a Tapered Element Oscillating Microbalance mass monitor (R&P Model 8500, FDMS TEOM) was operated at the site as well.

The objective of this QA assessment is to present data obtained using the SMPS 3034, to compare the data with those from the NanoSMPS and the FDMS TEOM, to evaluate our

experience of operating the SMPS 3034 in field environment and to suggest some improvements for instrument design and operation.

V.2 SMPS 3034 Measurement Method

The SMPS 3034 is designed using the same primary principles as the conventional SMPS (Figure V.2). One of the significant differences is that the three components of the SMPS 3034 (ESC, DMA and the CPC) are integrated into a single box, which makes instrument transport and set-up much more convenient, especially during field campaigns. Routine maintenance of the SMPS 3034 is easier due to replacement of the impactor at the ESC inlet by a mini-cyclone (resulting in less frequent, faster and easier inlet cleanings), and implementation of a patented water-removal technology from the butanol reservoir in the integrated CPC (resulting in much less frequent draining and refilling of butanol). The SMPS 3034 DMA is approximately 1/4 shorter than a conventional Long Differential Mobility Analyzer, thus combining high sensitivity towards smaller particles (similar to that of the NanoDMA) and a wide range of diameters in a scan, 10-470 nm (although not as wide as those from the Long DMA). Fewer particle losses and a faster instrument response of the SMPS 3034 are ensured by direct connection of the DMA outlet to the CPC inlet (which leads to shortening of the aerosol flow path), as well as by a higher sample flow (1 liter/min). In addition, this higher sample flow rate results in good counting statistics even at low particle concentrations. CPC saturator and condenser temperatures in the SMPS 3034 are controlled separately, and the temperature difference is 25^{o}C vs. 17^{o}C for a CPC 3010 and 27^{o}C for a CPC 3025. As a result the SMPS 3034 CPC can detect small particles with a higher efficiency than the CPC3010 but a slightly lower efficiency than the CPC 3025.

Other differences in design and operation between the conventional SMPS and the SMPS 3034 are fixed sheath-to-sample flow ratio of 4, automated reading of temperature and pressure leading to more accurate mean free path and viscosity values, and a maximum resolution of 32 channels/decade (SMPS3034) vs. 64 channels/decade (conventional SMPS).

An additional convenience for an instrument operator is that operational parameters (scan time, sheath and sample flow rates) are fixed (see Table V.1). On the other hand, these preset parameters make the SMPS 3034 less flexible and more suitable for routine measurement rather than for research purposes.

V.3 Measurements

The SMPS 3034 and the CPC 3022 sampled through a flow splitter (TSI Model 3708) connected to a port in the wall of a main inlet tube (stainless steel, 3” OD, flow speed 1.1 m/sec). Another port of the main inlet tube was used for the APS sampling. Inlet height was approximately 6.5 meters above the ground. The second main inlet tube was identical in design to the first one, with one of its ports used for sampling by the NanoSMPS. Both tubes were located within a few meters of each other. Quality assurance and maintenance procedures included daily operational parameter checks, dynamic filter blanks with a HEPA filter at the inlet (normally once a week, and daily on several occasions), weekly inlet flow audits, cyclone/impactor cleaning (as necessary) and replacing activated charcoal in a scrubber, which had to be installed at the exhaust port to absorb CPC butanol vapors. Operational parameters for the SMPS 3034, Nano

SMPS, APS and the CPC 3022 are listed in Table V.1. SMPS 3034 data were saved every 3 minutes, NanoSMPS data were saved every 2.5 minutes, CPC 3022 and APS data were saved every 5 minutes. All instruments were constantly operating for four weeks. Table V.1 also reports the percentage of data capture which is calculated as the ratio of valid data points over the maximum possible data points. Invalid points include data missed because of scheduled maintenance or removed during data processing (when it is clear that an instrument was malfunctioning).

Three-minute time series of SMPS 3034 number concentrations and number median diameter are shown in Figure V.3. A week-long data gap (01/14 – 01/20) was due a SMPS 3034 malfunction. A possible reason was identified as a cyclone-induced leak in the system, which resulted in high dynamic blank (up to 10000 particles/cm^3 at times). Data from this period had to be discarded which resulted in 75% data capture (the data capture for other TSI instruments ranged from 93 to 100%). It should be noted that when reviewing the original time series of particle number concentrations measured by the NanoSMPS, it was observed that occasional unusually high values (800, 000 particles/cm^3 or higher) had been recorded by the instrument. These concentration "spikes" are random, not correlated either with the second NanoSMPS, or with the CPC 3022 measurements, and are present in only one or two size bins. Spikes with the same characteristics (randomly occurring in the NanoSMPS data and not correlated to CPC 3022 measurements) were also observed previously during the summer 2001 PMTACS-NY field intensive, indicating that they are not specific to the winter 2004 data. These spikes were therefore considered artifacts and the corresponding samples were removed from the NanoSMPS data set. The total number of samples containing the artifacts was 28 during the whole campaign. Number concentration data from particle sizing and counting instruments were averaged over 30 minutes and 1 hour for data comparisons and analysis. Averaging intervals that had less than 75% valid values were removed from the data set.

Table V.1. Operation parameters and data completeness for the particle sizing and counting instruments

	SMPS 3034	**Nano SMPS**	**APS**	**CPC 3022**
Cycle length, min	**3**	**2.5**	**5**	**5**
Inlet sample flow, l/min	**1**	**0.6**	**1**	**1.5**
Sheath flow, l/min	**4**	**6***	**4**	**-**
Diameter range, nm	**10-470**	**3-104****	**542-19800*****	**-**
Operation period	**01/09 - 02/05**	**01/09 - 02/05**	**01/09 - 02/05**	**01/09 - 02/06**
Data capture, %	**75**	**93**	**100%**	**100**

*** - a dryer was installed in the bypass flow;**
**** - electrical mobility diameter, corresponds to physical diameter for spherical shape particles;**
***** - aerodynamic diameter, corresponds to physical diameters of approximately 443-16,167 nm, assuming density of 1.5 g/cm^3.**

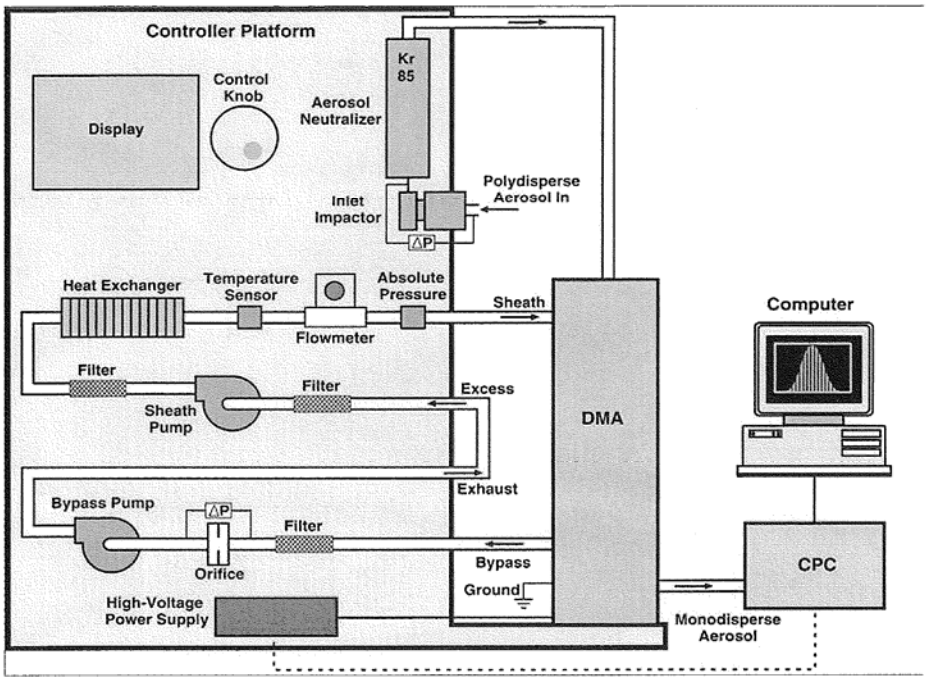

Figure V.1. Schematics of a "single box" Scanning Mobility Particle Sizer, TSI SMPS Model 3034 (courtesy of TSI, Inc.).

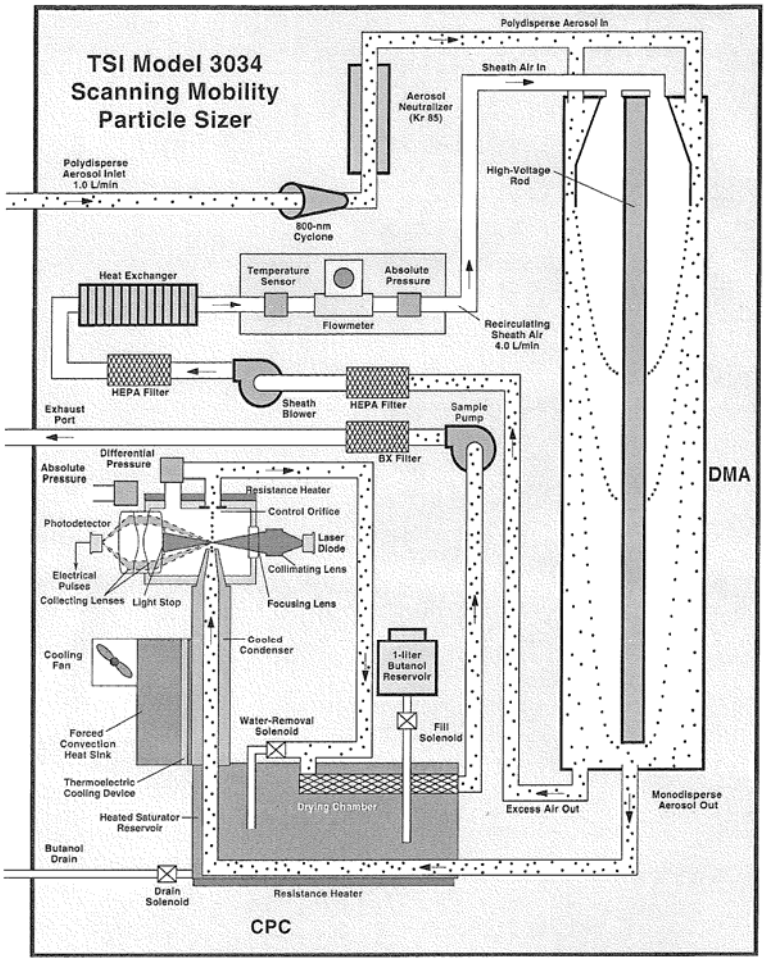

Figure V.2. Schematics of a conventional Scanning Mobility Particle Sizer with a Long DMA, TSI SMPS Model 3936 (courtesy of TSI, Inc.).

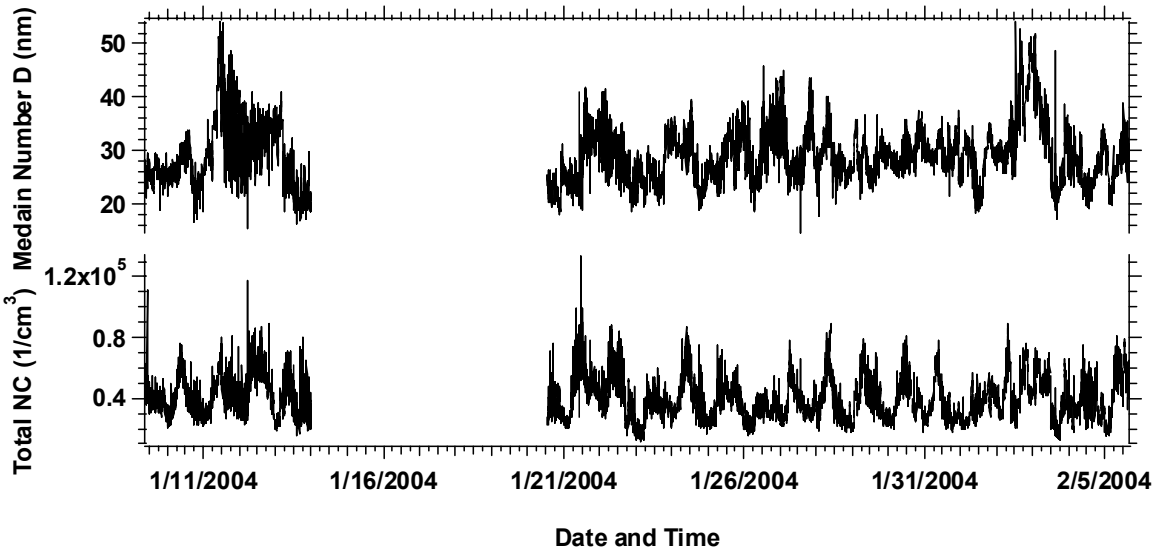

Figure V.3. Time series of 3-min aerosol number concentration and median number diameter from SMPS 3034.

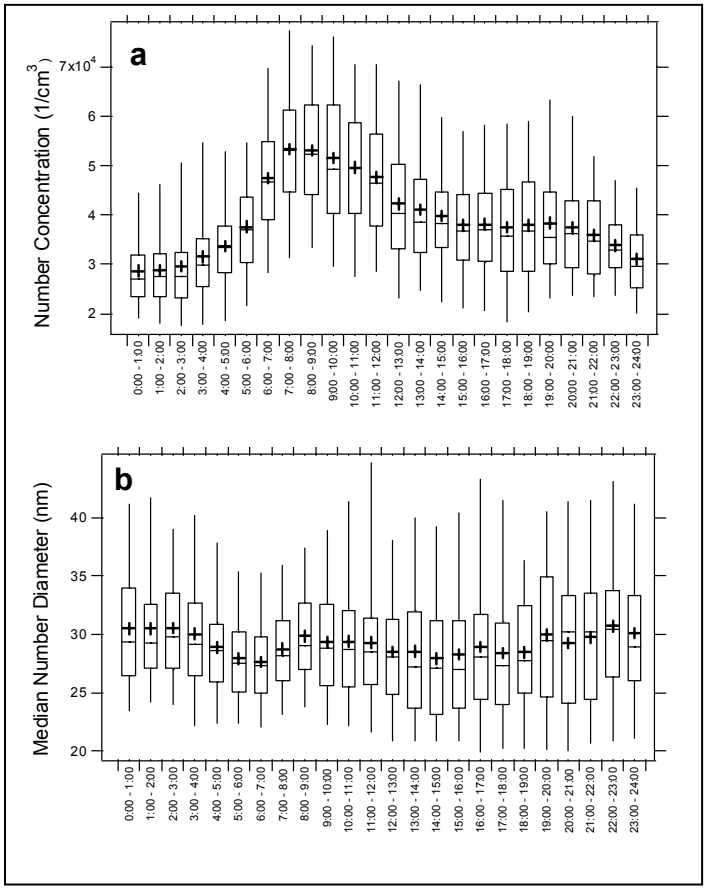

Figure V.4. Average diurnal patterns for number concentrations (a) and median number diameter (b) as measured by the SMPS 3034. The legends are as follows: boxes - 25 % percentiles, the medians and the 75 % percentiles; whiskers - 5 % and 95 % percentiles, crosses – the means**.**

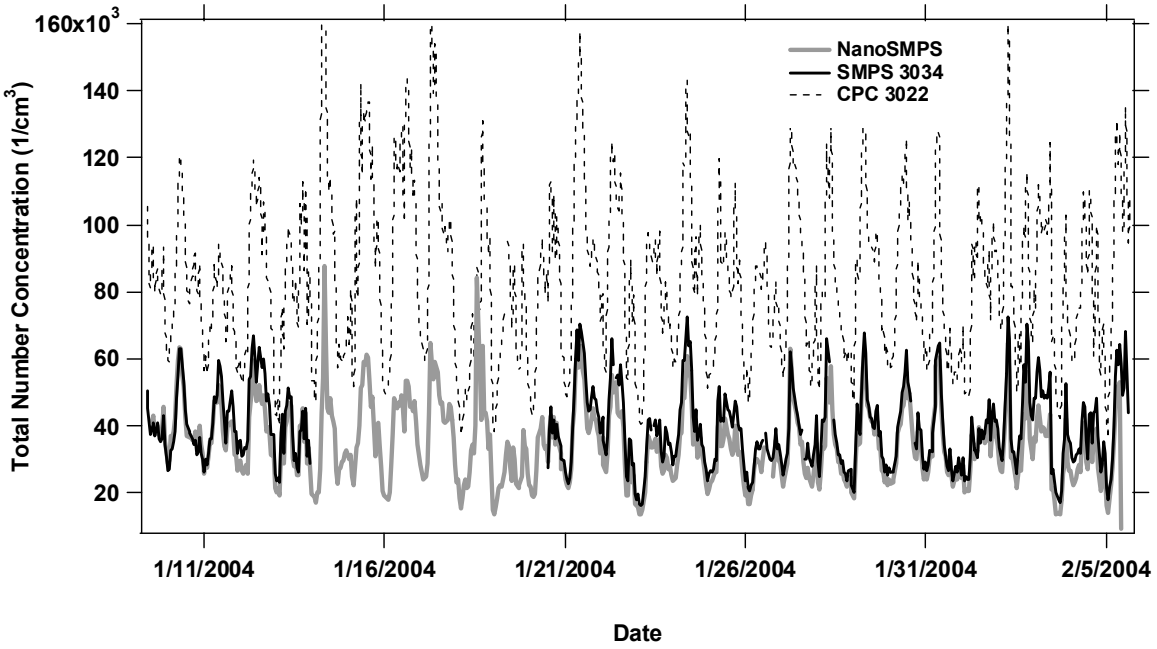

Figure V.5. Time series of hourly aerosol number concentrations from the SMPS 3034, the SMPS 3936 with the Nano DMA and the CPC 3022.

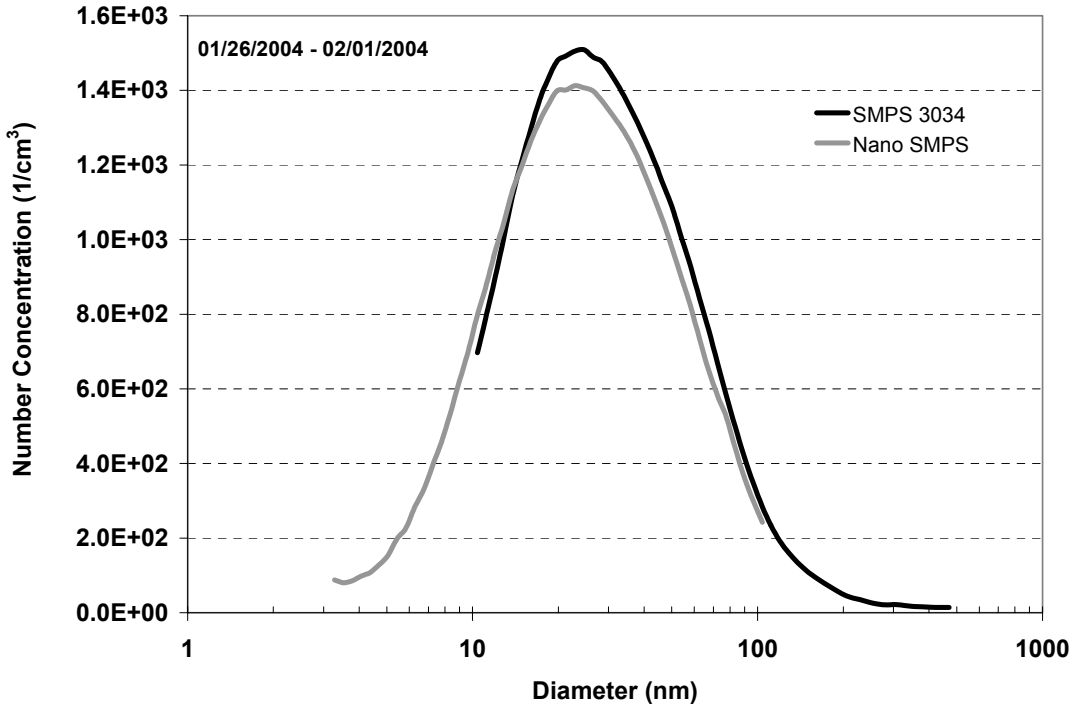

Figure V.6. Weekly average (01/26/04-02/01/04) size distributions as measured by the SMPS 3034 and the Nano SMPS.

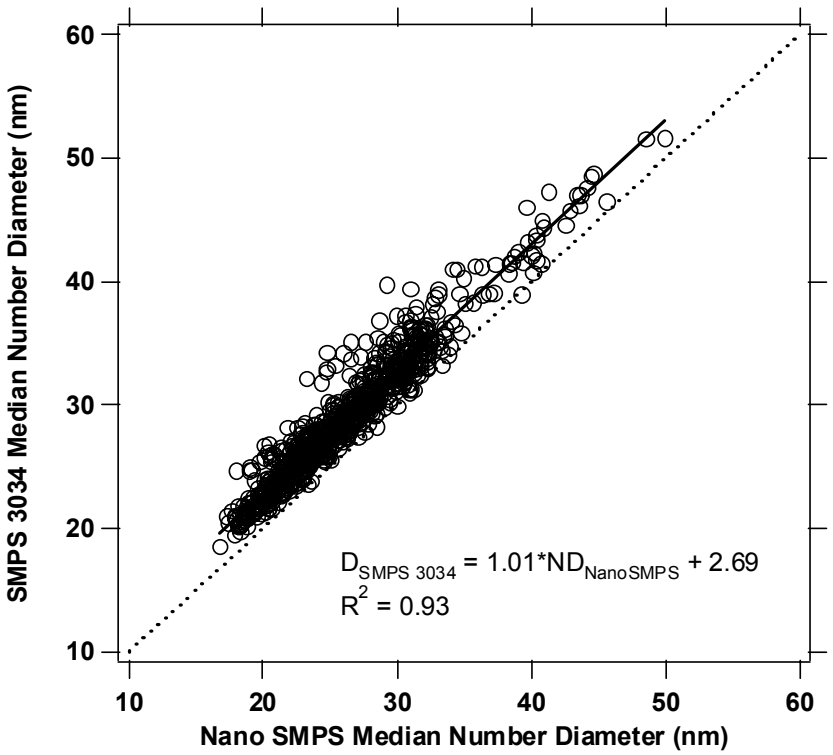

Figure V.7. SMPS 3034 median number diameter data (30-min averages) plotted vs. data from SMPS 3936 with the Nano DMA.

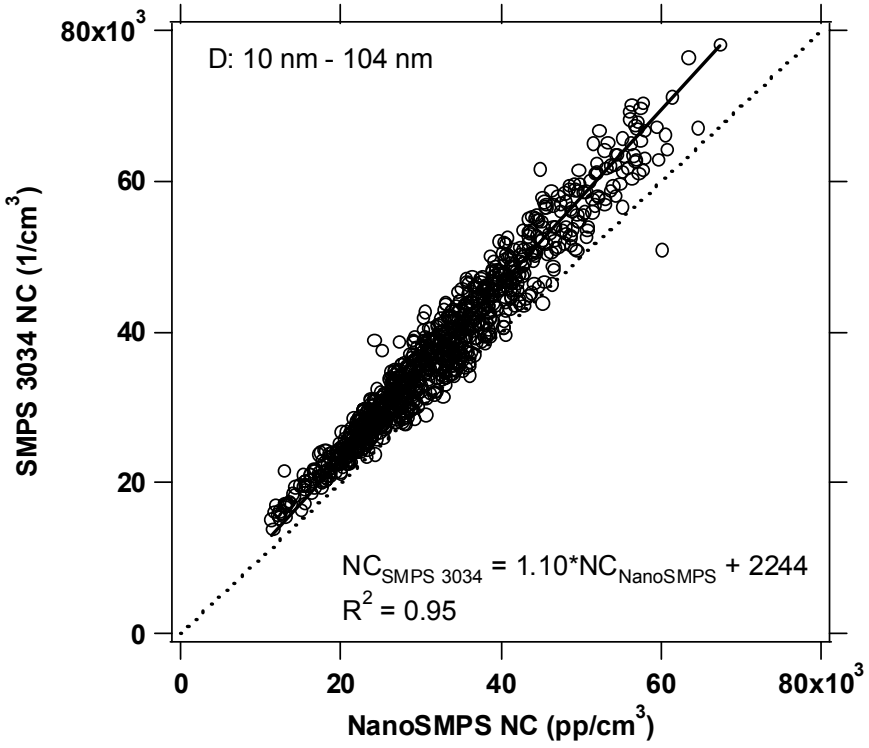

Figure V.8. SMPS 3034 number concentration data (30-min averages) plotted vs. data from SMPS 3936 with the Nano DMA. Only number concentrations from common size bins (10-104 nm) are considered in this comparison.

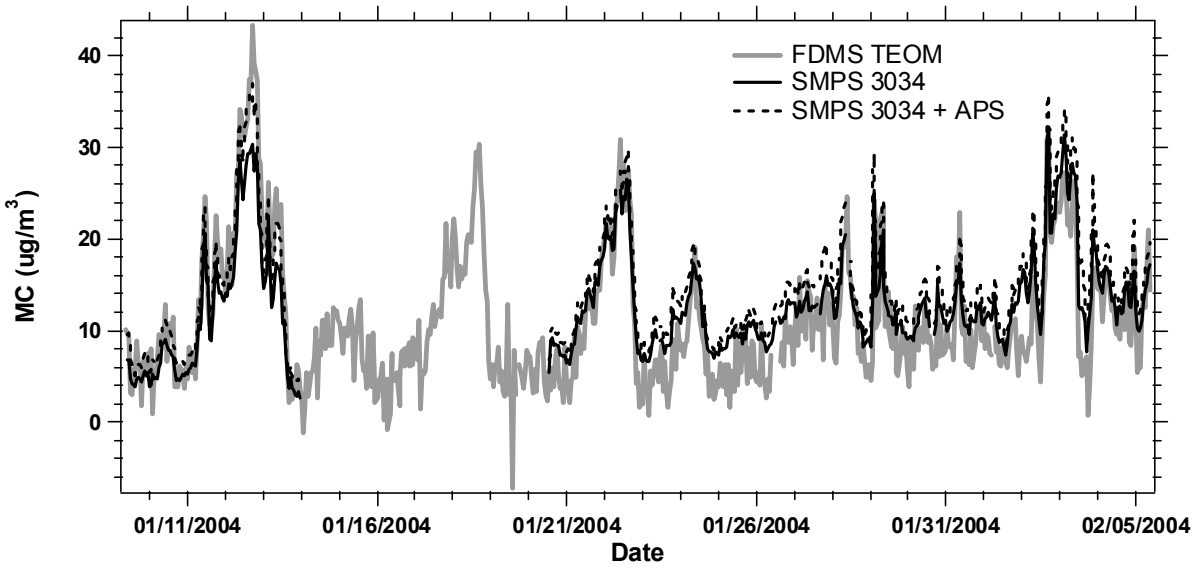

Figure V.9. Time series of hourly aerosol mass concentrations from the SMPS 3034, the APS and the FDMS TEOM. FDMS TEOM size cut-point is 2.5 □m. While the total mass concentration from the SMPS 3034 is plotted, the APS data include only mass concentrations corresponding to the particle diameters of 480 nm to 2.0 □m (corresponds to aerodynamic diameter of 2.5 □m). Particle density (SMPS3034 and APS) was assumed to be 1.5 g/cm^3.

V.4 Assessment and Conclusions

Observed 3-min total number concentrations as measured by the SMPS 3034 ranged from 1.3 x 10^4 particles/cm^3 to 1.3 x 10^5 particles/cm^3, while median number diameter ranged from 15 nm to 54 nm (Figure V.3). No extended "clean air" periods were detected during the campaign. Average diurnal patterns of the total number concentration and the median number diameter shown are presented in Figure V.4 as boxplots with the means, medians, and 5%, 25%, 75%, and 95% percentiles of the data shown for every hour of the day. The number concentration diurnal pattern shows a clear maximum (6 AM - noon) and a minimum (midnight – 2 AM), which are consistent with traffic patterns and perhaps residential heating in the urban New York City area. As particle number concentration starts to increase around 4-5 AM, particle median diameter decreases, which can be attributed to new particle formation. As day progresses (and particles age), particle diameter increases while particle concentration stays high. This phenomenon lasts until approximately noon, , and may be similarly correlated with traffic patterns.

Time series of hourly total particle number concentrations measured by the SMPS 3034, NanoSMPS and the CPC 3022 are shown in Figure V.5. Both SMPSs track CPC 3022 quite well, however, CPC-measured number concentrations are higher than SMPS total number concentrations by a factor of two. This discrepancy can be largely attributed to particle losses in the inlet and neutralizer of the electrostatic classifiers in the SMPSs. Agreement between total number concentrations from the SMPS 3034 and NanoSMPS is very good throughout the whole campaign. Aerosol size distributions as measured by the SMPS 3034 and the NanoSMPS over the week of 01/26/2005 – 02/01/2005 are shown in Figure V.6. Both instruments agree quite well over the entire overlap size range (10-104 nm). Figure V.7 shows the results of comparison of

the 30-min average particle number median diameter measured by the SMPS 3034 and the NanoSMPS throughout the whole campaign. The slope of the linear regression is 1.01, the intercept is approximately 3 nm and R^2 is 0.93. If the intercept is set to 0, the slope increases to 1.11. 30-min average number concentrations from the two instruments were compared as well. Total number concentrations in the diameter range of 10 – 104 nm measured by both instruments are shown in Figure V.8. The data are very well correlated (R^2 of 0.95). The slope of linear regression is 1.10, and 1.16 if intercept is set to 0, indicating that the number concentrations agree within 16% in the overlap range. The fact that the SMPS 3034 measures more particles can be attributed to a higher sample flow and shorter particle path inside the SMPS 3034. The reasons for the relatively high intercept of approximately 2.0×10^3 particle/cm^3 are not clear.

The time series of hourly total particle mass concentrations measured by the SMPS 3034 is shown in Figure V.9. Since there are no available data on density of aerosol particles in New York City area, we have used the value of 1.5 g/cm^3 to convert SMPS 3034–measured number concentration into mass concentration. This is a number is consistent with the lower value of density of urban atmospheric aerosol particles measured by McMurry et al. (2002) in Atlanta, GA and by the average density value inferred from measurements by Khlystov et al. (2004) in Pittsburg, PA. An FDMS TEOM monitor was chosen for comparison with the SMPS 3034 in order to evaluate the ability of the latter to efficiently detect changes in the aerosol mass concentration.

The FDMS TEOM monitor is a self-referencing continuous mass-measuring instrument, accounting for both non-volatile and semi-volatile components of a PM mass (more detailed description of the instrument can be found in (Felton et al, 2005)). During the campaign the FDMS TEOM monitor collocated with the particle sizing instruments had a 2.5 μm cyclone at the inlet and was operated at the TEOM filter temperature of 30^{o}C. The time series of hourly averaged mass concentration as measured by the FDMS TEOM monitor is also shown in Figure V.9. While the SMPS 3034 (black line) and the TEOM (gray line) data are well correlated with R^2 of 0.80, the SMPS 3034 under-estimates the aerosol mass concentration. This is not surprising considering that the largest particles the SMPS 3034 is capable of measuring are those with a diameter of 470 nm. In an attempt to close the mass balance, we have used APS data. The APS is a time-of-flight spectrometer that measures the velocity of particles in an accelerating airflow, and thus their aerodynamic diameters. The physical diameter of a spherical particle can be calculated by dividing its aerodynamic diameter by the square root of the particle density (Seinfeld and Pandis, 1998). The mass concentration of particles with the aerodynamic diameters of 580 nm – 2.5 μm (corresponding to the physical diameters of 480 nm – 2.0 μm, if particle density is 1.5 g/cm^3) was calculated and added to the total SMPS 3034-measured mass concentration (Figure. V.9, dashed line). Overall, this reconstructed "SMPS+APS" mass concentration stays well correlated with the FDMS TEOM data (R^2 = 0.82) throughout the campaign. However, while from the beginning of the campaign until 01/23/05 the "SMPS+APS" mass concentrations agree very well with the FDMS TEOM data, afterwards the TEOM monitor appears to "under-measure" the mass concentration. This may suggest that the particle density decreased during this period, relative to the first part of the campaign.

The new "single-box" SMPS (TSI Model 3034) was successfully deployed and operated during the PMTACS-NY Winter 2004 intensive campaign in Queens. The SMPS 3034 operated continuously from 01/09 to 02/05. Approximately 25% of the data had to be discarded due to the malfunction of the instrument (induced leak) at the beginning of the campaign. No other problems in instrument operation or maintenance were encountered during the winter 2004 field campaign.

Total particle number concentrations measured by the SMPS 3034 are highly correlated with those from the NanoSMPS, the CPC 3022 and the FDMS TEOM. The SMPS 3034 and NanoSMPS number concentrations agree within 16% in the overlap diameter range (10-104 nm) and the median number diameters agree within 3 nm. It appears that not only does the SMPS 3034 capture the main features of a size distribution "correctly", it is also more sensitive to small particles than the NanoSMPS. Due to the wide range of particle diameters over which the SMPS 3034 is measuring the number concentrations (10-470 nm), the instrument can be used in many cases as a replacement for the combination of NanoSMPS + SMPS with a Long DMA for measuring ultrafine particles. It was also shown that the SMPS 3034 mass concentration measurements track those of the FDMS TEOM very well (R^2=0.82).

Among many attractive qualities of the "single box" SMPS 3034 are its easy transport and set-up in field conditions. Since operation parameters are fixed, it makes it much easier to start and run the instrument, as well as compare the data from several SMPS 3034 instruments. On the other hand, fixed flows (and consequently the diameter range over which the number concentrations are measured) and scan time may limit use of the SMPS 3034 for research purposes. Perhaps adding an option to vary flow, as well as the scan time, may broaden the area of this instrument's use.

VI REFERENCES

Altshuller, A. (1993). Review: Natural Volatile Organic Substances and Their Effect on Air Quality in the United States. *Atmos. Environ.*, (27A)2132-2165.

Apel, E.C., Calvert, J.G., Riemer, D., Pos, W., Zika, R., Kleindienst, T., Lonnenman, W.A., Fuyng, K., Fujita, E., Shepson, P.B., Starn, T.K., Roberts, P.T. (1998). Measurements Comaprison of Oxygenated Volatile Organic Compounds at a Rural Site during the 1995 SOS Nashville Intensive. *J. Geophys. Res.* 103(D17):22295-22316.

Armstrong, B.H. (1967). Spectrum line profiles: the Voigt Function. *J. Quant. Spectrosc. Radiat. Transfer*, 7:61-88.

Chu, P.M., S.J. Wetzel, W.L. Lafferty, A. Perrin, J.-M. Flaud, Ph. Areas, G. Guelachvili (1998). Line intensities for the 8 μm bands of SO_2. *J. Mol. Spectrosc.*, 189:55-63.

Chylek, P., ., Ramaswamy, V., Srivastava, V., (1984). Graphitic carbon content of aerosols, clouds and snow and its climatic implications. *The Science of The Total Environment*, 36:117-120.

Dasgupta, P.K., Dong, S., Hwang, H., Yang, Y.-C., Genfa, Z. (1988). Continuous Liquid-Phase Fluorimetry Coupled to a Diffusion Scrubber for the Determination of Atmospheric Formaldehyde, Hydrogen Peroxide, and Sulfur Dioxide. *Atmos. Environ.,* 22:949-963.

Dong, S. and P.K. Dasgupta (1987). Fast Fluorometric Flow Injection Analysis of Formaldehyde in Atmospheric Water. *Environ. Sci. Technol.,* 21:581-588.

Fan, Q and P.K. Dasgupta (1994). Continuous Automated Determination of Atmospheric Formaldehyde at the Parts per Trillion Level. *Anal. Chem.,* 66:551-556.

Elkus, B., Wilson, K., (1977). Photochemical Air Pollution: Weekday-weekend differences. *Atmospheric Environment*, 11:509-515.

Felton, H.D., Schwab, J.J., Rattigan, O.V., and Demerjian, K.L. (2005). New York State Urban and Rural Measurements of Continuous PM2.5 Mass by FDMS TEOM and BAM: Evaluations and Comparisons with the FRM, *to be submitted to JAWMA*.

Finlayson-Pitts, B. J., and Pitts, J. N. (1986). *Atmospheric Chemistry: Fundamentals and Experimental Techniques*. JohnWiley and Sons, Inc., New York.

Fried, A., and 20 others L(2003). Tunable Diode Laser Measurements of Formaldehyde during the TOPSE 2000 study: Distributions, Trends, and Model Comparisons. *J. Geophys. Res. D.* 108(D4)8365-8376, doi:10.1029/2002D002208

Fried, A., Lee, Y.-N., Frost, G., Wert, B., Henry, B., Drummond, J.R., Huebler, G., Jobson, T. (2002). Airborne CH_2O Measurements over the North Atlantic during the 1997 NARE

Campaign: Instrument Comparisons and Distributins. *J. Geophys. Res.,* 107(D4):4039-4059, doi:10.1029/2000JD000260.

Friedfeld, S., Fraser, M.P., Ensor, K., Tribble, S., Rehle, D., Rehle, D., Leleux, D., Tittel, F. (2002). Statistical Analysis of Primary and Secondary Formaldehyde. *Atmos. Environ*., (36)4767-4775.

Gilpin, T., Apel, E., Fried, A., Wert, B., Calvert, J., Genfa, Z., Dasgupta, P., Harder, J.W., Heikes, B., Hopkins, B., Westberg, H., Kleindienst, T., Lee, Y.-N., Zhou, X., Lonnenman, W., Sewell, S. (1997). Intercomparison of Six Ambient [CH_2O] Measurement Techniques. *J. Geophys. Res.,* 102(D17):21611-21688.

Gray, H., A., Cass, G., R., Huntzicker, J., J., Heyerdahl, E., K., Rau, J., A., (1984). Elemental and organic carbon particle concentrations: A long term perspective. *The Science of The Total Environment*, 36:17-25.

Hansen, A., D., A., Rosen, H., Novakov, T., (1984). The aethalometer- an instrument for the real time measurement of optical absorption by aerosol particles. *The Science of The Total Environment*, 36:191-196.

Heikes, B., McCully, B., Zhou, X., Lee, Y.-N., Mopoper, K., Chen, X., Mackay, G., Karecki, D., Schiff, H., Campos, T., Atlas, E. (1996). Formaldehyde Methods Comparison in the Remote Lower Troposphere during the Mauna Loa Photochemistry Experiment 2. *J. Geophys. Res.,* (101):14741-14755.

Hering, S.V. and S.K. Friedlander, (1982). *Atmos. Environ*., 16:2647-2656.

Herndon, S.C., Nelson, D.D., Li. Y.Q., Zahniser, M.S. (2004). Determination of line strengths for selected transitions in the v2 band relative to the v1 and v5 bands of H_2CO. *J. Quant. Spectrosc. Radiat. Transfer*, 90(2):207-216.

Hildemann, L., M., Markowski, G., R., Cass, G., R., (1991). Chemical composition of emissions from urban sources of fine organic aerosol. *Environmental Science and Technology*, 25(4):744-759.

Humlicek, J. (1979). An efficient method for evaluation of the complex probability function: the Voigt function and its derivatives. *J. Quant. Spectrosc. Radiat. Transfer*, 21:309-313.

Ito, K., Xue, N., Thurston, G., (2004). Spatial variation of $PM_{2.5}$ chemical species and source apportioned mass concentration in New York City. *Atmospheric Environment*, 38:5269-5282.

Jacobson, M., (2001). Strong radiative heating due to the mixing state of BC in atmospheric aerosols. *Nature*, 409:695-697.

Jeong, C.-H., Lee, D.-W., Kim, E., Hopke, P.K., (2004). Measurement of real time $PM_{2.5}$ mass,sulfate and carbonaceous aerosols at multiple monitoring sites. *Atmospheric Environment*, 38:5247-5256.

Kawamura, K., Steinberg, S., Kaplan, I. (2000). Homologous Series of C1-C10 Monocarboxylic Acids and C1-C6 Carbonyls in Los Angeles Air and Motor Vehicle Exhausts. *Atmos. Environ.,* (34)4175-4191.

Kenny, L., C., Gussman, R., A., (2000). A direct approach to the design of cyclones for aerosol-monitoring applications. *Journal of Aerosol Science*, 31:1407-1420.

Khlystov, A., Stanier, C., and Pandis, S. (2004). An Algorithm for Combining ElectricalMobility and Aerodynamic Size Distributions Data When Measuring Ambient Aerosol, *Aerosol Sci. Technol.* 38 (S1): 229–238.

Lebron, F., A., (1975). Comparison of weekend-weekday ozone and hydrocarbon concentrations in the Baltimore-Washington metropolitan area. *Atmospheric Environment*, 9:861-863.

Lowenthal, D., H., Zielinska, B., Chow, J., C., Watson, J., G., Gautam, M., Ferguson, D., H., Neuroth, G., R., Stevens, K., D., (1994). Characterization of heavy-duty diesel vehicle emissions. *Atmospheric Environment*, 28:731-743.

Mandin, J.-Y., V. Dana, A. Perrin, J.-M. Flaud, C. Peyret-Camy, L. Régalia, A. Barbe (1997). The $\{\nu_1 + 2\,\nu_2, \nu_1 + \nu_3\}$ bands of $^{14}N^{16}O_2$: Line positions and intensities; line intensities in the $\nu_1 + \nu_2 + \nu_3 - \nu_2$ hot band, *J. Mol. Spectrosc*., 181, 379-388,

Mather, J.H., P.S. Stevens and W.H. Brune, 1997. OH and HO_2 measurements using laser-induced fluorescence. J. Geophysical Research, Vol. 102, No. D5, 6427-6436 (March 20).

McManus, J. B., P. L. Kebabian, and M. S. Zahniser, (1995). Atigmatic mirror multiple pass absorption cells for long pathlenght spectroscopy, *Appl. Opt*., 34:3336-3348

McMurry, P.H., Wang, X., Park, K., and Ehara, K. (2002). The Relationship between Mass and Mobility for Atmospheric Particles: a New Technique for Measuring Particle Density, *Aerosol Sci. Technol.* 36: 227–238.

Pandya, R., J., Solomon, G., Kinner, A., Balmes, J., R., (2002). Diesel exhaust and asthma: Hypotheses and molecular mechanisms of action. *Environmental Health Perspectives*, 110(1):103-112.

Park, S., Sakurai, H., Vollmers, K., and McMurry (2004). Aersol Size Distributions Measured at the South Pole during ISCAT, *Atmos. Environ*, 38: 5493-5500.

Possanzini, M., Di Palo, V., Petricca, M., Fratarcangeli, R., Brocco, D. (1996). Measurements of Lower Carbonyls in Rome Ambient Air. *Atmos. Environ.*, (30)3757-3764.

Robbins, R., (1994). Differences in the carbon composition of source profiles for diesel-and gasoline-powered vehicles. *Atmospheric Environment*, 28:2493-2505.

Rothman, , L. S., C. P. Rinsland, A. Goldman, S. T. Massie, D. P. Edwards, J. M. Flaud, A. Perrin, C. Camy-Peyret, V. Dana, J. Y. Mandin, J. Schroeder, A. McCann, R. R. Gamache, R. B. Wattson, K. Yoshino, K. V. Chance, K. W. Jucks, L. R. Brown, V. Nemtchinov and P. Varanasi, (1998). The HITRAN molecular spectroscopic database and hawks (HITRAN atmospheric workstation): 1996 edition, *J. Quantum Spectrosc. Radiat. Transfer*, 60:665-710

Samet, J. M., Dominici, F., Curriero, F. C., Coursac, I., and Zeger, S. L. (2000). Fine Particulate Air Pollution and Mortality in 20 U.S. Cities, *N. Engl. J. Med*. 343:1742–1749.

Seinfeld, J. H., and Pandis, S. N. (1998). *Atmospheric Chemistry and Physics*. John Wiley and Sons, Inc., New York.

Shen, S., Jaques, P.A., Zhu Y., Geller M.D., and Sioutas C. (2002) Evaluation of the SMPS–APS System as a Continuous Monitor for Measuring $PM_{2.5}$, PM_{10} and Coarse ($PM_{2.5-10}$) Concentrations, *Atmos. Environ*, 36: 3939-3950.

Singh, H. and 19 others (2000). Distribution and Fate of Selected Oxygenated Organic Species in the Troposphere and Lower Stratosphere over the Atlantic. *J. Geophys. Res. D* 105(D3)3795-3805.

Smith, M. A. H., C. P. Rinsland, B. Fridovich and K. N. Rao, (1985). Intensites and collision broadening paramters from Infrared Spectra, *Mol. Spectrosc.: Mod Res.*, 3:111-248

Stolzenburg, M.R. and S.V. Hering (2000). *Environ. Sci. Technol*., 34:907-914.

Stanier, C., Khlystov, A.Y, Chan, W.R., Mandiro, M., and Pandis, S. (2004). A Method for the In Situ Measurement of Fine Aerosol Water Content of Ambient Aerosols: The Dry-Ambient Aerosol Size

Stein, S.W., B.J. Turpin, X.-P. Cai, P.-F. Huang and P.H. McMurry (1994). *Atmos. Environ*., 28:1739-1746.

Wang, S.C., and Flagan, R.C. (1989). Scanning Electrical Mobility Spectrometer, *J. Aerosol. Sci.* 20: 1485-1489.

Watson, J., G., Chow, J.,C., (2001). Estimating middle-, neighborhood-, and urban-scale contributions to elemental carbon in Mexico City with a rapid response aethalometer. *Journal of Air and Waste Management Association*, 51:1522-1528.

Watson, J., G., Chow, J., C., (2002). A wintertime PM2.5 episode at Fresno, CA, supersite. *Atmospheric Environment*, 36:465-475.

Wert, B.P. and 23 others (2003). Signatures of Terminal Alkene Oxidation in Airborne Formaldehyde Measurements during TexAQS 2000. *J. Geophys. Res. D* 108(D3)4104-4117, doi:10.1029/2002JD002502.

Winkler, P. (1974). *J. Aerosol Sci*., 5:235-240.

Wongphatarakul, V., Friedlander, S., K., Pinto, J., P., (1998). A comparative study of $PM_{2.5}$ ambient aerosol chemical databases. *Environmental Science and Technology*, 32:3926-3934.

Zhu, Y., Hinds, W.C., Shen, S., and Sioutas, C. (2004). Seasonal trends of Concentration and Size Distribution of Ultrafine Particles Near Major Highways in Los Angeles, 38 (S1): 5–13.

APPENDIX A: Winter 2004 Intensive

Results of Audits Performed by DEC, Division of Air Resources, Bureau of Technical Support, Quality Assurance Section

New York State Department of Environmental Conservation
Division of Air Resources
Bureau of Quality Assurance, Ambient Monitoring Section
1 University Place, PO box #10, room C-115
Rensselaer, New York 12144
Phone: (518) 525-2700 • **FAX:** (518) 525-2706
Website: www.dec.state.ny.us

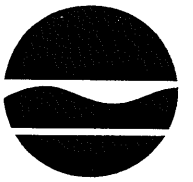

Erin M. Crotty
Commissioner

July 23, 2004

M E M O R A N D U M

TO: Ed Marion - Bureau of Air Quality Surveillance
Southern Monitoring Operations

FROM: Gary Belcher - Bureau of Quality Assurance
Ambient Monitoring Section

RE: Annual Continuous Air Monitoring Systems Audit Report for Queens College 2 (7096-15) and PS219 @ Queens College 2 (7096-14)

On June 24, 2004, Ambient Monitoring Section staff completed the site visit portion of the annual continuous air monitoring systems audit at the Queens College 2 monitoring site and the PS219 @ Queens College 2 monitoring site. The Queens College 2 monitoring site is located in a temporary 7 foot by 7 foot shelter in Parking Lot 6 on the grounds of the Queens College campus in Flushing, Queens. Parameters continuously monitored at this location are ambient sulfur dioxide, nitrogen oxides, ozone and carbon monoxide. An Horiba ambient air monitor and an ATEC carbonyl sampler are also located at this site.

Across a field to the West of this site on the rooftop of Public School 219 is located the particulate monitoring site Queens College 2 @ PS 219, site number 7096-14. Located at this site is a Rupprecht & Patashnick $PM_{2.5}$ Model 1400AB TEOM particulate sampler, a Rupprecht & Patashnick $PM_{2.5}$ Model Filter Dynamic Measuring System (FDMS) 1400AB TEOM System, a Rupprecht & Patashnick $PM_{2.5}$ Model 2300 Speciation particulate sampler, a manual Rupprecht & Patashnick $PM_{2.5}$ particulate sampler, a canister particulate

sampler, a Rupprecht & Patashnick Model 5400 Carbon Particulate Monitor and a meteorological tower. Despite the proximity, this site is not with 7096-15 because a separate ESC Data Logger is needed for some of the instrumentation at the site. This site was visited, photographs were taken and instrument identification numbers verified.

Data availability figures for continuous parameters for January 1 through December 31, 2003 for both sites were as follows:

Parameter	% of Available Hours
Sulfur Dioxide	**96.4%**
Ozone	**95.9%**
Carbon Monoxide	**87.8%**
Nitrogen Dioxide	**90.2%**
TEOM (PS219)	**97.0%**

See excerpts from the site supervisor's Second and Third Quarter QA Narratives for specific information regarding lost or missing data episodes.

Issues Affecting Data Quality, Data Availability or Safety:

Major Issues:

None

Additional Items:

1. A primary calibration must be performed for the TEI Model 49C analyzer as soon as possible. There was no calibration performed (as required) after a documented pump change on May 26, 2004.

2. Weekly check sheets were not initialed by the site supervisor past the third week in April. Review by the site supervisor should be accomplished no later than within 2 weeks.

3. The interior temperature probe appears to be malfunctioning. This should be addressed as soon as possible.

4. There was no chart recorder at the site, either to be used continuously for criteria data or for audit/ calibration documentation. Recent email communication with USEPA (copy attached at end of report) has indicated that strip chart operation is still required, unless a waiver is obtained. The chart recorder should be returned to operation at this site.

5. The Model 204 Equipment file for the Rupprecht & Patashnick $PM_{2.5}$ Model 1400AB TEOM particulate sampler located at the Queens College 2 @ PS 219 monitoring site needs to be updated to reflect the correct DEC number (#138525).

6. The Model 204 data processing system should be updated to reflect the removal of the TEI Model 48C Carbon Monoxide sampler (#137168) and the TEI Model 42 Oxides of Nitrogen sampler (#53077) and the installation of the TEI Model 48C Carbon Monoxide sampler (#137161) and the TEI Model 42 Oxides of Nitrogen sampler (#53081), respectively.

This air monitoring site continues to be well operated and maintained by the operator, Mike Christopherson.

cc: John Higgins - BQA
Pat Lavin - BAQS
Dave Wheeler - Region 2 BAQS
Randall Coon - BQA
Mike Christophersen - Region 2 BAQS
Section Circulation

New York State Department of Environmental Conservation
Division of Air Resources
Bureau of Quality Assurance, Ambient Monitoring Section
1 University Place, PO box #10, room C-115
Rensselaer, New York 12144
Phone: (518) 525-2707 • **FAX:** (518) 525-2706
Website: www.dec.state.ny.us

Erin
Comm

To: Randy Coon

From: Malcolm Baker MB

Subject: **QA Performance Audit**

Date: September 30, 2004

On September 8, 2004 QA staff conducted an annual performance audit at the Queen's College (7096-15) continuous air monitoring site. This site has continuous analyzers fc Ozone, Carbon Monoxide, NO-NO2-NOX and SO2.

The results of the audits are summarized below. No reply is required. The sites's zero air supply was not inspected because it had been removed by the operator in order to make room for audit equipment.

SO2: average %d= +0.2 %

Carbon Monoxide: average %d= +2.8%

Ozone: average %d= +2.5%

NOX: NO average %d= -3.0%
NOX average %d= -3.1%
NO2 average %d= -2.8%

Preliminary results were sent to the operator and the supervising engineer via GroupWise electronic mail on September 9, 2004.

MB:mb

New York State Department of Environmental Conservation
Division of Air Resources
Bureau of Quality Assurance, Ambient Monitoring Section
1 University Place, PO box #10, room C-115
Rensselaer, New York 12144
Phone: (518) 525-2707 • **FAX:** (518) 525-2706
Website: www.dec.state.ny.us

Erin M. Crot
Commissione

To: Randy Coon
From: Malcolm Baker MB
Subject: **PM 2.5 Performance Audits**
Date: December 3, 2004

On November 9, 2004 and November 16, 2004 QA staff conducted annual performance audits on the FRM and TEOM samplers located at the Canal Street Post Office (8100-02) and PS 219 (7096-14) air monitoring sites. Canal Street is a rooftop site with a PM-2.5 TEOM, a PM-2.5 FRM, a PM-10 FRM and a Met One Speciation sampler. This site was audited on November 9. The audit of the speciation sampler will be reported under separate cover.

PS 219 is the rooftop site associated with the Queen's College supersite. At this site are two TEOMs, one PM-2.5 FRM, and a R & P 2300 speciation sampler. Reported here is the November 16 audit of the PM-2.5 FRM. The audits of the TEOMs and speciation sampler located at PS 219 will be reported under separate cover.

No reply is required. The FRMs and TEOM at Canal Street passed all their audit criteria on November 9. The FRM at PS 219 failed the leak check but passed a leak check later that week after the "V" seals were cleaned by the operator. Preliminary results were sent to the operator and the supervising engineer via Groupwise electronic mail on November 10, 2004 and November 17, 2004.

MB:mb

IS 52, TEOM 23537: Leak check (Accu System) failed for both total and main flows. Total flow audit failed at 4.4%d. The operator reports that this unit was replaced on 10/29/04 and passed a flow audit on 11/17/04.

Dirk Felton of BAQS reports that ACCU System attachments will be removed when the current supply of filters is exhausted. This is thought to be late December or early January. Preliminary results were sent to the operators and the supervising engineer via Groupwise electronic mail on October 6, 2004.

MB:mb